haematologica
Journal of The Ferrata Storti Foundation

Phenotype-based drug screening reveals association between venetoclax response and differentiation stage in acute myeloid leukemia

by Heikki Kuusanmäki, Aino-Maija Leppä, Petri Pölönen, Mika Kontro, Olli Dufva, Debashish Deb, Bhagwan Yadav, Oscar Brück, Ashwini Kumar, Hele Everaus, Bjørn T. Gjertsen, Merja Heinäniemi, Kimmo Porkka, Satu Mustjoki, and Caroline A. Heckman

Haematologica 2019 [Epub ahead of print]

Citation: Heikki Kuusanmäki, Aino-Maija Leppä, Petri Pölönen, Mika Kontro, Olli Dufva, Debashish Deb, Bhagwan Yadav, Oscar Brück, Ashwini Kumar, Hele Everaus, Bjørn T. Gjertsen, Merja Heinäniemi, Kimmo Porkka, Satu Mustjoki, and Caroline A. Heckman.
Phenotype-based drug screening reveals association between venetoclax response and differentiation stage in acute myeloid leukemia.
Haematologica. 2019; 104:xxx
doi:10.3324/haematol.2018.214882

Phenotype-based drug screening reveals association between venetoclax response and differentiation stage in acute myeloid leukemia

Authors: Heikki Kuusanmäki[1, 2], Aino-Maija Leppä[1], Petri Pölönen[3], Mika Kontro[2], Olli Dufva[2], Debashish Deb[1], Bhagwan Yadav[2], Oscar Brück[2], Ashwini Kumar[1], Hele Everaus[4], Bjørn T. Gjertsen[5], Merja Heinäniemi[3], Kimmo Porkka[2], Satu Mustjoki[2,6] and Caroline A. Heckman[1]

Affiliations:

[1]Institute for Molecular Medicine Finland, Helsinki Institute of Life Science, University of Helsinki, Helsinki, Finland

[2]Hematology Research Unit, Helsinki University Hospital Comprehensive Cancer Center, Helsinki, Finland

[3]Institute of Biomedicine, School of Medicine, University of Eastern Finland, Kuopio, Finland

[4]Department of Hematology and Oncology, University of Tartu, Tartu, Estonia

[5]Centre for Cancer Biomarkers, Department of Clinical Science, University of Bergen, Bergen, Norway

[6]Translational Immunology Research Program and Department of Clinical Chemistry and Hematology, University of Helsinki, Helsinki, Finland

Contact information for correspondence:

Caroline A. Heckman, Ph.D. Institute for Molecular Medicine Finland, University of Helsinki, P.O. Box 20, FI-00014 Helsinki, Finland. Phone: +358 29 4125769; Email: caroline.heckman@helsinki.fi

Heikki Kuusanmäki, Ph.D. Institute for Molecular Medicine Finland, University of Helsinki, P.O. Box 20, FI-00014 Helsinki, Finland. Email: heikki.kuusanmaki@helsinki.fi

Running heads: Venetoclax response and maturation stage in AML

Keywords (4): Venetoclax, FAB subtype, biomarker, flow cytometry

Word count (abstract): 218/250
Word count (text): 3919/4000
Figures/Tables: 6/2
References: 49

ACKNOWLEDGEMENTS

We thank the patients and donors who participated in the study. We appreciate critical comments and input from colleagues at FIMM (Dimitrios Tsallos, Jarno Kivioja, Riku Turkki, Komal Javarappa, Joseph Saad, Samuli Eldfors, Muntasir Mamun Majumder, Aleksandr Ianevski and Krister Wennerberg). We would like to thank the FIMM High Throughput Biomedicine Unit for preparing the drug plates (Laura Turunen, Jani Saarela), and the FIMM Sequencing Lab for preparing the exome sequence data. We also thank Alun Parsons, Minna Suvela and Siv Knaappila for their help in patient sample processing, and clinicians Riikka Räty, Eeva Martelin, Tuija Lundán, Sanna Siitonen, Minna Lehto, Juha Lievonen and Sari Kytölä for providing the samples.

This study was supported by grants from the European Research Council (M-IMM), Academy of Finland, Finnish Cancer Organizations, Finnish Cancer Institute, Emil Aaltonen Foundation, Sigrid Juselius Foundation, Orion Research Foundation, Instrumentarium Science Foundation, State Funding for University-Level Health Research in Finland, Relander Foundation, Gyllenberg Foundation, Ida Montin Foundation, Finnish Hematology Association and TEKES - the Finnish Funding Agency for Technology and Innovation.

ABSTRACT

Ex vivo drug testing is a promising approach to identify novel treatment strategies for acute myeloid leukemia. However, accurate blast-specific drug responses cannot be measured with homogeneous “add-mix-measure” cell viability assays. In this study, we implemented a flow cytometry-based approach to simultaneously evaluate the *ex vivo* sensitivity of different cell populations in 34 primary acute myeloid leukemia samples to seven drugs and 27 rational drug combinations. Our data demonstrate that different cell populations present in acute myeloid leukemia samples have distinct sensitivity to targeted therapies. Particularly, blast cells of FAB M0/1 acute myeloid leukemia showed high sensitivity to venetoclax. In contrast, differentiated monocytic cells abundantly present in M4/5 subtypes showed resistance to Bcl-2 inhibition, whereas immature blasts in the same samples were sensitive, highlighting the importance of blast-specific readouts. Accordingly, in the total mononuclear cell fraction the highest *BCL2/MCL1* gene expression ratio was observed in M0/1 and the lowest in M4/5 acute myeloid leukemia. Of the seven tested drugs, venetoclax had the highest blast-specific toxicity, and combining venetoclax with either MEK inhibitor trametinib or JAK inhibitor ruxolitinib effectively targeted all venetoclax-resistant blasts. In conclusion, we show that *ex vivo* efficacy of targeted agents and particularly Bcl-2 inhibitor venetoclax is influenced by the cell type, and accurate blast-specific drug responses can be assessed with a flow cytometry-based approach.

INTRODUCTION

The treatment of acute myeloid leukemia (AML) with high-dose cytarabine and anthracycline-based intensive chemotherapy has remained the standard of care for the last four decades.[1] Despite the increase in overall survival, only 35 to 40% of adult patients under 60 years are cured with chemotherapy and allogeneic stem cell transplantation.[2] A number of novel targeted agents have been investigated in AML, but have usually generated clinical responses only in small patient subsets. Currently, genetic profiling is used for patient stratification and determination of treatment, evident by the recent approvals of midostaurin/gilteritinib and ivosidenib/enasidenib for treating AML patients with *FLT3* or *IDH1*/*IDH2* mutations, respectively.[3–5] Furthermore, Bcl-2 inhibitor venetoclax combined with a hypomethylating agent was recently approved for AML with increased efficacy in patients with *IDH1/2* and *NPM1* mutations.[6,7] However, the majority of AML patients lack actionable mutations and our understanding of the relationship between cancer genotype, phenotype and drug function remain limited. *Ex vivo* drug testing with primary patient samples may help to identify novel treatment options and patient subgroups with sensitivity to a specific targeted therapy.

AML is diagnosed when the bone marrow (BM) contains at least 20% of myeloid lineage blast cells, and hematological relapse is defined when the BM exceeds 5% of blasts. The non-blast cells of the AML BM are comprised of other cell types, mainly lymphocytes and more mature leukemic cells (monocytes, granulocytes) or healthy cells. The BM content and the maturity level of leukemic cells is reflected in the French-American-British (FAB) subtypes.[8] In FAB M0/1 subtypes, the differentiation blockade occurs at the early myeloid progenitor stage, whereas in FAB M4/5 subtypes the differentiation blockade is “leaky”. In addition to immature blasts in FAB M4/5 samples, leukemic cells often show myelomonocytic or monocytic differentiation, respectively. To achieve optimal response in patients, the drugs should target the less differentiated leukemic blasts.[9] However, due to cellular heterogeneity, blast-specific drug responses are challenging to measure with conventional cell viability assays such as CellTiter-Glo (CTG) or tetrazolium reduction assays (MTT/MTS).[10] Although enrichment of blasts is

possible, this can be time consuming and enrichment might deplete cell populations such as monocytes that secrete cytokines important for blast cell survival and drug responses.[11–13]

To evaluate the *ex vivo* sensitivity of AML patient samples at a cell population level, we applied a multiplexed, 96-well format flow cytometry (FC)-based drug sensitivity assay. We compared this approach with the CTG-based cell viability assay to study potential inconsistencies between these two methods. Furthermore, we aimed to identify drugs and drug combinations that could effectively target leukemic blasts in physiologically relevant concentrations. In addition to standard of care drugs, cytarabine and idarubicin, we selected five FDA-approved targeted small molecule inhibitors that have shown AML-selective responses in our earlier studies:[14,15] MEK inhibitor (trametinib), JAK1/2 inhibitor (ruxolitinib), mTORC1 inhibitor (everolimus), FLT3/broad range tyrosine kinase inhibitor (TKI, sunitinib) and Bcl-2 inhibitor (venetoclax). Most importantly, we demonstrate that targeted agents, particularly venetoclax, have different efficacies towards AML cells at distinct stages of myeloid differentiation.

METHODS

Methods are described in more detail in the *Online Supplemental Material.*

Patient samples

BM samples from 34 AML patients and three healthy volunteers were obtained from Helsinki University Hospital Comprehensive Cancer Center after informed consent (permit numbers 239/13/03/00/2010, 303/13/03/01/2011, Helsinki University Hospital Ethics Committee) and in compliance with the Declaration of Helsinki. Patient characteristics are presented in Supplemental Table 1.

Preparation of drug plates

The compounds (Supplemental Table 2) were dispensed on 96-well V-bottom plates (Thermo Fisher Scientific, Carlsbad, CA) and 384-well plates (Corning, Corning, NY) using an acoustic liquid handling device Echo 550 (Labcyte, Sunnyvale, CA). Drug plate layouts and concentrations are presented in Supplemental Figure 1. BM mononuclear cells (BM-MNCs) were isolated using Ficoll-Paque Premium (GE Healthcare, Little Chalfont, Buckinhamshire, UK) density gradient centrifugation. Fresh or frozen BM-MNCs were suspended in mononuclear cell medium (MCM; PromoCell, Heidelberg, Germany) supplemented with 10 µg/mL gentamicin and 2.5 µg/mL amphotericin B and plated in parallel on pre-drugged 96-well plates (100,000 cells/well in 100 µl) for FC analysis and 384-well plates (10,000 cells/well in 25 µl) for CellTiter-Glo® (CTG)-based cell viability assay. The cells were incubated with the drugs for 72 hours at 37°C and 5% CO_2.

Flow cytometry-based readouts

Following the 72-hour incubation with the drugs, cells were stained with an antibody mix (CD33, CD45, CD14, CD38 and CD34) followed by apoptosis (Annexin-V) and dead (7-AAD) cell staining. A detailed description of the methods is presented in *Online Supplemental Material* and the gating strategy is illustrated in Figure 1B.

Cell viability analysis using CellTiter-Glo®

Parallel to FC analysis, cell viability was measured with CellTiter-Glo® (CTG; Promega, Madison, WI) in 384-well plates as described earlier.[14] After the 72-hour incubation with the drugs, 25 µL CTG was added to each well. The luminescence signal was measured using a PHERAstar plate reader (BMG LABTECH, Ortenberg, Germany).

Calculation of the drug sensitivity and drug combination scores

Ex vivo drug sensitivity of AML and healthy BM cells to the tested drugs was calculated using a drug sensitivity score (DSS) as previously described.[16] Drug combination efficacies were calculated as the difference between observed and expected values. The expected value is computed using the Bliss independence model[17] as reference, which assumes that two drugs exhibit their effect independently.[18]

Gene expression and pathway analysis

Publicly available microarray data from the Hemap data set[19,20] (http://hemap.uta.fi/) and RNA-seq data (RSEM values) from the TCGA Research Network[21] (http://cancergenome.nih.gov/) also included in the Hemap resource were used for gene expression and pathway analysis. Beat AML data[22] was used to assess the correlation between venetoclax drug sensitivity and *BCL2* family and monocytic/granulocytic differentiation marker gene expression. For analysis of gene expression in healthy hematopoietic cell types Differentiation Map data was used.[23] Detailed methods are described in the *Online Supplemental Material.*

Statistical analysis

Statistical analysis was conducted with Graph Prism version 7.0 (GraphPad Software, San Diego, CA). Differences between drug responses were analyzed by Mann-Whitney U test, and for multiple t-tests p-values were adjusted using the Benjamin-Hochberg method ($q<0.10$ used to determine significance). The Kruskal-Wallis test was used when more than two groups were tested and significant comparisons were validated with post-hoc analysis

(Dunn’s test). Statistical dependence between two variables was assessed by Spearman’s rank correlation.

RESULTS

Analysis of the AML bone marrow compartment

To measure blast-specific drug responses in mononuclear cell (MNC) enriched BM AML samples, we tested 34 AML samples collected at diagnosis or relapse with seven drugs. Following a 72-hour drug treatment we analyzed the samples by both FC and CTG-based cell viability assays (Figure 1A). With the CTG assay we measured the overall BM-MNC sensitivity, while with the FC analysis we measured the number of viable cells in different cell populations. We used four cell surface markers (CD45, CD34, CD33, CD14) to identify the major leukocyte populations present in the AML BM: leukemic blasts, immature granulocytes, promonocytes/monocytes and lymphocytes (Figure 1B). In the studied samples, the fraction of blasts out of CD45+ positive leukocytes varied between 17-92% and the lymphocyte population ranged from 1 to 49% (Supplemental Table 3). As expected, we observed high numbers of monocytic cells in FAB M4/5 samples, whereas M0/1 samples mainly consisted of blasts and lymphocytes (Figure 1C). After 72-hours in culture, we observed monocytic maturation in several M5 samples,[24] and in many samples the granulopoietic cell population diminished or was completely lost (Supplemental Figure 2).

Flow cytometry *vs*. homogeneous cell viability assay-based drug sensitivity profiling

To determine the correlation between drug sensitivity of the samples measured by FC or CTG-based methods, we converted the cell viability readouts from each assay to drug sensitivity scores (DSS, a drug sensitivity metric based on area under the dose-response curve, higher DSS indicates higher sensitivity).[16] We observed a strong correlation between CTG and FC viability derived DSS when all live CD45+ leukocytes were used as the FC readout ($R=0.64$, $P<0.0001$, Figure 2A), and when the blast-specific drug responses were exclusively taken as the FC readout from samples with blast counts over 50% ($R=0.75$, $P<0.0001$, Figure 2B). However, we observed poor correlation between the FC and CTG results in a sample cohort with blast counts below 50% ($R=0.24$, $P=0.05$, Figure 2C). The most prominent differences were seen in the response to trametinib and venetoclax

(Supplemental Figure 3). The poor correlation was partly due to highly different drug sensitivities of the non-blast cell populations when compared to blasts as demonstrated in two samples with low blast counts (Figure 2 D-G). Our data shows that AML BM subpopulations have heterogeneous drug responses that confound the assessment of blast specific drug sensitivities when using homogenous cell viability assays in unsorted BM-MNC samples.

Ex vivo drug screening predicts induction therapy response

Next, we evaluated whether incomplete bone marrow blast clearance at d14/d28 after induction treatment was associated with decreased *ex vivo* drug sensitivity. We evaluated BM samples from 15 patients collected prior to anthracycline+cytarabine induction chemotherapy. Amongst these patients, five had >10% blast cells at d14 and/or d28 and were defined as chemoresistant as described in Supplemental Table S1. Additionally, we included samples from two patients resistant to induction (collected at the time of resistant disease) in the chemoresistant group. A combined DSS of cytarabine and idarubicin showed significantly lower values for the resistant patients both with FC and (P<0.05, 2H) and CTG (P<0.01, Figure 2I). Furthermore, we observed a significant difference between responders and non-responders when blast-specific idarubicin response was measured with FC (P<0.05, Figure 2H) or CTG (P<0.05, Figure 2I). These results are in line with a recent study demonstrating that a similar FC-based platform can predict induction therapy response in a larger AML cohort.[25]

Blasts are highly sensitive to Bcl-2 inhibition whereas monocytes and granulocytes are resistant

Using the FC approach, we were able to evaluate blast-specific drug responses and compare them to other cell types within the same or between samples. Amongst the seven tested drugs, venetoclax (IC50=3.0nM) and idarubicin (IC50=28.7nM) showed the highest toxicity against blasts (Table 1). However, between these two drugs venetoclax showed the most selective efficacy against blasts when compared to other cell populations and healthy CD34+ cells (Figure 3A, IC50 values in Supplemental Figure 4). Moreover, venetoclax was also effective against CD34+CD38- cells, which suggests

activity against leukemic stem cells (Supplemental Figure 5). Compared to blasts, monocytic cells (CD14+) were resistant to Bcl-2 inhibition (P<0.001, Mann Whitney U test), but sensitive to MEK and JAK inhibition (P<0.001, Figure 3A). The phenomenon was clearly observed in samples from patients diagnosed with acute monocytic leukemia (M5) that contained substantial fractions of both cell types (Figure 3 B-C).

Overall BM AML sample sensitivity to venetoclax is associated with FAB subtype

To follow-up on our findings, we hypothesized that AML samples with high monocytic cell content should have a distinct drug response profile when overall BM-MNC sensitivity is measured with the CTG assay. We re-analyzed our earlier published CTG-based drug sensitivity data of 37 AML samples comprised of FAB M1, M2, M4 and M5 samples that were screened with 296 compounds.[14,15] Amongst the 296 compounds, venetoclax showed the largest drug sensitivity difference between M1 and M5 AML (P<0.001, Supplemental Table 4, Figure 4A). Similarly, the CTG-based sensitivity of the AML sample cohort studied here showed a gradual decrease in venetoclax sensitivity from M0 towards M5 subtype (Figure 4B). When we limited our FC analysis to diagnostic samples, a significant but smaller difference in blast-specific venetoclax sensitivity was also associated with FAB subtype (*P*<0.05, Figure 4C). This significance was not observed when we also included relapse and chemorefractory samples in the analysis (Figure 4D) largely due to a high number of chemorefractory M1/2 samples in our cohort that were more resistant to venetoclax (*P*<0.001, Figure 4 D-E). Taken together, monocytic cells blur the high blast specific venetoclax effect in Ficoll-enriched M4/5 samples when measured with CTG but FAB subtype still has a significant effect on venetoclax response in blasts in our diagnosis AML sample cohort.

FAB subtype is associated with *BCL2* and *MCL1* gene expression

Anti-apoptotic Mcl-1 and Bcl-2 are considered the most important pro-survival factors in AML.[26,27] Furthermore, their expression and phosphorylation has been shown to be regulated through the Ras/Raf/MEK/ERK, PI3K/PTEN/AKT and JAK/STAT signal transduction pathways in different leukemias.[28–31] To

study whether the expression of *BCL2* family members and activity of signal transduction pathways is associated with FAB subtypes, we analyzed gene expression data of MNCs of diagnosis AML samples using publicly available microarray and RNA-seq data. *BCL2* was highly expressed in M0/1 AML and gradually decreased towards M5 samples and healthy monocytes (Figure 5A, Supplemental Figure S6). Notably, *MCL1* showed an opposite trend in expression and was most highly expressed in healthy monocytes (Figure 5A). We also detected higher expression of *BCL2A1*, *BCL2L11* (*BIM*), *BID* and *JAK2* in M4/5 AML. A more detailed analysis of the healthy myeloid compartment revealed that *BCL2* family expression is highly dependent on differentiation stage, which likely also influences the expression patterns seen between the different FAB subtypes (Figure 5B). Interestingly, high *BCL2* and low *MCL1* expression was also observed in FAB M3 AML and their heathy counterparts, colony forming unit (CFU) granulocytes (Figure 5A and 5B). High *BCL2/MCL1* expression ratio in CFU granulocytes might explain the neutropenia seen in venetoclax treated patients.

Next, we investigated whether common cytogenetic abnormalities (*RUNX1-RUNX1T1*, *CBFB-MYH11*, *MLL*, *PML-RARA*) or mutations (*FLT3*, *NPM1*, *RUNX1*, *CEBPA*) explain some of the variation we observed in *MCL1*, *BCL2* or *BCL-xL* gene expression within FAB subgroups (Supplemental Figure 7). AML samples with *RUNX1T1-RUNX1T1* fusions showed significantly different gene expression exclusively in the M2 subgroup and samples with *MLL* or *CBFB-MYH11* fusions exclusively in the M4 subgroup (Figure 5C, Supplemental Table 5). Particularly, M4 samples with MLL fusions had high *BCL2* but low *MCL1* expression levels compared to other M4 samples. To assess whether major signal transduction pathways are differentially active in FAB subtypes, we performed gene set enrichment analysis (GSEA). The analysis revealed significant enrichment of gene sets associated with inflammatory signaling and IL6/JAK/STAT pathway in M4/5 AML (Figure 5 D-E, Supplemental Table 6).

To study whether *ex vivo* venetoclax response is associated with differentiation markers and *BCL2* family expression, we analyzed the

published Beat AML data set which includes data from 562 AML patients.[22] Supporting our previous findings, samples that had high expression of monocytic/granulocytic cell markers (CD14, CD11b, CD86, CD68) were resistant to venetoclax (Figure 5F). High *BCL2* expression was associated with venetoclax sensitivity whereas high *MCL1* and *BCL2A1* expression was associated with resistance (Figure 5F). These findings were also presented earlier by two different research groups.[32,33]

Taken together, the gene expression data of mononuclear cell enriched AML samples indicate that M4/5 AML have low *BCL2* but high *MCL1* and *BCL2A1* expression and increased inflammatory signaling. Thus, the data support the decreased venetoclax sensitivity we observe with the total mononuclear cell fraction of M4/5 samples.

MEK and JAK inhibitors sensitize venetoclax-resistant blast cells to venetoclax

Next, we studied whether mutations might explain the observed differences in blast specific venetoclax responses, but did not find significant correlation between genetic lesions and venetoclax response in our limited patient cohort (Supplemental Table 7). However, as demonstrated earlier, we detected decreased venetoclax sensitivity in chemorefractory and M5 samples (Supplemental Table 7, Figure 4 A-E). When we divided the AML samples into two subgroups (sensitive DSS 21-43, IC50<20nM and resistant DSS 0-21, IC50>20nM) from the mid-point of venetoclax response range, we noticed that resistant blasts were sensitive to either MEK and/or JAK inhibitors (Figure 6A). This finding suggests that venetoclax resistant blasts are addicted to either JAK/STAT and/or MAPK pathways. Furthermore, venetoclax sensitive blasts were enriched for *NPM1* (8/25 in sensitive vs. 1/8 in resistant) and *IDH1/2 (*10/25 in sensitive and 1/8 in resistant) mutations supporting the good clinical activity of venetoclax seen in this patient group (Figure 6A, Supplemental Table 7).

To assess the efficacy and clinical relevancy of 27 drug combinations against blasts, we used concentrations achieved in patients' plasma during treatment.

The results demonstrated prominent inter-patient variability with the most synergistic drug combinations when blast-specific drug responses were measured by FC (Supplemental Figure 8). Of the 27 tested drug combinations, venetoclax plus kinase inhibitors showed the highest average synergistic and blast killing effect (Table 2, higher BLISS score and lower mean % live blasts). Importantly, blasts were highly sensitive to single-agent venetoclax in 76% (25/33) of the samples with IC50<20nM. Thus, we did not observe synergy in the majority of the samples with a single venetoclax concentration of 50nM as this concentration alone was sufficient to kill the blasts (Figure 5A). To study the drug combination effect in more detail, we conducted additional drug testing of venetoclax with a more detailed concentration range on 4 AML samples. We observed that with lower venetoclax concentrations (10nM) a synergistic effect with MEK and/or JAK inhibitors was also detected in samples that were sensitive to single agent 50nM venetoclax treatment (Supplemental Figure 9).

Importantly, venetoclax (50nM) plus ruxolitinib (300nM) showed high efficacy (apoptosis/death>70%) and synergism in 6/8 venetoclax resistant samples (Figure 5A and 5B). Strikingly, by combining venetoclax (50nM) with trametinib (25nM), all venetoclax resistant blasts were effectively targeted (Figure 6A and 6B). Although the combinations showed substantial toxicity to healthy CD34+ cells, they targeted most effectively leukemic blasts (Figure 6B). As a comparison, a drug combination used during induction treatment (cytarabine+idarubicin) showed remarkable inter-patient differences in blast toxicity and it was also toxic to healthy CD34+ cells (Figure 6B). Furthermore, the broad-spectrum tyrosine kinase and FLT3 inhibitor sunitinib (100nM) or mTOR inhibitor everolimus (10nM) were not as effective when combined with venetoclax (Figure 6A, Table 2). Our data demonstrate that by simultaneously inhibiting JAK and/or MEK signaling and Bcl-2, blast cells involving chemorefractory AML cells, can be effectively targeted *ex vivo* in physiologically relevant concentrations.

DISCUSSION

With FC-based drug testing we were able to simultaneously measure drug sensitivities of different cell populations in primary AML BM samples. Monocytic cells abundantly present in FAB M4/5 AML were markedly resistant to Bcl-2 inhibitor venetoclax, while less differentiated blast cells in the same M4/5 samples or in M0/1/2 samples were sensitive. Accordingly, the overall BM MNC sensitivity to venetoclax was strongly influenced by FAB subtype. Our study shows that FC-based, phenotypic drug testing can improve the current understanding of *ex vivo* drug effects and may help to identify blast-specific treatments for AML patients.

Along with our previous studies, several other groups have evaluated *ex vivo* drug responses of Ficoll-enriched AML mononuclear cells using high-throughput CTG or MTS based cell viability assays.[14,34–36] While these assays provide fast and robust readouts they fail to accurately measure blast specific drug responses. By using more accurate microscopy based screening, Snijder et al. recently demonstrated that blast specific or relative blast fraction-based readouts increase predictive accuracy to treatment outcome.[37] Similarly, Martinéz-Cuadrón et al. showed that a FC-based platform measuring blast specific effect in whole BM without MNC enrichment, predicted clinical response to induction therapy.[25] We also showed earlier that in chronic myeloid leukemia, CD34-depleted cells (mature granulopoietic cells) were insensitive to BCR-ABL-1 inhibitors *ex vivo* whereas CD34+ progenitor cells showed good sensitivity.[38] In accordance, we demonstrate here with a FC-based approach that blasts differ in their drug sensitivities in comparison to other cell populations in the same AML samples. The highest blast-specific efficacy was observed with venetoclax, whereas ruxolitinib and trametinib showed increased activity towards monocytic cells. Importantly, we demonstrate that in samples with low blast count, the overall mononuclear cell fraction sensitivity does not correlate well with the blast-specific drug sensitivity.

Consistent with our results, earlier studies have shown that primary AML samples are sensitive to venetoclax *ex vivo*.[15,39,40] Most of the studies have

used mononuclear cell fractions to assess cell viability and to measure protein and gene expression levels. We observed that mononuclear cells of M0/1 samples that mainly consisted of blasts, were sensitive to venetoclax compared to mononuclear cells of M4/5 samples when using a homogenous CTG-based cell viability assay. Earlier, high *ex vivo* sensitivity to Bcl-2 inhibition has been associated with M3 AML in a study by Niu et al., whereas Pan et al. found no associations with FAB subtypes.[39,40] Importantly, both study cohorts lacked comprehensive spectra of different subtypes, with none or only one M0/1 AML case. To support our observation, mononuclear cells of M0/1 samples had a high *BCL2/MCL1* gene expression ratio whereas M4/5 samples had a low ratio. Increased Bcl-2 protein expression has also been reported in M0/1 AML,[41] and increased Mcl-1 expression in M4/5 AML[26] of which the latter has been linked to elevated Mcl-1 expression in differentiating monocytes.[42] Accordingly, we observed high *MCL1/BCL2A1* but low *BCL2* expression in healthy monocytic and granulocytic cell populations.

By using a FC-based approach, we observed that several M5 samples contained venetoclax-sensitive blasts and a resistant monocytic cell fraction. This observation raises the question whether drug sensitivity profiling and gene/protein expression studies should focus on the immature blast cells and not the total MNC fraction especially in M4/5 samples. When we compared FC measured blast-specific venetoclax response between FAB subtypes, we observed a smaller but still significant difference between diagnosis M1 *vs.* M5 subgroups. In clinical trials, *NPM1*, *IDH1/2* and *RUNX1* mutations have shown to be promising biomarkers for venetoclax+HMA treatment.[7,43] Based on a study analyzing genotype and FAB subtype-specific patterns of 4373 adult *de novo* AML cases[44], both *IDH1/2* and *RUNX1* mutations are enriched in M0/1/2 AML whereas *NPM1* mutations are common in FAB M1/2/4/5 subtypes. Therefore, patient cohorts with mutated *IDH1/2* or *RUNX1* may be skewed to contain larger numbers of FAB M0/1/2 samples. To identify responders, it might be useful to evaluate the combined genetic and cell phenotype/FAB subtype information in a clinical setting.

With the FC method we also looked for effective combinations, since only 19% overall response rate was observed with venetoclax monotherapy in patients with high-risk relapsed/refractory (R/R) AML.[6] In our study, all venetoclax-resistant blasts showed sensitivity to MEK and/or JAK inhibitors suggesting that JAK/STAT and MAPK pathways play a major role in venetoclax resistance. We showed earlier that stromal cell secreted cytokines such as GM-CSF mediate resistance to venetoclax, which can be counteracted by JAK inhibition.[45] Moreover, the MAPK pathway plays a critical role in resistance through the proposed upregulation of *MCL1.*[28] Both of these studies also demonstrated remarkable antileukemic activity in murine xenograft models when inhibiting JAK or MEK kinases together with Bcl-2. In agreement with the good synergism between ruxolitinib or trametinib with venetoclax observed here and in a recent study by the Beat AML study group,[46] Kurtz et al. additionally showed that several different kinase inhibitors exhibited good synergism with venetoclax in AML samples.[47] However, a recent clinical study with MEK inhibitor cobimetinib and venetoclax in R/R AML was closed due to limited clinical activity demonstrating that *ex vivo* drug screening results might not directly translate into clinical setting.[48]

Inflammatory pathways are more active in M4/5 AML based on gene set enrichment analysis (GSEA), consistent with the observed high sensitivity of monocytic cells to ruxolitinib and trametinib. Earlier studies have demonstrated that leukemic cells of patients with M4/5 AML produce IL1/IL6[13] and have higher proliferative activity in cytokine-free medium.[49] Thus, secreted cytokines and culturing conditions may have a big role on the drug sensitivity profiles. While further investigation is warranted, results suggest that the JAK/STAT and MEK pathways are more active in differentiated monocytic cells as well as venetoclax resistant blasts.

In summary, we show that *ex vivo* sensitivity of AML patient samples to venetoclax is associated with cell composition. Furthermore, we demonstrate that FC-based drug screening could be implemented to identify effective targeted drugs and drug combinations against immature blasts, accelerating drug discovery and individualizing therapy for AML patients.

AUTHOR CONTRIBUTIONS

HK and AML designed the study, performed the experiments and wrote the manuscript. PP, OD, MH and AK performed gene expression and pathway analysis studies. MK, OB, BTG and HE collected clinical information and provided samples. OD and MK analyzed the data and performed critical revision of the manuscript. DD performed wet lab experiments. BY calculated the drug sensitivity and combination scores. CAH, SM and KP conceived the study, edited the manuscript and supervised the work. All the authors contributed to the writing and approved the final manuscript.

CONFLICT OF INTEREST

CAH has received research funding from Celgene, Novartis, Oncopeptides, Orion Pharma and Pfizer (unrelated to this project). SM has received honoraria and research funding from Novartis, Pfizer and Bristol-Myers Squibb and research funding from Ariad (unrelated to this project). KP has received research funding from Bristol-Myers Squibb, Pfizer, Novartis and Celgene (unrelated to this project).

REFERENCES

1. Tauro S. The blind men and the AML elephant: can we feel the progress? Blood Cancer J. 2016;6(5):e424.
2. Döhner H, Weisdorf DJ, Bloomfield CD. Acute Myeloid Leukemia. N Engl J Med. 2015;373(12):1136–1152.
3. Stone RM, Mandrekar SJ, Sanford BL, et al. Midostaurin plus Chemotherapy for Acute Myeloid Leukemia with a *FLT3* Mutation. N Engl J Med. 2017;377(5):454–464.
4. DiNardo CD, Stein EM, de Botton S, et al. Durable Remissions with Ivosidenib in *IDH1* -Mutated Relapsed or Refractory AML. N Engl J Med. 2018;378(25):2386–2398.
5. Stein EM, DiNardo CD, Pollyea DA, et al. Enasidenib in mutantIDH2relapsed or refractory acute myeloid leukemia. Blood. 2017;130(6):722–731.
6. Konopleva M, Pollyea DA, Potluri J, et al. Efficacy and Biological Correlates of Response in a Phase II Study of Venetoclax Monotherapy in Patients with Acute Myelogenous Leukemia. Cancer Discov. 2016;6(10):1106–1117.
7. DiNardo CD, Pratz K, Pullarkat V, et al. Venetoclax combined with decitabine or azacitidine in treatment-naive, elderly patients with acute myeloid leukemia. Blood. 2019;133(1):7-17.
8. Bennett JM, Catovsky D, Daniel MT, et al. Proposals for the classification of the acute leukaemias. French-American-British (FAB) co-operative group. Br J Haematol. 1976;33(4):451–458.
9. Bonnet D, Dick JE. Human acute myeloid leukemia is organized as a hierarchy that originates from a primitive hematopoietic cell. Nat Med. 1997;3(7):730–737.
10. Riss TL, Moravec RA, Niles AL, et al. Cell Viability Assays. Eli Lilly & Company and the National Center for Advancing Translational Sciences.
11. Panoskaltsis N, Reid CDL, Knight SC. Quantification and cytokine production of circulating lymphoid and myeloid cells in acute myelogenous leukaemia1. Leukemia. 2003;17(4):716–730.
12. Carey A, Edwards DK, Eide CA, et al. Identification of Interleukin-1 by Functional Screening as a Key Mediator of Cellular Expansion and Disease Progression in Acute Myeloid Leukemia. Cell Rep. 2017;18(13):3204–3218.
13. van der Schoot C, Jansen P, Poorter M, et al. Interleukin-6 and interleukin-1

production in acute leukemia with monocytoid differentiation. Blood. 1989;74(6):2081-2087.

14. Pemovska T, Kontro M, Yadav B, et al. Individualized systems medicine strategy to tailor treatments for patients with chemorefractory acute myeloid leukemia. Cancer Discov. 2013;3(12):1416–1429.
15. Kontro M, Kumar A, Majumder MM, et al. HOX gene expression predicts response to BCL-2 inhibition in acute myeloid leukemia. Leukemia. 2017;31(2):301–309.
16. Yadav B, Pemovska T, Szwajda A, et al. Quantitative scoring of differential drug sensitivity for individually optimized anticancer therapies. Sci Rep. 2014;4:5193.
17. BLISS CI. THE TOXICITY OF POISONS APPLIED JOINTLY1. Ann Appl Biol. 1939;26(3):585–615.
18. Zhao W, Sachsenmeier K, Zhang L, Sult E, Hollingsworth RE, Yang H. A New Bliss Independence Model to Analyze Drug Combination Data. J Biomol Screen. 2014;19(5):817–821.
19. Pölönen P, Mehtonen J, Lin J, et al. Hemap: An interactive online resource for characterizing molecular phenotypes across hematologic malignancies. Cancer Res. 2019;79(10):2466-2479.
20. Mehtonen J, Pölönen P, Häyrynen S, et al. Data-driven characterization of molecular phenotypes across heterogeneous sample collections. Nucleic Acids Res [Epub ahead of print].
21. Network TCGAR. Genomic and Epigenomic Landscapes of Adult De Novo Acute Myeloid Leukemia. N Engl J Med. 2013;368(22):2059–2074.
22. Tyner JW, Tognon CE, Bottomly D, et al. Functional genomic landscape of acute myeloid leukaemia. Nature. 2018;562(7728):526–531.
23. Novershtern N, Subramanian A, Lawton LN, et al. Densely Interconnected Transcriptional Circuits Control Cell States in Human Hematopoiesis. Cell. 2011;144(2):296–309.
24. Salem M, Delwel R, Mahmoud LA, Clark S, Elbasousy EM, Löwenberg B. Maturation of human acute myeloid leukaemia in vitro: the response to five recombinant haematopoietic factors in a serum-free system. Br J Haematol. 1989;71(3):363–370.
25. Martínez-Cuadrón D, Gil C, Serrano J, et al. A precision medicine test predicts

clinical response after idarubicin and cytarabine induction therapy in AML patients. Leuk Res. 2019;76:1–10.

26. Teh T-C, Nguyen N-Y, Moujalled DM, et al. Enhancing venetoclax activity in acute myeloid leukemia by co-targeting MCL1. Leukemia. 2018;32(2):303-312.
27. Glaser SP, Lee EF, Trounson E, et al. Anti-apoptotic Mcl-1 is essential for the development and sustained growth of acute myeloid leukemia. Genes Dev. 2012;26(2):120–125.
28. Konopleva M, Milella M, Ruvolo P, et al. MEK inhibition enhances ABT-737-induced leukemia cell apoptosis via prevention of ERK-activated MCL-1 induction and modulation of MCL-1/BIM complex. Leukemia. 2012;26(4):778–787.
29. Wang JM, Chao JR, Chen W, Kuo ML, Yen JJ, Yang-Yen HF. The antiapoptotic gene mcl-1 is up-regulated by the phosphatidylinositol 3-kinase/Akt signaling pathway through a transcription factor complex containing CREB. Mol Cell Biol. 1999;19(9):6195–206.
30. Shenoy AR, Kirschnek S, Häcker G. IL-15 regulates Bcl-2 family members Bim and Mcl-1 through JAK/STAT and PI3K/AKT pathways in T cells. Eur J Immunol. 2014;44(8):2500–2507.
31. Faderl S, Harris D, Van Q, Kantarjian HM, Talpaz M, Estrov Z. Granulocyte-macrophage colony-stimulating factor (GM-CSF) induces antiapoptotic and proapoptotic signals in acute myeloid leukemia. Blood. 2003;102(2):630–637.
32. Zhang H, Wilmot B, Bottomly D, et al. Biomarkers Predicting Venetoclax Sensitivity and Strategies for Venetoclax Combination Treatment. Blood. 2018;132(Suppl 1):175.
33. White BS, Khan SA, Ammad-ud-din M, et al. Comparative Analysis of Independent Ex Vivo functional Drug Screens Identifies Predictive Biomarkers of BCL-2 Inhibitor Response in AML. Blood. 2018;132(Suppl 1):2763.
34. Tyner JW, Yang WF, Bankhead A, et al. Kinase Pathway Dependence in Primary Human Leukemias Determined by Rapid Inhibitor Screening. Cancer Res. 2013;73(1):285-296.
35. Dietrich S, Oleś M, Lu J, et al. Drug-perturbation-based stratification of blood cancer. J Clin Invest. 2018;128(1):427–445.
36. Swords RT, Azzam D, Al-Ali H, et al. Ex-vivo sensitivity profiling to guide clinical decision making in acute myeloid leukemia: A pilot study. Leuk Res.

2018;64:34–41.
37. Snijder B, Vladimer GI, Krall N, et al. Image-based ex-vivo drug screening for patients with aggressive haematological malignancies: interim results from a single-arm, open-label, pilot study. Lancet Haematol. 2017;4(12):e595–e606.
38. Pietarinen PO, Eide CA, Ayuda-Durán P, et al. Differentiation status of primary chronic myeloid leukemia cells affects sensitivity to BCR-ABL1 inhibitors. Oncotarget. 2017;8(14):22606–22615.
39. Niu X, Wang G, Wang Y, et al. Acute myeloid leukemia cells harboring MLL fusion genes or with the acute promyelocytic leukemia phenotype are sensitive to the Bcl-2-selective inhibitor ABT-199. Leukemia. 2014;28(7):1557–1560.
40. Pan R, Hogdal LJ, Benito JM, et al. Selective BCL-2 Inhibition by ABT-199 Causes On-Target Cell Death in Acute Myeloid Leukemia. Cancer Discov. 2014;4(3):362–375.
41. Bogenberger JM, Kornblau SM, Pierceall WE, et al. BCL-2 family proteins as 5-Azacytidine-sensitizing targets and determinants of response in myeloid malignancies. Leukemia. 2014;28(8):1657–1665.
42. Yang T, Kozopas KM, Craig RW. The intracellular distribution and pattern of expression of Mcl-1 overlap with, but are not identical to, those of Bcl-2. J Cell Biol. 1995;128(6):1173–1184.
43. DiNardo CD, Rausch CR, Benton C, et al. Clinical experience with the BCL2-inhibitor venetoclax in combination therapy for relapsed and refractory acute myeloid leukemia and related myeloid malignancies. Am J Hematol. 2018;93(3):401-407.
44. Rose D, Haferlach T, Schnittger S, Perglerová K, Kern W, Haferlach C. Subtype-specific patterns of molecular mutations in acute myeloid leukemia. Leukemia. 2017;31(1):11–17.
45. Karjalainen R, Pemovska T, Popa M, et al. JAK1/2 and BCL2 inhibitors synergize to counteract bone marrow stromal cell–induced protection of AML. Blood. 2017;130(6):789–802.
46. Kurtz SE, Eide CA, Kaempf A, et al. Dual inhibition of JAK1/2 kinases and BCL2: a promising therapeutic strategy for acute myeloid leukemia. Leukemia. 2018;32(9):2025–2028.
47. Kurtz SE, Eide CA, Kaempf A, et al. Molecularly targeted drug combinations demonstrate selective effectiveness for myeloid- and lymphoid-derived

hematologic malignancies. Proc Natl Acad Sci U S A. 2017;114(36):E7554–E7563.

48. Daver N, Pollyea DA, Yee KWL, et al. Preliminary Results from a Phase Ib Study Evaluating BCL-2 Inhibitor Venetoclax in Combination with MEK Inhibitor Cobimetinib or MDM2 Inhibitor Idasanutlin in Patients with Relapsed or Refractory (R/R) AML. Blood. 2017;130(Suppl 1):813.
49. Lowenberg B, van Putten W, Touw IP, Delwel R, Santini V. Autonomous Proliferation of Leukemic Cells in Vitro as a Determinant of Prognosis in Adult Acute Myeloid Leukemia. N Engl J Med. 1993;328(9):614–619.

Table 1: Median drug sensitivity score (DSS) and IC50 values of the seven tested drugs against different cell populations

	Blasts (n=33)		**Monocytes (n=18)**		**Lymphocytes (n=31)**		**Granulocytes (n=5)**	
	DSS	**IC50 (nM)**	**DSS**	**IC50 (nM)**	**DSS**	**IC50 (nM)**	**DSS**	**IC50 (nM)**
	Median (Range)	**Median (Range)**	**Median (Range)**	**Median (Range)**	**Median (Range)**	**Median (Range)**	**Median (Range)**	**Median (Range)**
Venetoclax	**27.1** (0-43)	**3.0** (1-1000)	**7.1** (0-29)	**122.0** (1-1000)	**18.1** (9-30)	**20.3** (2-84)	**5.7** (0.3-9)	**113** (11-220)
Idarubicin	**22.0** (0-40.0)	**28.7** (2-212)	**16.1** (6-34)	**78.7** (13-390)	**16.5** (9-28)	**84.0** (18-227)	**19.0** (12-24)	**41.1** (26-154)
Cytarabine	**9.7** (0-36)	**894.2** (50-10000)	**7.5** (0-23)	**1071** (20-10000)	**4.8** (0-10)	**2550** (43-10000)	**9.5** (4-19)	**953** (305-1189)
Ruxolitinib	**5.0** (0-32)	**302.7** (50-3000)	**17.2** (0-37)	**93.3** (60-2896)	**0** (0-8)	**2511** (99-10000)	**0** (0.0-7)	**2476** (246-3 000)
Trametinib	**3.0** (0-27)	**18.9** (1-250)	**25.9** (0-42)	**2.4** (1-250)	**0** (0-1)	**> 250** (7-250)	**1.1** (0.0-7)	**165** (15-250)
Sunitinib	**1.0** (0-17)	**321.1** (8-1000)	**5.7** (3-22)	**223.7** (71-423)	**0** (0-4)	**> 1000** (6-492)	**4.4** (1-11)	**352** (92-434)
Everolimus	**0.0** (0-19)	**55.6** (1-100)	**4.6** (0-28)	**7.5** (3-28)	**0** (0-10)	**> 100** (2.5-100)	**0** (0.0-3)	**> 100** (33-100)

Table 2: Drug combination synergism and combination sensitivity in blasts

#	Drug I	Drug II	Drug III	Mean BLISS score*	Mean % of live blasts**
1	Venetoclax 50nM	Trametinib 25nM		0.083	11.3
2	Cytarabine 300nM	Trametinib 25nM		0.076	56.7
3	Trametinib 25nM	Everolimus 10nM		0.075	62.9
4	Venetoclax 50nM	Ruxolitinib 300nM		0.068	13.4
5	Idarubicin 10nM	Trametinib 25nM		0.057	51.3
6	Trametinib 25nM	Ruxolitinib 300nM		0.046	59.7
7	Venetoclax 50nM	Everolimus 10nM		0.040	18.6
8	Sunitinib 100nM	Trametinib 25nM		0.034	69.0
9	Venetoclax 50nM	Sunitinib 100nM		0.030	21.8
10	Idarubicin 10nM	Ruxolitinib 300nM		0.029	61.8
11	Venetoclax 50nM	Cytarabine 300nM		0.023	19.6
12	Sunitinib 100nM	Ruxolitinib 300nM		-0.004	73.3
13	Sunitinib 100nM	Everolimus 10nM		-0.001	80.8
14	Everolimus 10nM	Ruxolitinib 300nM		-0.018	73.9
15	Cytarabine 300nM	Sunitinib 100nM		-0.020	75.9
16	Idarubicin 10nM	Cytarabine 300nM		-0.026	64.9
17	Idarubicin 30nM	Cytarabine 1000nM		-0.029	40.1
18	Idarubicin 10nM	Everolimus 10nM		-0.038	69.5
19	Cytarabine 300nM	Everolimus 10nM		-0.046	80.1
20	Everolimus 10nM	Ruxolitinib 300nM	Trametinib 25nM	-0.051	52.4
21	Cytarabine 300nM	Ruxolitinib 300nM		-0.058	72.2
22	Sunitinib 100nM	Everolimus 10nM	Ruxolitinib 300nM	-0.067	63.8
23	Idarubicin 10nM	Ruxolitinib 300nM	Trametinib 25nM	-0.073	39.6
24	Idarubicin 10nM	Sunitinib 100nM		-0.088	74.7
25	Cytarabine 300nM	Ruxolitinib 300nM	Everolimus 10nM	-0.123	62.5
26	Cytarabine 300nM	Ruxolitinib 300nM	Trametinib 25nM	-0.129	54.4
27	Idarubicin 10nM	Ruxolitinib 300nM	Everolimus 10nM	-0.146	57.3

**Synergism calculated using BLISS score **Normalized to DMSO treated cells*

FIGURE LEGENDS

Figure 1. Study outline and gating strategy. (A) Schematic outline of the experimental setup. **(B)** Gating strategy of cell populations. Dead and apoptotic cells were stained with 7-AAD and Annexin V, respectively, and cells negative to these markers were gated as live cells. CD45dim/SSClow and CD34+ population was used as the standard gate for AML blast cells. For samples with blast cells negative for CD34, CD45dim/SSClow and CD33 positivity was used to identify blasts. Lymphocytes were gated based on CD45bright/SSClow and were confirmed to be CD33 negative. Immature granulocytes (present after Ficoll gradient centrifugation) were gated based on CD45dim/SSChigh, CD33+ and CD34-. Monocytes were identified based on CD14 positivity. Clinical immunophenotype data were obtained for all samples to validate the gated cell populations. The illustration shows patient sample 6323 at day 0. **(C)** Illustration of the immunophenotypic profiles of AML samples with different FAB subtypes and healthy bone marrow (BM) samples represented by CD45 *vs*. SSC plots at day 0.

Figure 2. Comparison of flow cytometric (FC) and CellTiter-Glo (CTG) based drug screening approaches. (A) Spearman's correlation between CTG and FC-based cell viability assays with CD45+ leukocytes as the FC readout, or **(B)** blasts in samples with clinical blast count >50%, or **(C)** blasts in samples with clinical blast count <50% as the FC readout. **(D)** Representative FC scatter plots of drug effects on different cell populations in AML sample 18 with low blast count (20%). Absolute cell counts inside the gates were calculated after 72h drug treatment and normalized to the cell counts in the DMSO-treated wells (represented as percentages). **(E)** Venetoclax dose response curves of different cell populations present in AML sample 18 assessed by FC and overall BM sensitivity with the CTG-based cell viability assay. **(F)** Representative FC scatter plots of drug effects on patient sample 5806 with acute monocytic leukemia (FAB M5). **(G)** Dose response curves of different cell populations after MEK inhibitor trametinib treatment calculated with FC or overall sensitivity calculated with CTG. **(H)** Comparison of the DSS values for idarubicin, cytarabine and idarubicin+cytarabine combination in blasts between induction treatment resistant and sensitive

patient samples using FC. **(I)** DSS measured with CTG from the same cohort. *P*-values calculated with Mann-Whitney U test.

Figure 3. Maturation stage of AML cells affects drug sensitivities. (A) DSS values for distinct cell populations in 33 AML samples (blue) and 2-3 healthy controls (orange). Cell population means were compared against blasts with Kruskal-Wallis test (Dunn's test, *P<0.05, **P<0.001, ***P<0.0001). HSPC=healthy hematopoietic stem/progenitor cells. **(B)** Representative FC scatter plots of the effects of venetoclax and trametinib on blasts, monocytic cells (CD14+) and lymphocytes after 72h drug treatment with the indicated concentrations. Absolute cell counts inside the gates were calculated after drug treatment and normalized to the cell counts in the DMSO-treatment wells (represented as percentages). **(C)** Inter- and intra-patient comparison of the DSS values in blasts and monocytic cell fraction calculated with Mann-Whitney U test.

Figure 4. Mononuclear cell (MNC) fraction sensitivity to venetoclax is dependent on FAB subtypes. (A) Venetoclax DSS values of AML samples with different FAB subtypes from an earlier published data set, and **(B)** from the present data set both measuring MNC fraction sensitivity with CTG based cell viability assay. **(C)** Blast-specific venetoclax sensitivity of diagnosis samples in FAB subgroups measured by FC from the present data set. **(D)** Blast-specific venetoclax sensitivity in different FAB subgroups measured by FC including chemorefractory and relapse samples. **(E)** Comparison of venetoclax DSS values between diagnosis, relapse and chemorefractory samples (induction resistant n=3, azacytidine resistant n=2). Black lines represent the mean of each subgroup. P-values calculated with the Kruskal-Wallis (and Dunn's) tests.

Figure 5. Cell differentiation is associated with low *BCL2* expression and venetoclax *ex vivo* resistance. (A) Heatmap of the median gene expression for each FAB class and control samples are shown for *BCL2* family genes in the Hemap AML data set. Sample groups are ordered based on the differentiation state between HSCs (hematopoietic stem cells) and healthy

monocytes. Z-scores were used to define high and low expression categories. Z-scores were further discretized to low and high categories, defined as having Z-score cutoff over 2 for high and less than -2 for low expression. P-values for FAB subgroup comparisons are presented in Supplemental Table 5. Similar analysis for TCGA data set is presented in Supplemental Figure 6. **(B)** Heatmap of the median gene expression of *BCL2* family genes for healthy hematopoietic cell types using Differentiation Map data set. **(C)** Significant *BCL2*, *MCL1* or *BCL-xL* gene expression differences between samples with *MLL*, *CBFB-MYH11* or *RUNX1-RUNX1T1* fusion genes when compared to non-fusion gene containing samples in FAB M2 and M4 groups. Values obtained from the Hemap data set. * P-value<0.05, ** P-value<0.001. **(D)** Pathway enrichment results with normalized enrichment scores (NES) and significance as FDR q-value are shown for pathways upregulated in M4 and M5 samples when compared to M0 and M1 samples. Pathways consistently enriched in both Hemap and TCGA data sets are shown here, while full results are shown in Supplemental Table 6. **(E)** Heatmap of IL6-JAK-STAT3 signaling pathway leading edge gene expression Z-scores using the Hemap data set. Z-scores were further discretized to low and high categories, defined as having Z-score cutoff over 2 for high and less than -2 for low expression. Samples are ordered based on FAB type. **(F)** Venetoclax drug response AUC and IC50 profiles, *BCL2* family genes and differentiation marker gene expression value Z-scores and FAB subtypes are shown as a heatmap. Samples are ordered based on drug sensitivity with sensitive samples on the left and resistant on the right. Pearson correlation Rho and FDR value is shown for each gene.

Figure 6. Inhibition of MEK and JAK pathways can overcome venetoclax resistance. (A) Heatmap showing characteristics of venetoclax sensitive (IC50<20nM, DSS>20) and resistant blasts (IC50>50nM, DSS<20) based on single agent venetoclax response measured by FC (top row). Blast-specific response of individual drugs is highlighted according to DSS values with red corresponding to high DSS value and blue to low DSS value. Blast-specific response to venetoclax combinations is highlighted according to percentage of apoptotic/dead cells with red corresponding to high percentage and blue to

low percentage of apoptotic/dead cells. The synergistic effect of the drug combination was assessed based on the BLISS synergistic score and is shown in the graph. Other characteristics covered include disease stage, molecular profiling, FAB subtype with M4 and M5 highlighted blue and FC-determined blast percentage. Overall BM venetoclax sensitivity measured with CTG (bottom row) is used to demonstrate how low blast cell percentage affects DSS values when compared to blast-specific DSS values. D=Diagnosis, R=Relapse, Rf=Refractory, CL=CMML transitioned to AML. **(B)** Dot scatter plots of venetoclax (50nm) + ruxolitinib (300nM), venetoclax (50nM) + trametinib (25nM), and cytarabine (1000nM) + idarubicin (30nM) responses in healthy CD45+ leukocytes, granulopoietic cells, lymphocytes, monocytes and blasts. Dark blue dots represent single agent toxicity to blasts. Cell population means were compared against blasts with the Kruskal-Wallis test (Dunn's test, *P<0.05, **P<0.001, ***P<0.0001). Orange dots represent healthy BM samples and light blue dots AML samples. Dark blue dots represent the single agent activity of venetoclax/trametinib/ruxolitinib to AML blasts.

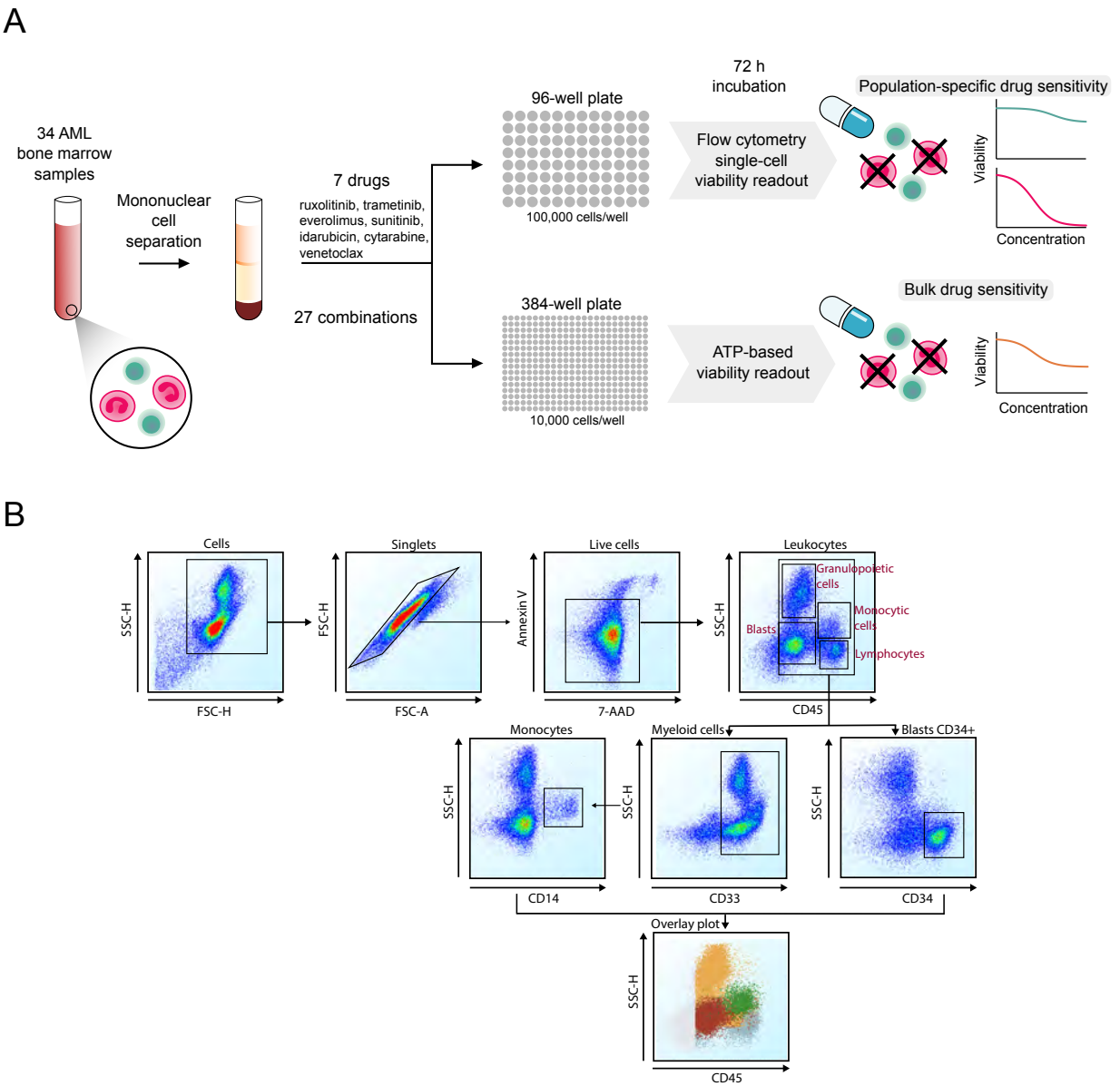
A
34 AML bone marrow samples
Mononuclear cell separation
7 drugs
ruxolitinib, trametinib, everolimus, sunitinib, idarubicin, cytarabine, venetoclax
27 combinations
96-well plate
100,000 cells/well
384-well plate
10,000 cells/well
72 h incubation
Flow cytometry single-cell viability readout
ATP-based viability readout
Population-specific drug sensitivity
Bulk drug sensitivity
Viability
Concentration
B
Cells
SSC-H
FSC-H
Singlets
FSC-H
FSC-A
Live cells
Annexin V
7-AAD
Leukocytes
SSC-H
CD45
Granulopoietic cells
Monocytic cells
Blasts
Lymphocytes
Monocytes
SSC-H
CD14
Myeloid cells
SSC-H
CD33
Blasts CD34+
SSC-H
CD34
Overlay plot
SSC-H
CD45
C
CD34+
CD33+
CD14+
CD33-/CD34-
Healthy BM (1690)
FAB M1 (6565)
FAB M5 (6525)
MDS → Multi Lin. Dysp. (3724)
SSC-H
CD45
1.
2.
3.
4.

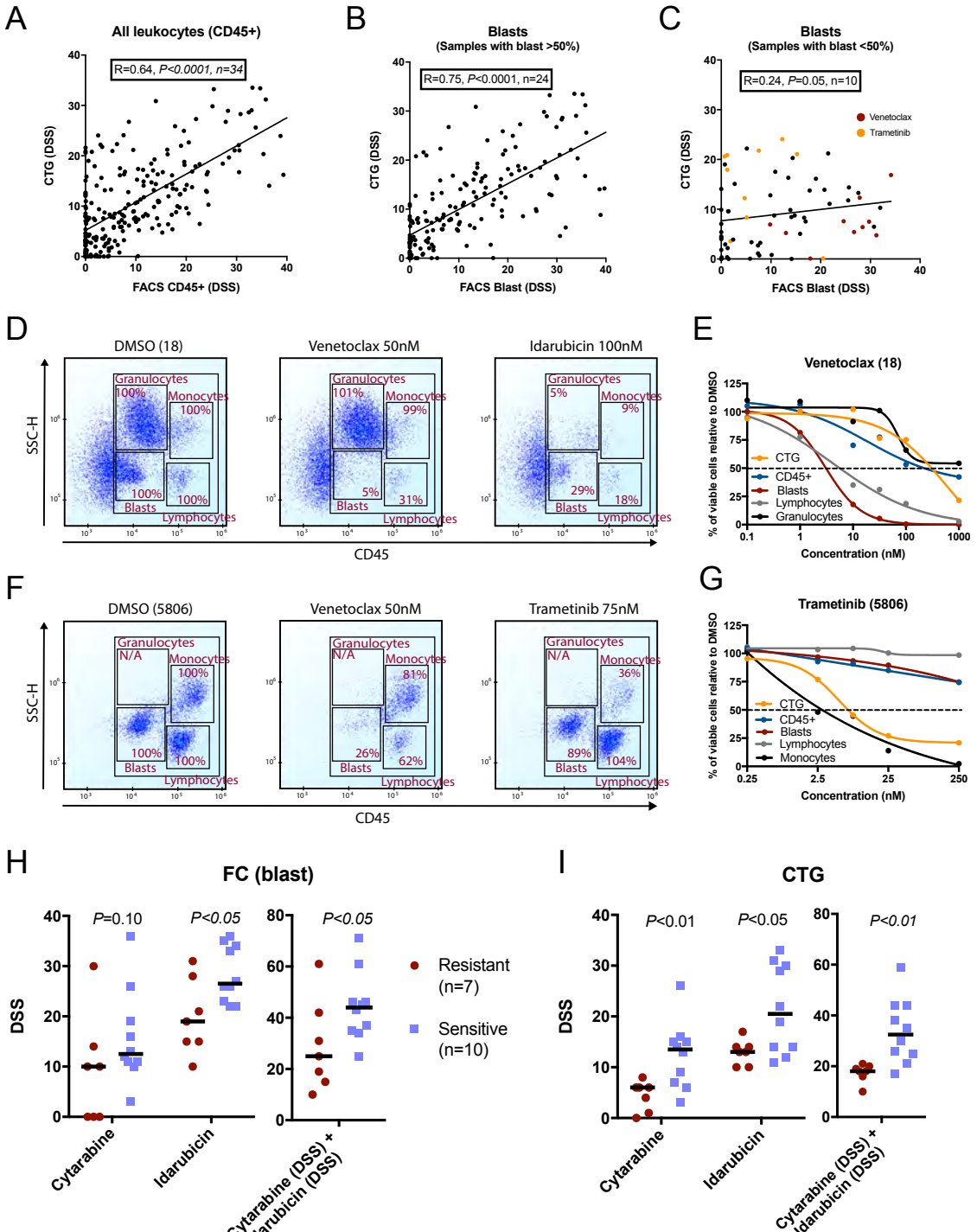
A
All leukocytes (CD45+)
R=0.64, P<0.0001, n=34
CTG (DSS)
FACS CD45+ (DSS)
B
Blasts
(Samples with blast >50%)
R=0.75, P<0.0001, n=24
CTG (DSS)
FACS Blast (DSS)
C
Blasts
(Samples with blast <50%)
R=0.24, P=0.05, n=10
Venetoclax
Trametinib
CTG (DSS)
FACS Blast (DSS)
D
DMSO (18)
Venetoclax 50nM
Idarubicin 100nM
Granulocytes
Monocytes
Blasts
Lymphocytes
100%
100%
100%
100%
101%
99%
5%
31%
5%
9%
29%
18%
SSC-H
CD45
E
Venetoclax (18)
% of viable cells relative to DMSO
CTG
CD45+
Blasts
Lymphocytes
Granulocytes
Concentration (nM)
F
DMSO (5806)
Venetoclax 50nM
Trametinib 75nM
Granulocytes
Monocytes
Blasts
Lymphocytes
N/A
100%
100%
81%
26%
62%
36%
89%
104%
SSC-H
CD45
G
Trametinib (5806)
% of viable cells relative to DMSO
CTG
CD45+
Blasts
Lymphocytes
Monocytes
Concentration (nM)
H
FC (blast)
P=0.10
P<0.05
P<0.05
DSS
Resistant (n=7)
Sensitive (n=10)
Cytarabine
Idarubicin
Cytarabine (DSS) + Idarubicin (DSS)
I
CTG
P<0.01
P<0.05
P<0.01
DSS
Cytarabine
Idarubicin
Cytarabine (DSS) + Idarubicin (DSS)

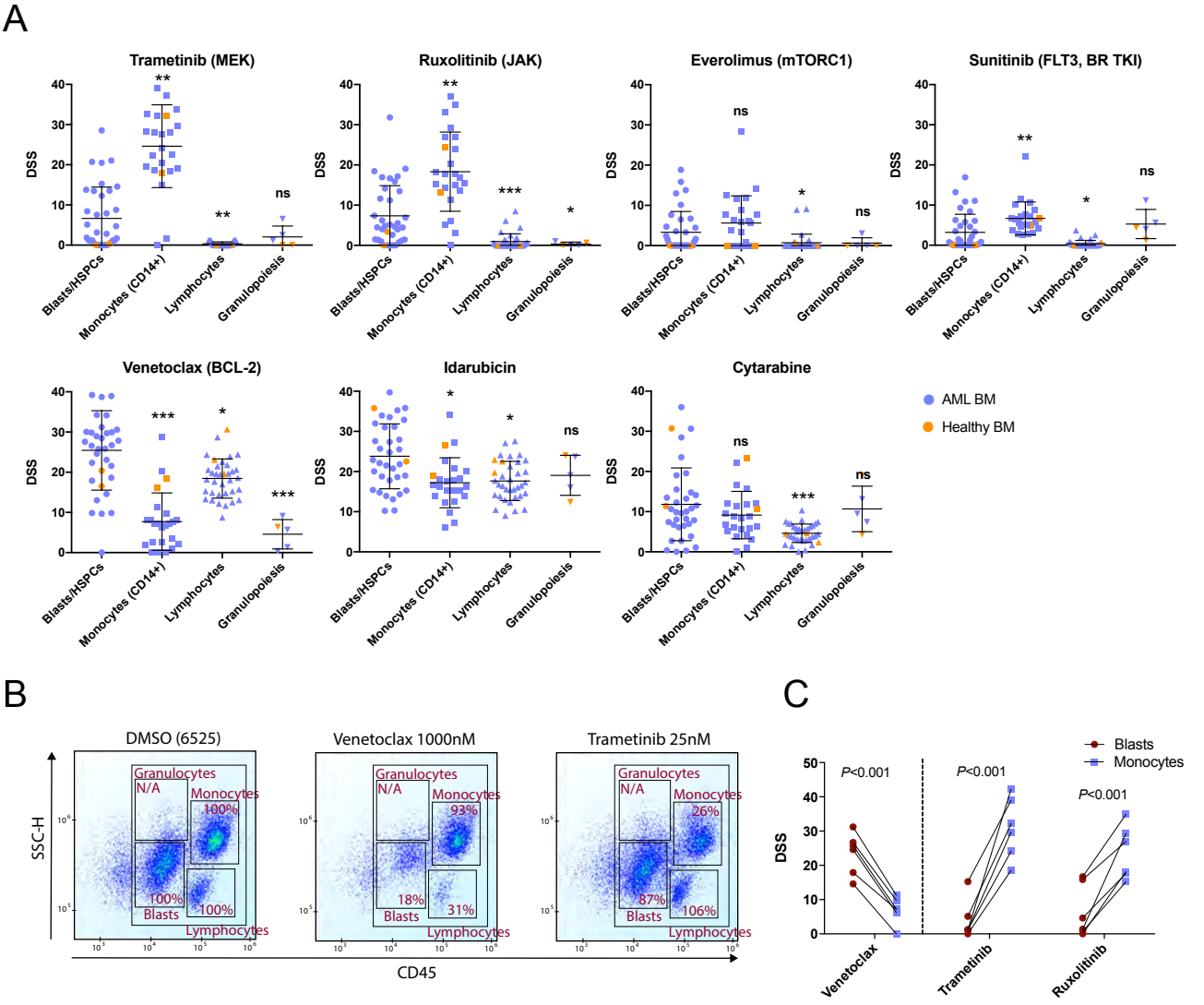
A
Trametinib (MEK)
Ruxolitinib (JAK)
Everolimus (mTORC1)
Sunitinib (FLT3, BR TKI)
Venetoclax (BCL-2)
Idarubicin
Cytarabine
DSS
Blasts/HSPCs
Monocytes (CD14+)
Lymphocytes
Granulopoiesis
AML BM
Healthy BM
B
DMSO (6525)
Venetoclax 1000nM
Trametinib 25nM
SSC-H
CD45
Granulocytes
N/A
Monocytes
100%
93%
26%
Blasts
100%
18%
87%
Lymphocytes
100%
31%
106%
C
Blasts
Monocytes
P<0.001
Venetoclax
Trametinib
Ruxolitinib

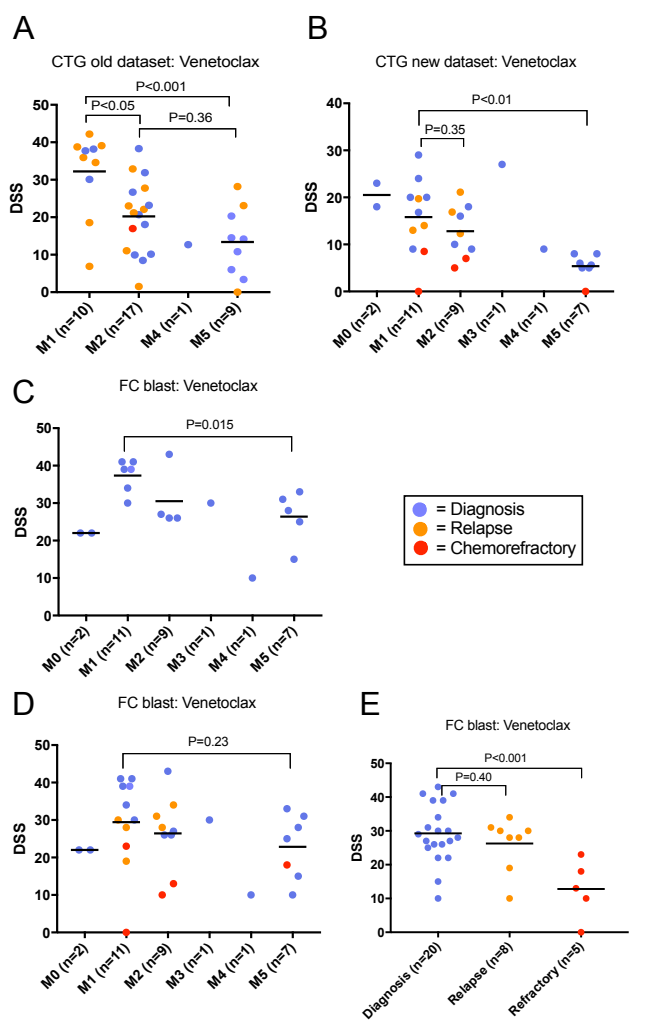
A
CTG old dataset: Venetoclax
P<0.001
P<0.05
P=0.36
DSS
M1 (n=10)
M2 (n=17)
M4 (n=1)
M5 (n=9)
B
CTG new dataset: Venetoclax
P<0.01
P=0.35
DSS
M0 (n=2)
M1 (n=11)
M2 (n=9)
M3 (n=1)
M4 (n=1)
M5 (n=7)
C
FC blast: Venetoclax
P=0.015
DSS
M0 (n=2)
M1 (n=11)
M2 (n=9)
M3 (n=1)
M4 (n=1)
M5 (n=7)
= Diagnosis
= Relapse
= Chemorefractory
D
FC blast: Venetoclax
P=0.23
DSS
M0 (n=2)
M1 (n=11)
M2 (n=9)
M3 (n=1)
M4 (n=1)
M5 (n=7)
E
FC blast: Venetoclax
P<0.001
P=0.40
DSS
Diagnosis (n=20)
Relapse (n=9)
Refractory (n=5)

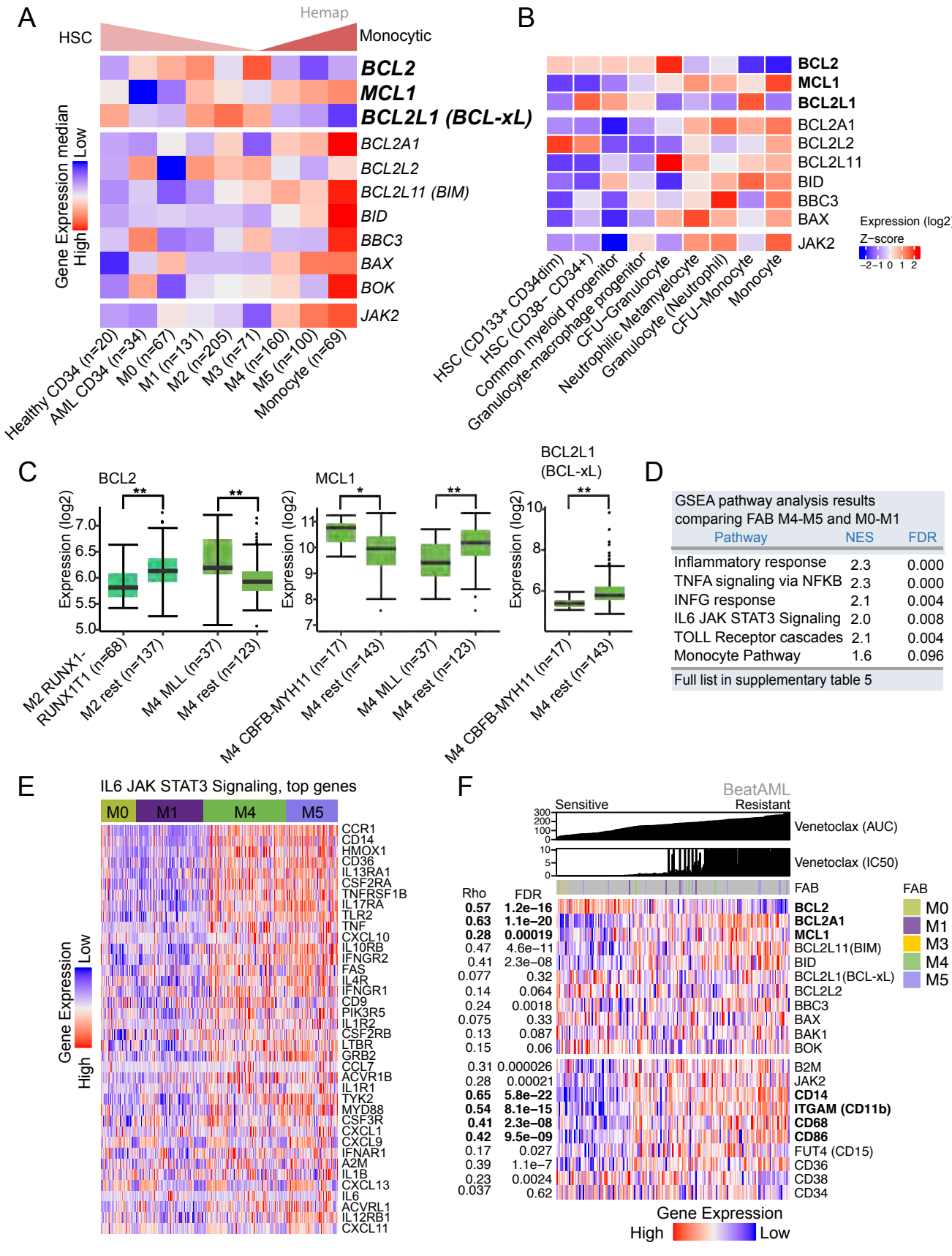
A
Hemap
HSC
Monocytic
BCL2
MCL1
BCL2L1 (BCL-xL)
BCL2A1
BCL2L2
BCL2L11 (BIM)
BID
BBC3
BAX
BOK
JAK2
Gene Expression median
Low
High
Healthy CD34 (n=20)
AML CD34 (n=34)
M0 (n=67)
M1 (n=131)
M2 (n=205)
M3 (n=71)
M4 (n=160)
M5 (n=100)
Monocyte (n=69)
B
BCL2
MCL1
BCL2L1
BCL2A1
BCL2L2
BCL2L11
BID
BBC3
BAX
JAK2
Expression (log2)
Z−score
−2 −1 0 1 2
HSC (CD133+ CD34dim)
HSC (CD38− CD34+)
Common myeloid progenitor
Granulocyte-macrophage progenitor
CFU−Granulocyte
Neutrophilic Metamyelocyte
Granulocyte (Neutrophil)
CFU−Monocyte
Monocyte
C
BCL2
MCL1
BCL2L1 (BCL-xL)
Expression (log2)
M2 RUNX1-RUNX1T1 (n=68)
M2 rest (n=137)
M4 MLL (n=37)
M4 rest (n=123)
M4 CBFB-MYH11 (n=17)
M4 rest (n=143)
M4 MLL (n=37)
M4 rest (n=123)
M4 CBFB-MYH11 (n=17)
M4 rest (n=143)
D
GSEA pathway analysis results comparing FAB M4-M5 and M0-M1
Pathway | NES | FDR
Inflammatory response | 2.3 | 0.000
TNFA signaling via NFKB | 2.3 | 0.000
INFG response | 2.1 | 0.004
IL6 JAK STAT3 Signaling | 2.0 | 0.008
TOLL Receptor cascades | 2.1 | 0.004
Monocyte Pathway | 1.6 | 0.096
Full list in supplementary table 5
E
IL6 JAK STAT3 Signaling, top genes
M0
M1
M4
M5
Gene Expression
Low
High
CCR1
CD14
HMOX1
CD36
IL13RA1
CSF2RA
TNFRSF1B
IL17RA
TLR2
TNF
CXCL10
IL10RB
IFNGR2
FAS
IL4R
IFNGR1
CD9
PIK3R5
IL1R2
CSF2RB
LTBR
GRB2
CCL7
ACVR1B
IL1R1
TYK2
MYD88
CSF3R
CXCL1
CXCL9
IFNAR1
A2M
IL1B
CXCL13
IL6
ACVRL1
IL12RB1
CXCL11
F
BeatAML
Sensitive
Resistant
Venetoclax (AUC)
Venetoclax (IC50)
FAB
Rho
FDR
0.57 1.2e−16 BCL2
0.63 1.1e−20 BCL2A1
0.28 0.00019 MCL1
0.47 4.6e−11 BCL2L11(BIM)
0.41 2.3e−08 BID
0.077 0.32 BCL2L1(BCL-xL)
0.14 0.064 BCL2L2
0.24 0.0018 BBC3
0.075 0.33 BAX
0.13 0.087 BAK1
0.15 0.06 BOK
0.31 0.000026 B2M
0.28 0.00021 JAK2
0.65 5.8e−22 CD14
0.54 8.1e−15 ITGAM (CD11b)
0.41 2.3e−08 CD68
0.42 9.5e−09 CD86
0.17 0.027 FUT4 (CD15)
0.39 1.1e−7 CD36
0.23 0.0024 CD38
0.037 0.62 CD34
FAB
M0
M1
M3
M4
M5
Gene Expression
High
Low

A

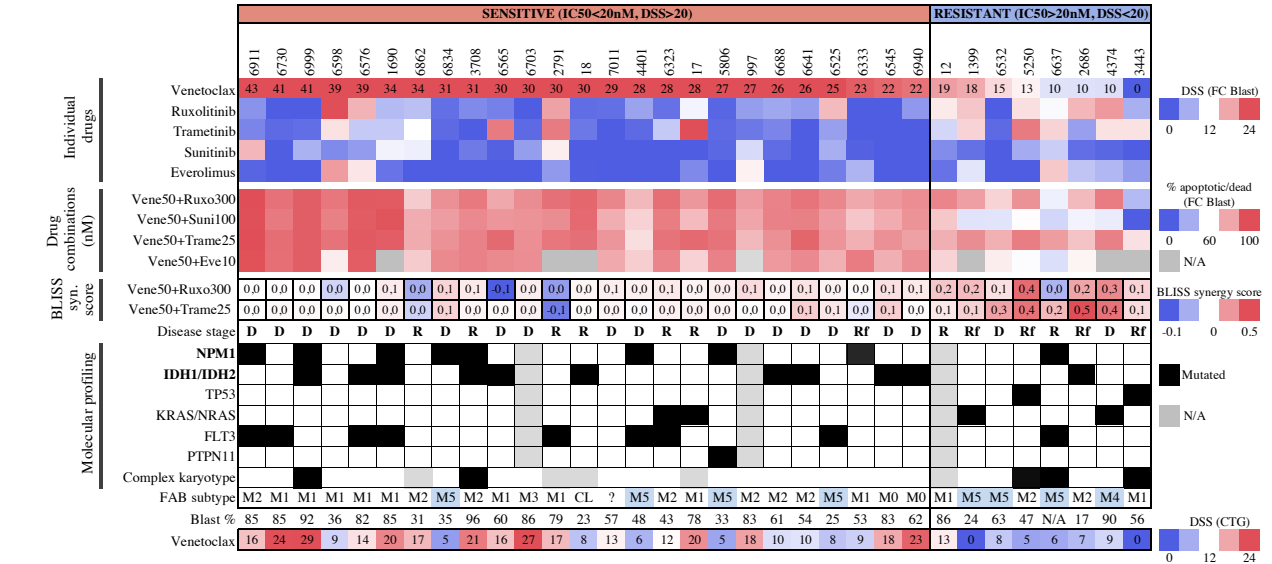
SENSITIVE (IC50<20nM, DSS>20)
RESISTANT (IC50>20nM, DSS<20)
6911 6730 6999 6598 6576 1690 6862 6834 3708 6565 6703 2791 18 7011 4401 6323 17 5806 997 6688 6641 6525 6333 6545 6940 12 1399 6532 5250 6637 2686 4374 3443
Individual drugs
Venetoclax 43 41 41 39 39 34 34 31 31 30 30 30 30 29 28 28 28 27 27 26 26 25 23 22 22 19 18 15 13 10 10 10 0
Ruxolitinib
Trametinib
Sunitinib
Everolimus
DSS (FC Blast)
0 12 24
Drug combinations (nM)
Vene50+Ruxo300
Vene50+Suni100
Vene50+Trame25
Vene50+Eve10
% apoptotic/dead (FC Blast)
0 60 100
N/A
BLISS syn. score
Vene50+Ruxo300 0,0 0,0 0,0 0,0 0,0 0,1 0,0 0,1 0,1 -0,1 0,0 0,0 0,0 0,1 0,0 0,1 0,0 0,0 0,1 0,0 0,1 0,0 0,0 0,1 0,1 0,2 0,2 0,1 0,4 0,0 0,2 0,3 0,1
Vene50+Trame25 0,0 0,0 0,0 0,0 0,0 0,0 0,0 0,1 0,0 0,0 0,0 -0,1 0,0 0,0 0,0 0,0 0,0 0,0 0,0 0,0 0,1 0,1 0,0 0,1 0,0 0,1 0,1 0,3 0,4 0,2 0,5 0,4 0,1
BLISS synergy score
-0.1 0 0.5
Disease stage D D D D D D R D R D D R R D D R R D D D D D Rf D D R Rf D Rf R Rf D Rf
Molecular profiling
NPM1
IDH1/IDH2
TP53
KRAS/NRAS
FLT3
PTPN11
Complex karyotype
Mutated
N/A
FAB subtype M2 M1 M1 M1 M1 M1 M2 M5 M2 M1 M3 M1 CL ? M5 M2 M1 M5 M2 M2 M2 M5 M1 M0 M0 M1 M5 M5 M2 M5 M2 M4 M1
Blast % 85 85 92 36 82 85 31 35 96 60 86 79 23 57 48 43 78 33 83 61 54 25 53 83 62 86 24 63 47 N/A 17 90 56
Venetoclax 16 24 29 9 14 20 17 5 21 16 27 17 8 13 6 12 20 5 18 10 10 8 9 18 23 13 0 8 5 6 7 9 0
DSS (CTG)
0 12 24

B

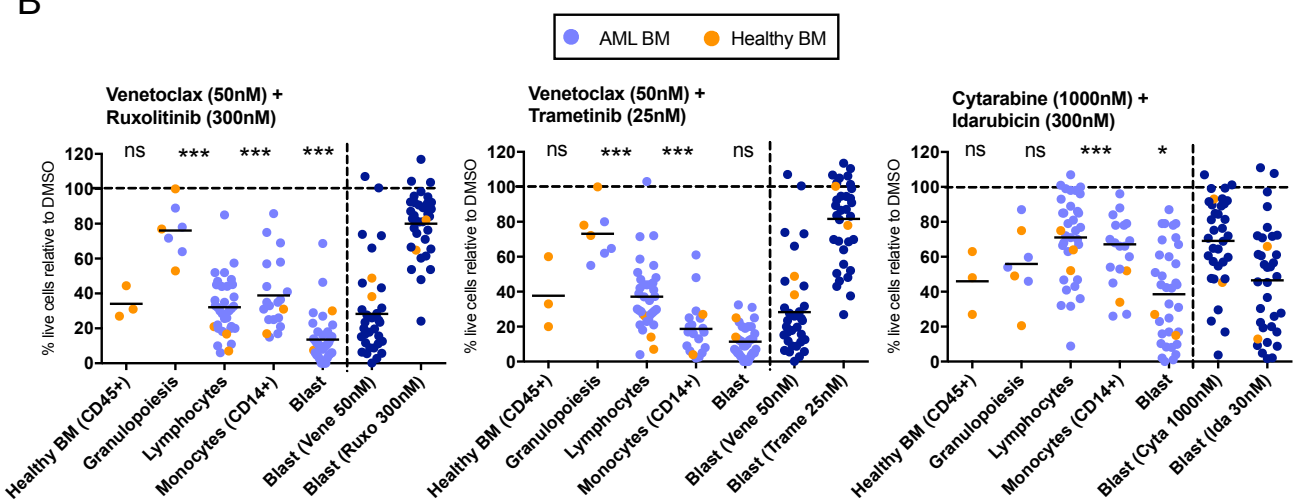
AML BM
Healthy BM
Venetoclax (50nM) + Ruxolitinib (300nM)
Venetoclax (50nM) + Trametinib (25nM)
Cytarabine (1000nM) + Idarubicin (300nM)
% live cells relative to DMSO
ns *** *** ***
ns *** *** ns
ns ns *** *
Healthy BM (CD45+)
Granulopoiesis
Lymphocytes
Monocytes (CD14+)
Blast
Blast (Vene 50nM)
Blast (Ruxo 300nM)
Blast (Trame 25nM)
Blast (Cyta 1000nM)
Blast (Ida 30nM)

Supplemental Material

Phenotype-based drug screening reveals an association between venetoclax response and differentiation stage in acute myeloid leukemia

Authors: Heikki Kuusanmäki[1, 2], Aino-Maija Leppä[1], Petri Pölönen[3], Mika Kontro[2], Olli Dufva[2], Debashish Deb[1], Bhagwan Yadav[2], Oscar Brück[2], Ashwini Kumar[1], Hele Everaus[4], Bjørn T. Gjertsen[5], Merja Heinäniemi[3], Kimmo Porkka[2], Satu Mustjoki[2,6], Caroline A. Heckman[1]

Affiliations:

[1]Institute for Molecular Medicine Finland, Helsinki Institute of Life Science, University of Helsinki, Helsinki, Finland

[2]Hematology Research Unit, Helsinki University Hospital Comprehensive Cancer Center, Helsinki, Finland

[3]Institute of Biomedicine, School of Medicine, University of Eastern Finland, Kuopio, Finland

[4]Department of Hematology and Oncology, University of Tartu, Tartu, Estonia

[5]Centre for Cancer Biomarkers, Department of Clinical Science, University of Bergen, Bergen, Norway

[6]Translational Immunology Research Program and Department of Clinical Chemistry and Hematology, University of Helsinki, Helsinki, Finland

Table of contents

Supplemental Methods

Patient samples

BM samples of 34 AML patients and three healthy volunteers were obtained from Helsinki University Hospital Comprehensive Cancer Center after informed consent (permit numbers 239/13/03/00/2010, 303/13/03/01/2011, Helsinki University Hospital Ethics Committee) and in compliance with the Declaration of Helsinki. Cytogenetic analysis was performed at hospital laboratories by fluorescence *in situ* hybridization and chromosomal banding analysis. Exome sequencing was performed as earlier described.[1] Patient characteristics are presented in Supplemental Table 1.

Preparation of drug plates

The compounds (Supplemental Table 2) were dissolved in 100% DMSO and dispensed on 96-well V-bottom plates (Thermo Fisher Scientific, Carlsbad, CA) and 384-well plates (Corning, Corning, NY) using an acoustic liquid handling device Echo 550 (Labcyte, Sunnyvale, CA). The plates contained several DMSO controls, 7 drugs (1,000-10,000-fold dilution series) and 27 drug combinations with one chosen concentration for each drug. Drug plate layouts and concentrations are presented in Supplemental Figure 1.

BM mononuclear cells (BM-MNCs) were isolated using Ficoll-Paque Premium (GE Healthcare, Little Chalfont, Buckinhamshire, UK) density gradient centrifugation. Fresh BM-MNCs were suspended in mononuclear cell medium (MCM; PromoCell, Heidelberg, Germany) supplemented with 10 µg/mL gentamicin and 2.5 µg/mL amphotericin B and plated in parallel on pre-drugged 96-well plates (100,000 cells/well in 100 µl) for FC analysis and 384-well plates (10,000 cells/well in 25 µl) for CTG-based cell viability assay. The cells were incubated with the drugs for 3 days at 37°C and 5% CO_2. Eleven of the 34 AML samples were viably frozen. Cells were treated with DNase I after thawing and after washing dispensed on the drug plates.

Flow cytometry-based readouts

Following 72h incubation with the drugs, cells were centrifuged (500xg, 6 min) in the 96-well plates and media discarded by inverting the plates. Cells were suspended in 25 µL of antibody mix containing staining buffer (10% FBS and 0.02% NaN_3 in RPMI-1640 medium) and the following antibodies: BD Biosciences (Santa Jose, CA): CD33 (BV421, clone WM53, dilution 1:600), CD45 (BV786, clone HI30, 1:50), CD34 (PE-Cy7, clone 8G12, 1:50), CD14 (APC, clone M5E2, 1:100) and Cytogonos (Salamanca, Spain): CD38 (FITC, clone LD38, 1:50). Cells were stained for 30 min at room temperature (RT) in the

dark and subsequently washed with 100 µL staining buffer followed by centrifugation (500xg, 6 min) and supernatant removal. Apoptotic and dead cells were discriminated by 7-aminoactinomycin D (7-AAD) and PE-Annexin V (BD Biosciences) staining with both dyes diluted 1:50 in 25 µL Annexin V binding buffer. The plates were incubated for 20 min at RT before FC analysis. FC analysis was performed using the iQue Screener PLUS instrument (Intellicyt, Albuquerque, NM). All media/cells were extracted from each well using 16 s sip time/well and pump speed of 32 rpm resulting in 35 min reading time for a 96-well plate. ForeCyt software (Intellicyt) was used to gate cells and acquire population counts. Analysis was done from viable CD45 positive singlet cells and the gating strategy is illustrated in manuscript Figure 1B. The cell count of a well was normalized to its 6 adjacent DMSO controls.

Data sets

Gene expression was analyzed from AML microarray data (log2 expression) from the Hemap data set (http://hemap.uta.fi/)[2,3] and TCGA RNA-seq data (RSEM values) generated by the TCGA Research Network (http://cancergenome.nih.gov/).[4] The data were generated using RNA extracted from the mononuclear cell fraction of AML patients. Beat AML RNA-seq count matrix was obtained from the authors (Tyner 2018).[5] Genes with expression > 1 cpm in more than 1 % of samples were kept and data were normalized using limma voom and quantile normalization. Beat AML *ex vivo* drug sensitivity data was obtained from Supplemental Table 41586_2018_623_MOESM3_ESM.xlsx (Tyner 2018). For analysis of gene expression in healthy hematopoietic cell types Differentiation Map data was used.[6]

Gene expression analysis

The two-tailed Wilcoxon test followed by Benjamini-Hochberg adjustment of *P*-values and fold change was computed to compare gene expression levels for *BCL2*, *BCL2L1, BCL2A1*, *MCL1*, *BCL2L2*, *BCL2L11*, *BID*, *BBC3*, *BAX*, *BAK1*, *BOK*, *B2M*, and *JAK2*. Comparisons were first done between FAB M0, M1, and M2 groups to M3, M4, and M5 groups individually for each *BCL2* family gene. Fusion gene status for *RUNX1-RUNX1T1*, *CBFB-MYH11*, *MLL*, *PML-RARA*, mutation status of *FLT3*, *NPM1*, *RUNX1*, *CEBPA*, plus complex and normal karyotype groups were next tested within each FAB group to investigate whether these events could explain some of the variance observed in *BCL2*, *BCL2L1* and *MCL1* expression levels.

For analysis of gene expression in hematopoietic cell types using Differentiation Map data,[6] log2-transformed expression values of Affymetrix HG_U133AAofAv2 probe sets

were downloaded from GEO (GSE24759). Affymetrix probe set identifiers were converted to gene symbols using biomaRt[7] and probes representing the same gene were averaged to obtain expression values for each gene. Heatmap of selected genes was plotted using Z-scores across median expression values of myeloid and stem cell populations.

Analysis of venetoclax drug sensitivity and *BCL2* family gene expression in Beat AML data set

Pearson correlation and correlation test of significance was computed for venetoclax AUC drug response values and *BCL2* family and differentiation markers CD14, CD11b, CD68, CD86, CD15, CD36, CD38, CD34 gene expression values. NA values were omitted and P-values were adjusted using the Benjamini-Hochberg method.

Pathway analysis

The command line version of GSEA[8] was used to perform gene set enrichment analysis comparing combined M0, M1 to M4, and M5 FAB group pathway profiles. Log2 expression values for Hemap and RSEM values for TCGA AML data sets were used in the analysis. Sample permutation and multiple hypotheses testing correction were used to obtain FDR q-values. Gene sets used in the analysis included KEGG, Biocarta, Hallmarks, Reactome from MsigDB v5.0, Wikipathways (06.2015) and PID V4. FDR q-values below 0.1 were defined as significant.

References

1. Pemovska T, Kontro M, Yadav B, et al. Individualized systems medicine strategy to tailor treatments for patients with chemorefractory acute myeloid leukemia. Cancer Discov 2013;3(12):1416–29.
2. Pölönen P, Mehtonen J, Lin J, et al. Hemap: An interactive online resource for characterizing molecular phenotypes across hematologic malignancies. Cancer Res 2019;canres.2970.2018.
3. Mehtonen J, Pölönen P, Häyrynen S, et al. Data-driven characterization of molecular phenotypes across heterogeneous sample collections. Nucleic Acids Res [Epub ahead of print].
4. Network TCGAR. Genomic and Epigenomic Landscapes of Adult De Novo Acute Myeloid Leukemia. N Engl J Med 2013;368(22):2059–2074.
5. Tyner JW, Tognon CE, Bottomly D, et al. Functional genomic landscape of acute myeloid leukaemia. Nature 2018;562(7728):526–531.
6. Novershtern N, Subramanian A, Lawton LN, et al. Densely Interconnected Transcriptional Circuits Control Cell States in Human Hematopoiesis. Cell 2011;144(2):296–309.
7. Durinck S, Spellman PT, Birney E, Huber W. Mapping identifiers for the integration of genomic datasets with the R/Bioconductor package biomaRt. Nat Protoc 2009;4(8):1184–91.
8. Subramanian A, Tamayo P, Mootha VK, et al. Gene set enrichment analysis: A knowledge-based approach for interpreting genome-wide expression profiles. Proc Natl Acad Sci 2005;102(43):15545–15550.

Supplemental Tables

Supplemental Table S1. Patient characteristics

#	BM or PB	Sample_ID	Fresh/Frozen	Previous malignancies or predisposing conditions	Diagnosis (ICD-O)	Risk class at the time of diagnosis	Disease state at sample collection	Time from diagnosis (months)	FAB	Cytogenetics	Mol. Genetics	Therapy at diagnosis	D0	D14	D28	Sens/ Res	FC (DSS)			CTG (DSS)		
																	Cytarabine	Idarubicin	Ida+Cyt	Cytarabine	Idarubicin	Ida+Cyt
1	BM	1399_3	Frozen	CMML	Acute monocytic leukemia	Intermediate	Refractory	2	M5	Trisomy 19	KRAS, NRAS	Cytarabine + Idarubicin	10	30	40	Res	30	31	61	6	10	16
2	BM	3443_6	Frozen	No	Acute myeloid leukemia without maturation	High	Refractory	4	M1	At diagnosis, del 17p, -2 (both), -17 (both), -5.	None	Cytarabine + Idarubicin	79	1	60	Res	0	19	19	0	10	10
3	BM	997_1	Frozen	No	Acute myeloid leukemia with maturation	Intermediate	Diagnosis	0	M2	Normal	NA	Hydroxyurea	90	NA	NA		23	33	56	18	34	52
4	PB	2791_7	Frozen	Breast cancer	Therapy-related acute myeloid leukemia	High	Relapse	15	M1	NA	FLT3-ITD	Cytarabine + Idarubicin	90	<5	1		8	28	36	8	29	37
5	BM	1690_2	Frozen	No	Acute myeloid leukemia without maturation	Intermediate	Diagnosis	0	M1	Normal	IDH2, NPM1, FLT3-ITD	Cytarabine + Idarubicin	90	<5	1	Sens	11	23	34	3	14	17
6	BM	4374_2	Frozen	No	Acute myelomonocytic leukemia	Low	Diagnosis	0	M4	Normal	DNMT3, NRAS	Cytarabine + Idarubicin	50	1	1	Sens	36	35	71	26	33	59
7	BM	18	Fresh	CMML	AML/CMML		Relapse		CMML/M1	NA	IDH2, DNMT3, ASXL1	NA	NA	NA	NA		7	18	25	3	13	16
8	BM	2686_4	Fresh	No	Acute myeloid leukemia with maturation	Intermediate	Refractory*	45	M2	Normal	IDH2	Cytarabine + Idarubicin	42	4	4		14	14	28	9	20	29
9	BM	6333_3	Frozen	NHL	Acute myeloid leukemia without maturation	Low	Refractory		M1	Normal	NPM1, TET2	Azacitidine	70	42			7	25	32	8	17	25
10	BM	5250_4	Fresh	MDS	Acute myeloid leukemia with maturation	High	Refractory		M2	46;XX;del(5q);-21;+der(21);	TP53	Azacitidine	8	7			7	14	21	1	10	11
11	BM	6532_2	Fresh	Breast cancer	Acute monocytic leukemia	Intermediate	Diagnosis	0	M5b	Normal	FGFR4, TET2	Cytarabine + Idarubicin	45		1	Sens	13	22	35	6	19	25
12	BM	6545_2	Fresh	No	Acute leukemia with mnimal differentation	Intermediate	Diagnosis	0	M0	46;XY;del(6q);del(12q);	DNMT3, IDH2	Hydroxyurea	85	NA			4	19	23	4	26	30
13	PB	17	Fresh	MDS	Acute myeloid leukemia without maturation		Relapse		M1	NA	SETBP1, NRAS, EZH2, DDX41, ASXL1	Cytarabine + Daunorubicin	NA	NA	NA		19	31	50	12	28	40
14	BM	6565_3	Fresh	Endometrium ca	Acute myeloid leukemia without maturation	Intermediate	Diagnosis	0	M1	47;XX;+8;abn(22) (14/20) / 46;XX (6/20)	IDH2, DNMT3	Azacitidine	46				7	15	22	4	16	20
15	BM	6576_2	Fresh	No	Acute myeloid leukemia without maturation	Intermediate	Diagnosis	0	M1	NA	IDH2, FLT3	Cytarabine + Idarubicin + Lenalinomide	80	<5	<5	Sens	12	34	46	15	29	44
16	BM	6598_2	Fresh	Prostata ca	Acute myeloid leukemia without maturation	Intermediate	Diagnosis	0	M1	Normal	CEBPA, TET2	Azacitidine	70	1	1		12	40	52	7	14	21
17	BM	6525_2	Fresh	MDS	Acute monocytic leukemia	Intermediate	Diagnosis	0	M5b	46;XY;del(9q) (5/20) / 46;XY (15/20)	FLT3-ITD	Cytarabine + Idarubicin	65	27	10	Res	14	28	42	8	13	21
18	BM	6641_2	Fresh	Prostata ca	Acute myeloid leukemia with maturation	High	Diagnosis	0	M2	Normal	IDH1, ASXL, BCOR	Cytarabine + Idarubicin/Daunorubicin	42	38	2	Res	10	15	25	6	13	19
19	BM	6637_4	Frozen	No	Acute monocytic leukemia	High	Relapse	3	M5a	47;XY;+i(5p);-7;+8 / 46;XY;	FLT3, NPM1	Cytarabine + Idarubicin	84	0	3		6	13	19	13	13	26
20	BM	6688_2	Fresh	No	Acute myeloid leukemia with maturation	High	Diagnosis	0	M2	47;XY;+8 (13/20) / 46;XY (7/20)	U2AF1, ASXL1, IDH1	Azacitidine	50	51	49		6	19	25	8	16	24
21	BM	6703_2	Fresh	No	Acute promyelocytic leukemia	Low	Diagnosis	0	M3	46;XY;t(15;17) (2/20) / 46;XY (18/20)	NA	ATRA	60	NA	NA		1	20	21	3	18	21
22	BM	12	Fresh	MDS	Acute myeloid leukemia without maturation		Relapse		M2	46;XX;del(5q);(del7q)	NA	NA	NA	NA	NA		3	10	13	1	7	8
23	BM	6730_2	Fresh	No	Acute myeloid leukemia without maturation	High	Diagnosis	0	M1	47; XX t(11q23) (MLL-gene) (7/20); 47; XX +2	FLT3-ITD	Cytarabine + Idarubicin + Lenalinomide	85	NA	2	Sens	16	27	43	14	30	44
24	BM	3708_3	Fresh	No	Acute myeloid leukemia with maturation	Low	Relapse	9	M2	45;X;-X;del(6q);rob(13;14);+ marker chromosc	CEBPA, CSFR8, IDH2, NPM1	Cytarabine + Idarubicin	65	0	1		11	23	34	11	27	38
25	BM	5806_2	Frozen	No	Acute monocytic leukemia	Low	Diagnosis	0	M5	Normal	PTPN11, TET2, NPM1	Cytarabine + Idarubicin	41	<5	1	Sens	19	26	45	16	14	30
26	BM	4401_2	Frozen	No	Acute monocytic leukemia	Intermediate	Diagnosis	0	M5	Normal	FLT3-ITD, NPM1	Cytarabine + Idarubicin	65	<5		Sens	3	22	25	15	11	26
27	BM	6834_2	Frozen	No	Acute monocytic leukemia	Intermediate	Diagnosis	0	M5b	Normal	NPM1	Cytarabine + Idarubicin	70	<5		Sens	11	26	37	9	12	21
28	BM	6862_2	Fresh	No	AML inv(16)(p13.1q22)	Low	Relapse		NA	NA	KIT	Cytarabine + Daunorubicin	61	<5	<5		13	22	35	16	21	37
29	BM	6911_2	Fresh	No	Acute myeloid leukemia with maturation	Intermediate	Diagnosis	0	M2	Normal	NPM1, CEBPA	Cytarabine + Idarubicin	63	5	1	Sens	28	33	61	13	22	35
30	BM	6940_2	Fresh	No	Acute leukemia with mnimal differentation	Intermediate	Diagnosis	0	M0	Normal	IDH2	Cytarabine + Idarubicin	75	10	36	Res	0	15	15	1	17	18
31	BM	6323_3	Fresh	No	Acute myeloid leukemia with maturation	Intermediate	Relapse**	10	M2	Normal	WT1, NRAS, FLT3-ITD	Cytarabine + Idarubicin	24	19	12	Res	10	21	31	6	14	20
32	BM	6999_2	Fresh	No	Acute myeloid leukemia without maturation	Low	Diagnosis	0	M1	46; XY; -7, -21, +2 marker chromosomes	NPM1, IDH2, DNMT3	Cytarabine + Idarubicin	91	<5	4	Sens	10	36	46	7	31	38
33	BM	7011_2	Fresh	No	MPAL (Myel 93%, B 7%)	High	Diagnosis	0	M2	Normal	None	Cytarabine + Idarubicin	62	74	NA	Res	0	10	10	4	14	18
34	BM	3724_2	Fresh	MDS	AML with multilineage dysplasia	Intermediate	Diagnosis	0	Mult. Dysp	Normal	TET2, RUNX1, SRSF2, NSD1	Azacitidine	35	NA	NA		NA	NA	NA	NA	NA	NA

*Refractory to Cytarabine+Idasanutlin

** 2nd induction treatment at the time of relapse

Supplemental Table S2. Compound list

Drug name	Mechanism/Targets	Approval status	Supplier	Supplier Ref	Label name	Solvent	conc (nM)
Ruxolitinib	JAK1&2 inhibitor	Approved	ChemieTek	CT-INCB	INCB018424 (free base, Ruxolitinib)	DMSO	10-3000
Trametinib	MEK1/2 inhibitor	Approved	ChemieTek	CT-GSK112	GSK1120212	DMSO	0.25-250
Sunitinib	Broad TK inhibitor	Approved	LC Laboratories	S-8803	Sunitinib maleate (Sutent, SU-11248)	DMSO	0.1-1000
Everolimus	binds FKBP12, causes inhibition of mTORC1	Approved	LC Laboratories	E-4040	Everolimus	DMSO	0.1-100
Idarubicin	Topoisomerase II inhibitor	Approved	Sigma-Aldrich	I1656	Idarubicin HCl	DMSO	1-1000
Cytarabine	Anti-metabolite, interferes with DNA synthesis	Approved	National Cancer Institute	NSC 63878-P/19	Cytarabine HCl	DMSO	10-10000
Venetoclax	Selective Bcl-2 inhibitor	Approved	ChemieTek	CT-A199	ABT-199	DMSO	0.1-1000

Supplemental Table S3. Summary of the cell populations present in the BM samples at day 0 and day 3

Cell population	N=34 (n) Day0/Day3	Median (% of CD45+) Day0/Day3	Range (% of CD45+) Day0/Day3
Blasts (CD45dim/SSClow)	34/34	72/63	18-92
Blasts (CD34+)	21/21	55/56	10-86
Lymphocytes	33/33	7/7	1-49
Monocytes (CD14+)	17/18	4/8	0-61
Immature granulocytes	13/9	4/3	0-60
FAB subclassification		**N=34, n (%)**	
M0		2 (6)	
M1		11 (33)	
M2		9 (26)	
M3		1 (3)	
M4		1 (3)	
M5		7 (20)	
Multi. lin. dysp.		1 (3)	
CMML->AML		1 (3)	

* Percentages were calculated from the CD45+ cell fraction and cell population smaller than 0.5% was considered to be absent.

Supplemental Table S4. Sensitivity of different FAB subtypes to 296 compounds

#	Drug	DSS (M1 vs. M5)	M1 Mean (n=10)	M2 Mean (n=16)	M4 Mean (n=2)	M5 mean (n=9)	P value*	FDR
1	Venetoclax	19,0	32,2	20,2	12,2	13,2	0,0005	0,075
2	Navitoclax	15,8	32,3	22,8	15,2	16,5	0,0011	0,103
3	(5Z)-7-Oxoze	11,4	24,1	12,7	14,6	12,7	0,0004	0,075
4	Tipifarnib	8,8	19,1	10,9	11,1	10,3	0,0014	0,103
5	Quizartinib	8,0	13,9	2,0	5,4	5,9	0,1098	0,414
6	Vistusertib	7,8	19,6	11,2	16,2	11,7	0,0359	0,309
7	Ruboxistaurin	7,4	16,8	7,7	8,9	9,3	0,0052	0,218
8	Foretinib	7,0	15,7	3,5	9,0	8,7	0,1517	0,472
9	Idarubicin	7,0	23,4	18,4	19,2	16,4	0,0462	0,335
10	GSK650394	6,9	9,0	1,8	3,7	2,0	0,0112	0,224
11	Nintedanib	6,8	15,9	8,0	12,7	9,1	0,1285	0,432
12	Quisinostat	6,8	27,5	20,8	24,5	20,8	0,0129	0,224
13	Sunitinib	6,6	13,6	2,2	7,7	7,0	0,0897	0,395
14	AZD8055	6,4	21,7	11,2	15,7	15,3	0,1013	0,411
15	AZD7762	6,3	17,2	5,6	12,5	10,9	0,2460	0,534
16	Pictilisib	6,2	19,5	9,6	11,6	13,2	0,0407	0,334
17	Vorinostat	6,2	15,3	9,0	13,4	9,1	0,0038	0,218
18	Cabozantinib	6,2	9,4	1,6	3,9	3,3	0,0463	0,335
19	Teniposide	6,1	18,5	13,5	10,4	12,4	0,0247	0,271
20	Tamatinib	6,1	11,8	3,4	8,5	5,7	0,1154	0,427
21	Lestaurtinib	6,0	16,9	6,4	11,0	10,8	0,0458	0,335
22	Tacrolimus	6,0	7,4	1,5	0,8	1,3	0,0299	0,291
23	Panobinostat	5,9	27,8	21,7	26,0	21,9	0,0182	0,265
24	Nutlin-3	5,9	9,6	6,1	4,0	3,8	0,0115	0,224
25	Daunorubicin	5,9	17,7	14,7	12,7	11,8	0,0124	0,224
26	Sorafenib	5,8	8,1	0,5	1,9	2,3	0,1362	0,438
27	Belinostat	5,8	24,5	17,6	22,5	18,7	0,0051	0,218
28	Omipalisib	5,7	21,2	11,0	17,4	15,5	0,2098	0,511
29	Sapanisertib	5,6	17,7	8,3	10,0	12,1	0,0720	0,371
30	Ponatinib	5,6	17,3	5,6	14,8	11,7	0,1858	0,504
31	Mitoxantrone	5,5	11,7	6,8	5,4	6,1	0,0231	0,270
32	Tosedostat	5,2	8,7	3,7	7,3	3,4	0,0280	0,286
33	ZSTK474	5,2	20,7	11,5	13,7	15,5	0,1070	0,411
34	Crenolanib	5,1	15,8	6,4	13,1	10,7	0,2598	0,545
35	AZD1775	5,0	13,9	5,9	9,8	8,9	0,1041	0,411
36	Omacetaxine	5,0	36,5	31,9	34,2	31,5	0,1060	0,411
37	Idelalisib	4,9	13,3	4,8	4,4	8,4	0,1106	0,414
38	Everolimus	4,9	10,6	4,1	1,9	5,7	0,1959	0,504
39	BMS-754807	4,9	11,6	5,4	4,0	6,7	0,1566	0,473
40	Tubastatin A	4,8	7,5	3,0	5,2	2,7	0,0166	0,259
41	Gandotinib	4,8	11,4	5,1	8,8	6,6	0,1267	0,432
42	Momelotinib	4,7	14,3	7,1	11,0	9,6	0,0530	0,344
43	Ipatasertib	4,7	8,1	3,4	7,9	3,3	0,0877	0,395
44	UCN-01	4,7	20,8	12,5	19,0	16,1	0,2374	0,534
45	APR-246	4,6	6,7	4,2	1,5	2,1	0,0198	0,265
46	Doramapimod	4,6	11,2	4,3	10,5	6,6	0,1588	0,475
47	Dexamethaso	4,6	7,4	8,4	2,6	2,8	0,1626	0,476
48	Dactolisib	4,5	11,8	6,7	10,4	7,3	0,0816	0,378
49	Tubacin	4,5	8,9	3,3	6,9	4,4	0,0080	0,218
50	8-chloro-aden	4,5	18,1	11,2	15,6	13,6	0,0721	0,371
51	AZ 3146	4,5	10,7	3,5	9,0	6,2	0,0813	0,378
52	GSK-J4	4,4	18,3	16,6	13,9	13,9	0,0086	0,218
53	PF 431396	4,4	12,1	6,6	10,7	7,7	0,0785	0,375
54	Alvocidib	4,3	25,8	21,0	25,5	21,5	0,0104	0,224
55	OSI-027	4,3	11,9	4,8	8,6	7,6	0,0726	0,371
56	Midostaurin	4,2	13,3	4,1	11,0	9,1	0,3589	0,625
57	Temsirolimus	4,1	9,0	3,6	8,0	4,9	0,2422	0,534
58	Vinblastine	4,1	9,6	7,7	8,3	5,5	0,0237	0,270
59	Mitomycin C	4,1	6,5	4,7	3,8	2,5	0,0200	0,265
60	Sonolisib	4,1	7,0	3,2	3,2	2,9	0,0151	0,248

61	Rebastinib	4,0	5,0	0,0	0,3	1,0	0,0778	0,375
62	Carfilzomib	4,0	29,3	27,3	27,6	25,3	0,0304	0,291
63	Dinaciclib	4,0	26,8	23,4	28,9	22,8	0,0710	0,371
64	Valrubicin	4,0	16,0	13,8	11,8	12,0	0,0540	0,344
65	Serdemetan	4,0	11,1	7,6	6,4	7,1	0,0583	0,344
66	NVP-RAF265	3,9	9,8	4,8	6,7	5,9	0,1256	0,432
67	Azacitidine	3,8	6,0	2,0	5,9	2,2	0,0079	0,218
68	Unknown [FIN	3,8	12,4	NA	NA	8,6	0,5101	0,763
69	Palbociclib	3,8	8,8	3,7	8,5	5,0	0,0279	0,286
70	Ralimetinib	3,6	12,1	3,5	11,9	8,5	0,3327	0,600
71	BMS-911543	3,6	9,8	3,5	13,0	6,2	0,2442	0,534
72	Entinostat	3,6	12,3	7,0	13,7	8,7	0,1217	0,432
73	Regorafenib	3,6	13,0	5,6	10,4	9,4	0,2107	0,511
74	GSK269962	3,5	8,5	4,9	5,1	5,0	0,1183	0,432
75	Tandutinib	3,5	4,9	0,7	2,2	1,4	0,1222	0,432
76	AVN944	3,4	8,7	5,8	8,2	5,3	0,0930	0,399
77	Dovitinib	3,3	5,4	1,3	2,2	2,1	0,0605	0,344
78	Apitolisib	3,3	16,8	9,3	13,4	13,6	0,2479	0,534
79	Etoposide	3,2	7,7	6,8	5,3	4,5	0,0993	0,411
80	Vandetanib	3,2	3,9	0,4	0,9	0,7	0,0708	0,371
81	Erlotinib	3,2	6,1	2,3	4,6	2,9	0,0324	0,300
82	Methylprednis	3,2	6,0	6,2	6,6	2,8	0,2303	0,528
83	Canertinib	3,2	13,2	9,5	13,8	10,0	0,0572	0,344
84	Tanespimycin	3,1	18,8	12,3	22,4	15,7	0,3360	0,601
85	GSK2636771	3,1	5,7	1,5	4,2	2,6	0,1318	0,433
86	Mocetinostat	3,0	14,2	11,1	16,2	11,2	0,2083	0,511
87	Alvespimycin	3,0	14,6	8,9	14,5	11,6	0,1529	0,472
88	PF-3845	3,0	4,9	2,0	3,0	2,0	0,0088	0,218
89	Dacomitinib	2,9	6,0	1,7	4,4	3,1	0,0218	0,268
90	Melphalan	2,9	5,3	2,7	0,0	2,3	0,3371	0,601
91	Luminespib	2,9	24,5	17,0	27,5	21,6	0,3616	0,626
92	KX2-391	2,9	12,2	9,8	10,0	9,2	0,2350	0,534
93	Veliparib	2,9	3,4	0,7	0,5	0,6	0,0206	0,265
94	Linifanib	2,8	4,9	0,9	1,9	2,1	0,1766	0,493
95	Raloxifene	2,7	3,9	1,7	2,6	1,2	0,0510	0,344
96	Gefitinib	2,7	6,8	2,4	5,6	4,0	0,1003	0,411
97	Dactinomycin	2,7	24,3	22,9	25,1	21,6	0,2284	0,528
98	Doxorubicin	2,6	10,7	9,0	9,0	8,1	0,1792	0,496
99	Prednisolone	2,6	4,5	4,2	5,1	1,9	0,1836	0,503
100	TGX-221	2,6	7,0	2,3	4,2	4,4	0,1670	0,480
101	Fludarabine	2,5	13,6	11,1	14,0	11,1	0,0576	0,344
102	SGC0946	2,5	4,0	2,3	2,8	1,5	0,0365	0,309
103	Valproic acid	2,5	4,4	2,6	2,2	2,0	0,0765	0,375
104	Seliciclib	2,4	4,1	1,7	3,0	1,7	0,0557	0,344
105	VER 155008	2,4	7,4	3,4	7,6	5,0	0,1926	0,504
106	BIIB021	2,4	21,5	13,7	22,5	19,1	0,4969	0,760
107	AZD1480	2,4	5,0	1,8	3,7	2,6	0,1972	0,504
108	PF-04691502	2,3	24,1	16,3	21,3	21,8	0,5985	0,809
109	MK-2206	2,3	7,0	3,1	5,5	4,7	0,3583	0,625
110	PF-04708671	2,2	3,5	1,9	1,8	1,2	0,0746	0,374
111	Fasudil	2,2	5,9	2,4	3,1	3,6	0,2489	0,534
112	Cladribine	2,2	15,1	12,8	15,3	12,8	0,3229	0,600
113	Linsitinib	2,2	5,9	4,0	3,0	3,7	0,3403	0,603
114	Bleomycin	2,1	7,7	4,4	4,6	5,6	0,2409	0,534
115	Fostamatinib	2,0	8,1	2,7	8,3	6,2	0,4931	0,760
116	Afatinib	2,0	4,7	1,3	4,1	2,8	0,1490	0,469
117	Axitinib	1,8	7,7	4,2	5,4	5,9	0,5199	0,763
118	Ridaforolimus	1,7	7,1	4,2	4,4	5,4	0,5107	0,763
119	Plicamycin	1,7	17,2	18,9	16,8	15,5	0,7034	0,846
120	Clofarabine	1,6	23,8	22,3	25,2	22,2	0,5186	0,763
121	Tamoxifen	1,5	5,5	3,1	5,8	3,9	0,3134	0,600
122	PF-670462	1,5	4,7	2,3	5,9	3,2	0,5231	0,763

123	Ibrutinib	1,5	2,3	1,3	0,5	0,8	0,1277	0,432
124	Finasteride	1,5	2,7	0,5	0,5	1,2	0,2290	0,528
125	Sotrastaurin	1,5	4,7	1,1	6,0	3,2	0,5684	0,782
126	Aminoglutethi	1,5	1,5	0,0	0,0	0,0	0,2947	0,600
127	I-BET151	1,5	11,3	8,2	15,5	9,9	0,5146	0,763
128	Iniparib	1,4	1,5	1,0	0,3	0,1	0,1942	0,504
129	CUDC-101	1,4	19,3	14,6	25,0	17,9	0,5902	0,801
130	Neratinib	1,3	7,0	3,9	8,1	5,7	0,3678	0,629
131	Rabusertib	1,3	1,8	0,7	2,0	0,5	0,2128	0,512
132	RD162	1,3	2,1	1,2	0,3	0,8	0,1376	0,438
133	Lomeguatrib	1,3	1,5	0,3	0,1	0,3	0,0903	0,395
134	Pazopanib	1,2	6,6	2,3	5,9	5,3	0,6611	0,830
135	Ruxolitinib	1,2	7,2	4,1	8,2	6,0	0,6431	0,829
136	Lenalidomide	1,2	4,9	2,7	8,5	3,7	0,6180	0,824
137	Tepotinib	1,2	1,4	0,2	0,1	0,2	0,2480	0,534
138	PFI-1	1,1	7,1	4,4	10,8	6,0	0,5617	0,780
139	8-amino-aden	1,1	23,1	16,7	24,3	22,0	0,6315	0,829
140	Tretinoin	1,1	2,4	1,3	1,3	1,3	0,6590	0,830
141	Flutamide	1,1	1,2	0,5	0,9	0,2	0,0462	0,335
142	Tofacitinib	1,0	2,3	1,3	3,3	1,3	0,4838	0,752
143	Selumetinib	1,0	11,1	6,6	12,0	10,0	0,7605	0,881
144	IOX-2	1,0	1,7	1,6	0,6	0,7	0,2016	0,506
145	PAC-1	1,0	5,9	5,3	5,4	4,9	0,3732	0,635
146	AT 101	0,9	13,8	14,2	15,1	12,9	0,6602	0,830
147	Tacedinaline	0,9	1,5	0,6	0,1	0,6	0,3168	0,600
148	Chlorambucil	0,9	1,5	1,4	0,1	0,6	0,0908	0,395
149	Uramustine	0,9	1,3	0,6	0,2	0,4	0,3463	0,610
150	SB 743921	0,9	1,4	1,9	3,0	0,6	0,3044	0,600
151	Clomifene	0,8	5,6	3,5	8,2	4,8	0,5380	0,764
152	XAV-939	0,8	0,9	0,1	0,3	0,1	0,1920	0,504
153	AZD1152-HQ	0,8	2,6	1,5	2,7	1,8	0,6619	0,830
154	JQ1	0,8	15,2	11,7	21,4	14,5	0,7849	0,896
155	Simvastatin	0,8	1,9	1,0	0,6	1,2	0,3675	0,629
156	Bosutinib	0,8	9,9	7,4	10,8	9,2	0,6822	0,837
157	Exemestane	0,7	1,9	1,1	3,1	1,1	0,3908	0,648
158	Buparlisib	0,7	12,5	6,7	8,2	11,7	0,8111	0,909
159	Bortezomib	0,7	28,7	27,5	29,4	28,0	0,6421	0,829
160	Dabrafenib	0,7	1,3	0,4	0,3	0,6	0,1606	0,475
161	Obatoclax	0,7	1,8	1,0	0,4	1,1	0,5553	0,779
162	Vincristine	0,6	7,7	7,5	10,2	7,1	0,7388	0,871
163	Thioguanine	0,6	2,0	2,1	2,3	1,4	0,5331	0,764
164	Mitotane	0,6	0,6	0,0	0,0	0,0	0,3121	0,600
165	Enzastaurin	0,6	0,8	0,4	0,0	0,2	0,4721	0,739
166	UNC0638	0,6	5,7	6,1	7,2	5,1	0,3912	0,648
167	Rofecoxib	0,6	0,6	0,0	0,0	0,0	0,1662	0,480
168	Nilutamide	0,6	1,1	0,6	0,5	0,5	0,5224	0,763
169	Amonafide	0,6	8,6	7,6	12,0	8,0	0,7087	0,846
170	C646	0,5	3,2	4,1	4,6	2,7	0,7060	0,846
171	Tivantinib	0,5	1,4	0,8	2,4	0,8	0,5353	0,764
172	UNC0642	0,5	5,7	5,4	7,7	5,2	0,4850	0,752
173	Olaparib	0,5	1,7	0,7	4,0	1,2	0,5621	0,780
174	Arsenic(III) ox	0,5	0,6	0,1	0,0	0,1	0,2559	0,541
175	AT-406	0,5	2,8	1,8	4,0	2,3	0,7444	0,874
176	Vismodegib	0,4	0,7	0,1	0,0	0,3	0,3763	0,636
177	Perifosine	0,4	0,5	0,1	0,0	0,1	0,1051	0,411
178	Lasofoxifene	0,4	0,6	0,2	1,1	0,2	0,2928	0,600
179	Rucaparib	0,4	1,6	0,7	3,6	1,2	0,6643	0,830
180	Bimatoprost	0,4	0,5	0,1	0,0	0,1	0,2287	0,528
181	Bicalutamide	0,4	1,6	0,5	4,4	1,2	0,8001	0,904
182	Fulvestrant	0,4	2,5	0,6	2,5	2,1	0,7922	0,898
183	Toremifene	0,3	3,2	2,4	6,3	2,8	0,8039	0,905
184	Topotecan	0,3	9,2	9,3	12,4	8,9	0,8522	0,931

185	Letrozole	0,3	0,7	0,3	1,2	0,3	0,6642	0,830
186	Binimetinib	0,3	6,8	4,6	6,4	6,5	0,9069	0,962
187	Brivanib	0,3	0,3			0,0	0,1702	0,485
188	Plerixafor	0,3	0,3	0,2	0,0	0,0	0,3306	0,600
189	MK-0752	0,3	0,3	0,2	0,0	0,0	0,3306	0,600
190	Volasertib	0,2	6,3	4,3	6,7	6,0	0,9005	0,962
191	Abiraterone	0,2	1,9	1,0	0,1	1,7	0,8969	0,962
192	UNC1215	0,2	0,2	0,5	0,0	0,0	0,3306	0,600
193	Anagrelide	0,2	0,4	0,1	0,0	0,2	0,6684	0,831
194	Chloroquine	0,2	9,1	8,6	9,7	8,9	0,9176	0,962
195	Vinorelbine	0,2	11,1	10,6	15,3	10,9	0,9433	0,973
196	Enzalutamide	0,2	1,2	0,6	1,3	1,0	0,8593	0,932
197	Levamisole	0,2	0,2			0,0	0,4005	0,655
198	Bendamustin	0,2	0,5	0,8	0,6	0,4	0,5852	0,798
199	Crizotinib	0,1	1,1	1,2	0,7	0,9	0,8447	0,931
200	Allopurinol	0,1	0,3	0,3	0,4	0,2	0,7603	0,881
201	2-methoxyest	0,1	1,8	2,0	1,9	1,7	0,9003	0,962
202	PF-4800567	0,1	1,5	0,5	0,7	1,4	0,9087	0,962
203	Irinotecan	0,1	2,7	3,7	7,3	2,6	0,9481	0,974
204	Vemurafenib	0,1	1,4	0,8	1,3	1,3	0,9298	0,962
205	Sonidegib	0,1	0,5	0,6	2,5	0,5	0,9168	0,962
206	Sirolimus	0,1	4,9	2,6	6,3	4,8	0,9849	0,991
207	AZD4547	0,1	3,0	1,3	1,9	2,9	0,9638	0,984
208	Metformin	0,1	0,3	0,0	0,0	0,2	0,8563	0,932
209	CPI-613	0,1	0,1	0,1	0,1	0,0	0,5010	0,760
210	Galunisertib	0,0	0,0			0,0	0,3306	0,600
211	Streptozocin	0,0	0,3	0,0	0,0	0,2	0,9200	0,962
212	Megestrol ace	0,0	1,1	1,7	3,1	1,1	0,9820	0,991
213	Mercaptopurir	0,0	0,0	0,8	0,2	0,0	0,9598	0,983
214	Fluorouracil	0,0	0,9	0,5	0,3	0,9	0,9980	0,998
215	Pentostatin	0,0	0,0	0,1	0,4	0,0	0,3306	0,600
216	Imiquimod	0,0	0,2	0,3	0,9	0,2	0,9229	0,962
217	Pemetrexed	0,0	0,0	1,3	0,0	0,0	0,3306	0,600
218	TAK-901	0,0	6,4	4,1	7,8	6,4	0,9873	0,991
219	Pilaralisib	0,0	2,5	1,8	2,8	2,6	0,9818	0,991
220	Lapatinib	0,0	0,0	0,1	0,0	0,1	0,5642	0,780
221	1-methyl-D-try	0,0	0,3	0,2	0,0	0,3	0,8861	0,957
222	Anastrozole	-0,1	0,0			0,1	0,3306	0,600
223	Pipobroman	-0,1	0,0	0,2	0,2	0,1	0,1558	0,473
224	Bexarotene	-0,1	2,3	1,9	2,0	2,3	0,9719	0,989
225	Methotrexate	-0,1	0,1	1,8	0,0	0,2	0,6770	0,835
226	Ifosfamide	-0,1	0,0	0,2	0,0	0,1	0,3306	0,600
227	Tarenflurbil	-0,1	0,5	0,1	0,2	0,6	0,8258	0,922
228	Roxadustat	-0,1	0,1	0,1	0,1	0,2	0,5008	0,760
229	Niraparib	-0,2	2,0	1,0	4,0	2,1	0,8520	0,931
230	Deferoxamine	-0,2	2,8	2,8	1,0	2,9	0,9285	0,962
231	Estramustine	-0,2	0,0	0,4	0,0	0,2	0,1732	0,488
232	Temozolomid	-0,2	0,0	0,2	0,8	0,2	0,1242	0,432
233	15D-PGJ2	-0,3	0,0	0,1	0,8	0,3	0,1971	0,504
234	AT9283	-0,3	1,6	0,9	3,3	1,9	0,8379	0,931
235	Pravastatin	-0,3	0,5	0,7	0,0	0,8	0,5810	0,796
236	Cytarabine	-0,3	10,0	9,1	15,4	10,3	0,8438	0,931
237	VX-11E	-0,3	3,0	2,6	5,3	3,3	0,7713	0,885
238	Hydroxyurea	-0,3	0,1	0,1	0,7	0,5	0,3862	0,648
239	Fingolimod	-0,3	6,1	6,5	7,6	6,4	0,6440	0,829
240	GSK343	-0,3	2,7	2,7	3,5	3,0	0,7868	0,896
241	Ixabepilone	-0,4	0,3	0,6	1,1	0,7	0,3256	0,600
242	Celecoxib	-0,4	0,3	0,1	2,1	0,7	0,4031	0,656
243	Cyclophospha	-0,4	0,0	0,0	0,0	0,4	0,3306	0,600
244	Goserelin	-0,4	0,4	0,1	0,0	0,8	0,4284	0,682
245	Sepantronium	-0,4	19,2	22,6	22,7	19,6	0,9187	0,962
246	Carboplatin	-0,5	2,9	4,0	4,2	3,4	0,7345	0,870

247	4-hydroxytam	-0,5	4,1	4,4	6,0	4,5	0,7078	0,846
248	Altretamine	-0,5	0,0	0,0	2,6	0,5	0,3306	0,600
249	Vatalanib	-0,5	1,0	0,8	0,9	1,5	0,6559	0,830
250	Thalidomide	-0,5	0,0	0,1	2,1	0,6	0,1992	0,504
251	Stattic	-0,6	16,1	15,2	21,4	16,7	0,7563	0,881
252	Thio-TEPA	-0,6	0,7	0,8	0,5	1,3	0,5137	0,763
253	Carmustine	-0,6	0,2	0,2	1,9	0,8	0,2040	0,507
254	Busulfan	-0,6	0,9	0,4	2,8	1,6	0,5368	0,764
255	Nelarabine	-0,7	4,2	6,7	7,0	4,9	0,6925	0,844
256	Atorvastatin	-0,7	4,9	5,1	5,3	5,7	0,6324	0,829
257	Bryostatin 1	-0,7	1,2	1,5	0,4	1,9	0,6840	0,837
258	Varespladib	-0,7	0,1	0,1	0,0	0,8	0,1308	0,433
259	Nilotinib	-0,8	5,9	3,4	9,7	6,7	0,7619	0,881
260	SNS-032	-0,8	29,9	27,6	35,0	30,7	0,8509	0,931
261	StemRegenin	-0,8	1,1	1,2	4,5	1,9	0,4693	0,739
262	Infigratinib	-0,8	0,1	0,5	1,6	1,0	0,0551	0,344
263	BI 2536	-0,9	6,8	6,0	10,0	7,6	0,6436	0,829
264	Decitabine	-0,9	1,1	1,6	1,2	1,9	0,3916	0,648
265	Refametinib	-0,9	12,5	9,1	14,3	13,4	0,7685	0,885
266	Galiellalacton	-0,9	3,6	2,9	6,5	4,5	0,5466	0,770
267	Prednisone	-1,0	0,0	0,2	4,5	1,0	0,2231	0,528
268	Auranofin	-1,0	5,3	6,6	7,6	6,3	0,6061	0,812
269	Floxuridine	-1,1	0,0	1,7	1,3	1,1	0,0604	0,344
270	Imatinib	-1,2	2,4	2,4	3,6	3,6	0,6052	0,812
271	Capecitabine	-1,2	0,0	0,0	6,0	1,2	0,3281	0,600
272	Masitinib	-1,2	5,6	3,9	6,4	6,8	0,6757	0,835
273	PF-00477736	-1,2	8,8	5,0	12,8	10,1	0,7056	0,846
274	Tivozanib	-1,3	9,0	4,8	10,7	10,3	0,7238	0,860
275	Mechlorethan	-1,4	1,3	0,8	3,3	2,7	0,1341	0,436
276	Motesanib	-1,4	2,0	1,2	2,8	3,4	0,5354	0,764
277	Cediranib	-1,5	0,0	0,3	2,5	1,5	0,1060	0,411
278	Danusertib	-1,6	6,1	4,6	9,1	7,7	0,4569	0,723
279	Saracatinib	-1,7	3,9	2,0	8,7	5,5	0,4250	0,680
280	Trametinib	-1,7	9,3	6,7	13,1	11,1	0,6263	0,829
281	Oxaliplatin	-1,9	9,8	10,7	18,1	11,7	0,6365	0,829
282	ABT-751	-1,9	3,9	3,9	11,1	5,8	0,2510	0,535
283	Cisplatin	-2,0	3,3	5,0	7,1	5,3	0,2949	0,600
284	Camptothecin	-2,1	7,6	9,0	15,3	9,7	0,3137	0,600
285	Gemcitabine	-2,1	4,5	6,0	8,7	6,7	0,2626	0,547
286	Indibulin	-2,3	0,4	2,3	6,0	2,7	0,0344	0,309
287	Dasatinib	-2,3	7,2	5,0	12,7	9,5	0,5397	0,764
288	Alisertib	-2,4	3,5	3,7	3,7	5,9	0,1989	0,504
289	TAK-733	-2,7	7,6	6,2	13,6	10,3	0,4251	0,680
290	Pimasertib	-2,9	10,8	8,9	15,0	13,8	0,4118	0,666
291	Patupilone	-3,5	1,8	4,5	9,2	5,2	0,0574	0,344
292	Daporinad	-3,7	19,3	16,4	35,1	23,0	0,3978	0,654
293	Mepacrine	-4,5	8,5	12,7	17,9	12,9	0,2282	0,528
294	Pevonedistat	-4,7	4,3	6,0	17,4	9,0	0,0682	0,371
295	Docetaxel	-5,2	2,2	5,9	10,8	7,5	0,0456	0,335
296	Paclitaxel	-5,9	2,7	4,7	8,0	8,6	0,0082	0,218

*P-value calculated from M1 vs. M5 data set

• Mean AML sample sensitivities to individual drugs of different FAB subtypes. Earlier published data of 37 AML samples screened with 296 compounds and cell viability measured with CTG were re-analyzed and the mean DSS values calculated. The difference between mean DSS values of M1 and M5 subtypes was calculated with Student's t-test (two-sample, unpaired). The Benjamini-Hochberg method was used to adjust P-values.

• The venetoclax concentration range used in the earlier study was 1-10 000nM compared to 0.1-1 000nM range used in this study.

Supplemental Table S5. Differential BCL2 family gene expression values and P-values between FAB subgroups

a-b: Significant genes between M4-M5 and M0-M1

Genes tested:
BCL2
BCL2L1
BCL2A1
MCL1
BCL2L2
BCL2L11
BID
BBC3
BAX
BAK1
BOK
B2M
JAK2

Groups tested (Two-Tailed Wilcoxon test):
M0 vs. M3
M0 vs. M4
M0 vs. M5
M1vs. M3
M1 vs. M4
M1 vs. M5
M2 vs. M3
M2 vs. M4
M2 vs. M5

c-d: Significant genes between M0 to M5 genetic subtype

Genes tested:
BCL2
BCL2L1
BCL2A1
MCL1
BCL2L2
BCL2L11
BID
BBC3
BAX
BAK1
BOK
B2M
JAK2

Groups tested (Two-Tailed Wilcoxon test):	GroupA (FAB M0,M1,M2,M3,M4,M5)	GroupB (FAB M0,M1,M2,M3,M4,M5)
Mutations	FLT3, NPM1, RUNX1, CEBPA	Wild Type (wt)
Fusion genes	RUNX1-RUNX1T1, CBFB-MYH11, MLL, PML-RARA	Wild Type (wt)
Karyotype	Complex Karyotype, Normal Karyotype	Rest of the samples

Each feature above was tested within FAB group, for example FLT3mut M0 vs FLT3wt M0

a. TCGA AML statistics M0 to M5

gene	Fold Change	P-Value	GroupA	GroupB	adj. P-Value
MCL1	0.72440113623124	0.048	M3	M4	0.0713142857142857
MCL1	0.67384379952626	0.017	M3	M5	0.0285161290322581
MCL1	0.597334564870145	0.012	M0	M5	0.0211525423728814
MCL1	0.631354136387117	0.011	M2	M5	0.0200701754385965
MCL1	0.678723547036657	0,03	M2	M4	0.00863396226415094
MCL1	0.642151545812753	0,03	M0	M4	0.00856470588235294
JAK2	0.773888815346665	0.033	M0	M4	0.052
JAK2	0.699606396318039	0.011	M2	M5	0.0200701754385965
JAK2	0.679568306951877	0,01	M1	M5	0.00455
JAK2	0.499076657371927	0.000013	M3	M5	0.0000614545454545454
JAK2	0.600471536254176	0.000009	M2	M4	0.000052
JAK2	0.583272862301762	0.0000021	M1	M4	0.00001456
JAK2	0.428357042957174	0.00000021	M3	M4	0.00000312
BOK	1.54184627027858	0.045	M3	M4	0.0678260869565217
BID	0.813289987666822	0,01	M2	M4	0.00354545454545455
BID	0.776599593468677	0.00041	M1	M4	0.00115243243243243
BID	0.685163233790136	0.000056	M0	M4	0.000215703703703704
BID	0.647843814892762	0.0000066	M2	M5	0.0000403764705882353
BID	0.684362276564345	0.0000063	M3	M4	0.0000403764705882353
BID	0.545781664515838	0.00000062	M0	M5	0.00000586181818181818
BID	0.618617284002548	0.00000057	M1	M5	0.00000586181818181818
BID	0.545143644630444	0.000000011	M3	M5	0.000000286
BCL2L11	0.571237226256204	0.00049	M1	M4	0.00130666666666667
BCL2L11	0.518313964432618	0.00045	M2	M4	0.00123157894736842
BCL2L11	0.459479190226749	0.000079	M1	M5	0.000273866666666667
BCL2L11	0.416909945140552	0.000071	M2	M5	0.000263714285714286
BCL2L11	0.439693357498595	0.000021	M3	M4	0.0000949565217391304
BCL2L11	0.475146610456495	0.000013	M0	M4	0.0000614545454545454
BCL2L11	0.353670836852854	0.0000019	M3	M5	0.0000141142857142857
BCL2L11	0.382187941851004	0.00000083	M0	M5	0.00000719333333333333
BCL2L1	1.41463723737829	0.027	M0	M4	0.043875
BCL2L1	1.40968712777108	0.025	M0	M5	0.0412698412698413
BCL2L1	1.41053072827582	0.015	M1	M5	0.026
BCL2L1	1.41548380018217	0,03	M1	M4	0.00863396226415094
BCL2L1	1.44531566059559	0,01	M2	M5	0.00429565217391304
BCL2L1	1.45039087962541	0.00069	M2	M4	0.001794
BCL2L1	1.77868680485133	0.00022	M3	M5	0.000653714285714286
BCL2L1	1.78493265505983	0.00011	M3	M4	0.000369032258064516
BCL2A1	0.445150499370007	0.039	M1	M5	0.0596470588235294
BCL2A1	0.16072427211598	0.00079	M3	M5	0.00200390243902439
BCL2A1	0.337025246228384	0.00018	M1	M4	0.000567272727272727
BCL2A1	0.121684997459121	9.7e-10	M3	M4	0.00000010088
BCL2	1.52880222775951	0,03	M3	M4	0.00943703703703704
BCL2	1.84192495804133	0,03	M0	M4	0.007904
BCL2	1.39104266197784	0,02	M1	M4	0.00530612244897959
BCL2	3.21292852946006	0.000054	M0	M5	0.000215703703703704
BCL2	2.18618354461221	0.000035	M2	M5	0.000151666666666667
BCL2	2.66673855089834	0.000013	M3	M5	0.0000614545454545454
BCL2	2.42644014070869	0.0000011	M1	M5	0.0000088
BBC3	0.531225691245345	0.002	M1	M5	0.00442553191489362
BBC3	0.460562893240659	0.00016	M2	M5	0.00052
BBC3	0.389527911000017	0.000054	M0	M5	0.000215703703703704
BAX	1.20608646064382	0.032	M1	M4	0.355555555555556
BAX	0.702687605752078	0,01	M0	M4	0.00354545454545455
BAX	0.660069790274895	0,00	M1	M5	0.00115243243243243
BAX	0.585123270193253	0.000078	M3	M5	0.000273866666666667
BAX	0.553893105953214	0.00000038	M2	M5	0.00000494
BAX	0.384568499599897	0.0000000036	M0	M5	0.0000001872
BAK1	0.76660312575102	0.017	M0	M4	0.0285161290322581
BAK1	0.713069343531053	0.00022	M3	M4	0.000653714285714286
BAK1	0.585381362174925	0.00000045	M2	M5	0.0000052
BAK1	0.57414068232008	0.00000017	M1	M5	0.00000294666666666667
BAK1	0.482835670297674	0.000000017	M0	M5	0.0000003536
BAK1	0.449118067598852	0.000000011	M3	M5	0.000000286
B2M	0.726301782391095	0.038	M2	M5	0.0589850746268657
B2M	0.621269729010482	0.012	M0	M5	0.0211525423728814
B2M	0.801357118148607	0.007	M2	M4	0.0132363636363636
B2M	0.685471152216891	0,01	M0	M4	0.00392888888888889
B2M	0.609466592436113	0.00089	M1	M5	0.00220380952380952
B2M	0.672448290729189	0.000013	M1	M4	0.0000614545454545454

b. Hemap AML statistics M0 to M5

gene	Fold Change	P-Value	GroupA	GroupB	adj. P-Value
MCL1	0.756176785661429	0.022	Healthy_CD34	M4	0.0308571428571429
MCL1	0.897566303440181	0.014	M2	M5	0.0204324324324324
MCL1	0.824092344440203	0.0604166666666667	M3	M4	0.0132338028169014
MCL1	0.782532086129728	0.0305555555555556	M1	Monocyte	0.00714586466165414
MCL1	0.716764145897184	0.0131944444444444	Healthy_CD34	M5	0.00333658536585366
MCL1	0.781139882370789	0.00077	M3	M5	0.00140949152542373
MCL1	0.622786601933196	0.00022	Healthy_CD34	Monocyte	0.000448301886792453
MCL1	0.779883133564879	0.00013	M2	Monocyte	0.000278019801980198
MCL1	0.675073066525414	0.000012	M0	M4	0.000031609756097561
MCL1	0.678721802368145	0.000011	M3	Monocyte	0.0000297
MCL1	0.639887628291896	0.0000015	M0	M5	0.00000498461538461539
MCL1	0.555989643070353	0.000000011	M0	Monocyte	0.0000000495
MCL1	0.436369274334818	0.0000000031	AML_CD34	M4	0.0000000171692307692308
MCL1	0.413625300518563	4.7e-10	AML_CD34	M5	0.00000000290057142857143
MCL1	0.359393388826824	1.3e-11	AML_CD34	Monocyte	1.08e-10
JAK2	0.864378529268028	0.026	M0	M4	0.0357707006369427
JAK2	0.745111320985678	0.00012	M0	M5	0.000261818181818182
JAK2	0.627058275288162	0.000093	Healthy_CD34	M4	0.000207092783505155
JAK2	0.64363469166669	0.000054	M0	Monocyte	0.000124085106382979
JAK2	0.672356052923596	0.0000091	AML_CD34	M4	0.0000255272727272727
JAK2	0.774418232375781	0.0000078	M1	M4	0.0000221684210526316
JAK2	0.466920968078552	0.0000076	Healthy_CD34	Monocyte	0.000021888
JAK2	0.540536586708859	0.0000033	Healthy_CD34	M5	0.0000103304347826087
JAK2	0.500650659590277	0.00000027	AML_CD34	Monocyte	0.00000106036363636364
JAK2	0.579584163423004	0.00000015	AML_CD34	M5	0.00000061320754716981
JAK2	0.576648335583184	0.0000000058	M1	Monocyte	0.000000028472727272727273
JAK2	0.73146900693134	0.0000000035	M2	M4	0.000000018439024390243 9
JAK2	0.667563772794714	0.0000000032	M1	M5	0.00000001728
JAK2	0.544667426131783	2.5e-11	M2	Monocyte	0.0000000002
JAK2	0.630540694337041	0.000000000001	M2	M5	9.81818181818182e-12
JAK2	0.408291720434451	0.000000000000009	M3	Monocyte	1.08e-13
JAK2	0.548321278188971	3.4e-16	M3	M4	5.24571428571429e-15
JAK2	0.472663744045003	2.2e-17	M3	M5	4.752e-16
BOK	0.960534983989802	0.041	M1	M4	0.05535
BOK	1.13706238658765	0.025	AML_CD34	M4	0.0348387096774194
BOK	0.907101817774019	0.013	Healthy_CD34	M4	0.0191020408163265
BOK	0.924643538260555	0.0388888888888889	M0	M5	0.00876521739130435
BOK	1.14933801920959	0.0229166666666667	AML_CD34	M5	0.00556875
BOK	0.916978474163954	0.0104166666666667	M3	Monocyte	0.00267768595041322
BOK	0.914767780048233	0.000077	M0	M4	0.000175073684210526
BOK	0.824267508376797	0.000016	Healthy_CD34	Monocyte	0.0000411428571428571
BOK	0.906554149773801	0.000011	M2	Monocyte	0.0000297
BOK	0.872821289130368	0.000000044	M1	Monocyte	0.00000018635294 1176471
BOK	0.831233433810154	7.6e-11	M0	Monocyte	5.472e-10
BID	0.766713435917683	0.011	AML_CD34	M5	0.0163862068965517
BID	0.849565151102682	0.0194444444444444	M0	M5	0.00476220472440945
BID	0.749383640572565	0.00277777777777778	Healthy_CD34	M4	0.000771428571428571
BID	0.691159853840777	0.000012	Healthy_CD34	M5	0.000031609756097561
BID	0.806218675668972	0.0000037	M1	M4	0.0000114171428571429
BID	0.785469082912321	0.000000011	M2	M4	0.0000000495
BID	0.743579058669234	0.0000000036	M1	M5	0.00000001851428571 42857
BID	0.660580953438376	2.6e-10	M3	M4	0.00000000165176470588235
BID	0.242636393352739	1.1e-10	Healthy_CD34	Monocyte	7.425e-10
BID	0.724441617283424	5.1e-11	M2	M5	3.79862068965517e-10
BID	0.269159995032075	3.6e-12	AML_CD34	Monocyte	3.1104e-11
BID	0.609256741820024	1.6e-12	M3	M5	1.50260869565217e-11
BID	0.298245656249035	9.5e-18	M0	Monocyte	2.28e-16
BID	0.213883745763837	5.4e-22	M3	Monocyte	2.916e-20
BID	0.261038513689036	1.1e-25	M1	Monocyte	1.188e-23
BID	0.254320184014578	1.1e-29	M2	Monocyte	2.376e-27
BCL2L2	0.886162909880358	0.049	Healthy_CD34	Monocyte	0.0653333333333333
BCL2L2	1.09000899861673	0.043	AML_CD34	M4	0.0576894409937888
BCL2L2	1.08835058879277	0.015	M1	M4	0.021744966442953

BCL2L2	1.13966520249199	0.0381944444444444	AML_CD34	M5	0.00867153284671533
BCL2L2	1.10814871470204	0.0368055555555556	M3	M5	0.00848
BCL2L2	1.09824948356787	0.0319444444444444	M2	M5	0.00741492537313433
BCL2L2	0.915831208869128	0.0180555555555556	M0	M5	0.0044928
BCL2L2	1.13793124252447	0.00625	M1	M5	0.00163361344537815
BCL2L2	0.875927646732203	0.000027	M0	M4	0.0000655280898876404
BCL2L2	0.837245298706436	0.0000056	M0	Monocyte	0.0000165698630136986
BCL2L11	0.817514995100885	0.027	Healthy_CD34	M5	0.0369113924050633
BCL2L11	0.848369350164473	0.026	M3	M4	0.0357707006369427
BCL2L11	0.804971212282638	0.011	AML_CD34	M5	0.0163862068965517
BCL2L11	0.754850754422285	0.0256944444444444	Healthy_CD34	M4	0.0061953488372093
BCL2L11	0.840374526023186	0.00056	M2	M4	0.00104275862068966
BCL2L11	0.743268478891676	0.00038	AML_CD34	M4	0.00073945945945946
BCL2L11	0.779030915984434	0.000097	M3	Monocyte	0.000213795918367347
BCL2L11	0.693155728144975	0.00009	Healthy_CD34	Monocyte	0.0002025
BCL2L11	0.815980634372373	0.000039	M1	M5	0.0000915652173913043
BCL2L11	0.682520088474534	0.0000056	AML_CD34	Monocyte	0.0000165698630136986
BCL2L11	0.771689520196486	0.0000012	M2	Monocyte	0.00000418064516129032
BCL2L11	0.761794880178923	0.00000027	M0	M5	0.00000106036363636364
BCL2L11	0.753434005664875	0.0000000046	M1	M4	0.000000023106976744186
BCL2L11	0.691854772279476	1.3e-10	M1	Monocyte	8.50909090909091e-10
BCL2L11	0.703401703288796	1.1e-10	M0	M4	7.425e-10
BCL2L11	0.645911681170291	4.8e-11	M0	Monocyte	3.70285714285714e-10
BCL2L1	1.23514116549936	0.0291666666666667	Healthy_CD34	Monocyte	0.00692519083969466
BCL2L1	1.07811377589905	0.00037	M3	M4	0.000726545454545455
BCL2L1	1.18023580503551	0.00035	M1	M4	0:07
BCL2L1	1.28825483079069	0.000025	M1	M5	0.0000613636363636364
BCL2L1	1.17678626086264	0.0000015	M3	M5	0.00000498461538461539
BCL2L1	1.45527999378235	0.0000000077	M1	Monocyte	0.00000003696
BCL2L1	1.32935927074322	0.0000000019	M3	Monocyte	0.0000000110918918918919
BCL2L1	1.35500909914626	3.3e-12	M2	M4	2.97e-11
BCL2L1	1.47902394614099	4.2e-14	M2	M5	4.77473684210526e-13
BCL2L1	1.67078275796019	2.9e-17	M2	Monocyte	5.69454545454545e-16
BCL2A1	0.603205655280486	0.016	M0	M5	0.0227368421052632
BCL2A1	0.596707068712228	0.0375	M0	M4	0.00857647058823529
BCL2A1	0.345547528073482	0.0166666666666667	Healthy_CD34	M5	0.00418064516129032
BCL2A1	0.341824800169698	0.00042	Healthy_CD34	M4	0.00080283185840708
BCL2A1	0.28172567820071	0.000022	AML_CD34	M5	0.0000546206896551724
BCL2A1	0.278690529752977	0.0000016	AML_CD34	M4	0.00000523636363636364
BCL2A1	0.374678752531045	0.00000077	M1	M5	0.000002772
BCL2A1	0.370642181773966	0.0000000022	M1	M4	0.0000000125052631578947
BCL2A1	0.0799863363728203	5.7e-10	Healthy_CD34	Monocyte	0.00000000342
BCL2A1	0.168637817917145	9.4e-13	M3	M5	9.66857142857143e-12
BCL2A1	0.0652130402641195	2.4e-13	AML_CD34	Monocyte	2.592e-12
BCL2A1	0.237973171726627	6.1e-15	M2	Monocyte	7.75058823529412e-14
BCL2A1	0.139628289961294	6.8e-16	M0	Monocyte	9.792e-15
BCL2A1	0.166821012240966	1.4e-16	M3	M4	2.32615384615385e-15
BCL2A1	0.0390357914128408	8.1e-22	M3	Monocyte	3.4992e-20
BCL2A1	0.0867295474483146	1.6e-22	M1	Monocyte	1.152e-20
BCL2	1.10852854722758	0.011	M0	M4	0.0163862068965517
BCL2	1.12965016010982	0.0451388888888889	M2	Monocyte	0.0101007194244604
BCL2	1.14320921051288	0.0298611111111111	M0	M5	0.00703636363636364
BCL2	1.24274535135676	0.00037	AML_CD34	M4	0.000726545454545455
BCL2	1.25330124292858	0.00138888888888889	M0	Monocyte	0.000419417475728155
BCL2	1.28162502945577	0.00014	AML_CD34	M5	0.000296470588235294
BCL2	1.40504662454973	0.000051	AML_CD34	Monocyte	0.000118451612903226
BCL2	1.21015862067505	0.0000032	M1	M5	0.0000101647058823529
BCL2	1.25163755775748	0.000002	M3	M5	0.00000644776119402985
BCL2	1.17344696434873	0.0000013	M1	M4	0.00000445714285714286
BCL2	1.21366758664751	0.00000047	M3	M4	0.0000017503448275862 1
BCL2	1.32669793899957	0.000000034	M1	Monocyte	0.00000014688
BCL2	1.37217133347778	0.000000012	M3	Monocyte	0.000000052897959 1836735
BBC3	1.08735067843387	0.036	M2	M5	0.0489056603773585
BBC3	1.1364551357906	0.016	M3	M4	0.0227368421052632
BBC3	0.851102061291693	0.0270833333333333	M0	M5	0.00648
BBC3	0.850944926121981	0.00026	M1	M4	0.000524859813084112

BBC3	1.2424010332266	0.00022	M3	M5	0.000448301886792453
BBC3	1.42318522051382	0.000019	AML_CD34	M4	0.0000482823529411765
BBC3	0.778524230718742	0.0000075	M0	M4	0.000021888
BBC3	1.55586149664336	0.00000091	AML_CD34	M5	0.00000322229508196721
BBC3	0.650752849876492	0.00000069	M3	Monocyte	0.00000252610169491525
BBC3	0.526027081239692	0.0000004	Healthy_CD34	Monocyte	0.00000151578947368421
BBC3	0.56953957207223	1.6e-15	M2	Monocyte	2.16e-14
BBC3	0.445795743169111	0000000000000000006	M0	Monocyte	1.85142857142857e-17
BBC3	0.487265021136612	0000000000000000002	M1	Monocyte	7.2e-18
BAX	0.823110029233584	0.022	M0	Monocyte	0.0308571428571429
BAX	0.835050751146335	0.016	M0	M5	0.0227368421052632
BAX	0.83847187377086	0.0458333333333333	M3	M4	0.0101828571428571
BAX	0.862473143881513	0.0118055555555556	M2	M4	0.00300983606557377
BAX	0.635242232867981	0.00049	Healthy_CD34	M4	0.000920347826086957
BAX	0.774814742671967	0.00045	M1	Monocyte	0.000852631578947368
BAX	0.786054852800087	0.00013	M1	M5	0.000278019801980198
BAX	0.712807237267295	0.000039	M3	Monocyte	0.0000915652173913043
BAX	0.540036315076058	0.000034	Healthy_CD34	Monocyte	0.0000816
BAX	0.547870533141794	0.00002	Healthy_CD34	M5	0.0000502325581395349
BAX	0.723147814705684	0.0000095	M3	M5	0.0000263076923076923
BAX	0.733211355251049	0.0000056	M2	Monocyte	0.0000165698630136986
BAX	0.743847931875533	0.00000032	M2	M5	0.00000123428571428571
B2M	1.05933244069107	0.013	M0	M5	0.0191020408163265
B2M	0.791942053967213	0.0465277777777778	AML_CD34	Monocyte	0.010263829787234
B2M	0.878561612689705	0.01875	Healthy_CD34	M5	0.00462857142857143
B2M	0.940042948213445	0.0104166666666667	M2	M5	0.00267768595041322
B2M	0.907336981677027	0.00069	M1	M5	0.00127384615384615
B2M	0.902768665865441	0.00022	M0	Monocyte	0.000448301886792453
B2M	1.10616742128612	0.000016	M0	M4	0.0000411428571428571
B2M	0.858784204432078	0.000000096	M3	Monocyte	0.000000398769230769231
B2M	0.748714817466613	0.0000000097	Healthy_CD34	Monocyte	0.0000000455478260869565
B2M	0.773237337945192	7.1e-17	M1	Monocyte	1.278e-15
B2M	0.801109534284861	1.4e-18	M2	Monocyte	3.78e-17

c. TCGA AML statistics genetics

gene	Fold Change	P-Value	GroupA	GroupB	adj. P-Value
MCL1	0.612859626142771	0.047	M4_RUNX1	M4_RUNX1_not	0.361725
JAK2	0.761148575989693	0.036	M2_FLT3	M2_FLT3_not	0.361725
JAK2	0.794749503608146	0.036	M1_NPM1	M1_NPM1_not	0.361725
JAK2	0.614777539697286	0,07	M4_FLT3	M4_FLT3_not	0.248181818181818
JAK2	1.79764869623807	0,03	M0_RUNX1	M0_RUNX1_not	1,1
BID	0.796901173779609	0.038	M3_FLT3	M3_FLT3_not	0.361725
BID	1.29841650735952	0.044	M5_NPM1	M5_NPM1_not	0.361725
BID	1.37888295459029	0.032	M5_Normal_Karyotype	M5_Normal_Karyotype_not	0.361725
BID	0.77017062307226	0,00	M4_CBFB_MYH11	M4_CBFB_MYH11_not	0.248181818181818
BID	1.42741802412088	0.0000035	M4_Normal_Karyotype	M4_Normal_Karyotype_not	0.0003185
BID	1.48735375973883	0.0000021	M4_NPM1	M4_NPM1_not	0.00028665
BCL2L2	1.35997650794728	0.00052	M1_NPM1	M1_NPM1_not	0.028392
BCL2L11	0.447384827550487	0.049	M2_RUNX1_RUNX1T1	M2_RUNX1_RUNX1T1_not	0.361725
BCL2L11	0.574565334213617	0.045	M4_RUNX1	M4_RUNX1_not	0.361725
BCL2L1	0.50518820365958	0.00000059	M4_CBFB_MYH11	M4_CBFB_MYH11_not	0.00016107
BCL2A1	0.524821962664371	0.049	M2_RUNX1_RUNX1T1	M2_RUNX1_RUNX1T1_not	0.361725
BCL2A1	9.17791640704799	0.024	M5_Normal_Karyotype	M5_Normal_Karyotype_not	0.361725
BCL2A1	2.23617761433255	0.031	M4_NPM1	M4_NPM1_not	0.361725
BCL2	0.517243912716571	0.041	M5_Normal_Karyotype	M5_Normal_Karyotype_not	0.361725
BCL2	1.78971339359243	0.039	M4_RUNX1	M4_RUNX1_not	0.361725
BCL2	0.669238387241732	0.014	M4_Normal_Karyotype	M4_Normal_Karyotype_not	0,2
BCL2	0.56972559673218	0.00091	M4_NPM1	M4_NPM1_not	0.041405
BCL2	0.449887221345994	0.00039	M2_RUNX1_RUNX1T1	M2_RUNX1_RUNX1T1_not	0.0266175
BBC3	1.62075304760719	0,00	M2_NPM1	M2_NPM1_not	0.361725
BBC3	0.60069607522619	0.047	M4_RUNX1	M4_RUNX1_not	0.361725
BBC3	0.437927810847697	0,05	M2_CEBPA	M2_CEBPA_not	0.203233333333333
BAX	1.37645223345365	0.023	M4_FLT3	M4_FLT3_not	0.361725
BAX	1.30017034863702	0.037	M4_Normal_Karyotype	M4_Normal_Karyotype_not	0.361725
BAX	1.40607959152019	0.016	M4_NPM1	M4_NPM1_not	0,2
BAX	1.45011434698119	0,02	M2_FLT3	M2_FLT3_not	0,6
BAK1	1.22853967071203	0.048	M1_CEBPA	M1_CEBPA_not	0.361725
BAK1	0.742482316638929	0.037	M4_RUNX1	M4_RUNX1_not	0.361725
BAK1	0.752623373705534	0.018	M5_Normal_Karyotype	M5_Normal_Karyotype_not	2,3
B2M	0.723942465080778	0.035	M1_FLT3	M1_FLT3_not	0.361725
B2M	0.648215513896212	0.013	M3_FLT3	M3_FLT3_not	0,2

d. Hemap AML statistics genetics

gene	Fold Change	P-Value	GroupA	GroupB	adj. P-Value
MCL1	1.44828834340019	0:02	M2_FLT3	M2_FLT3_not	0.122553191489362
MCL1	0.506196272152554	0.016	M4_PML_RARA	M4_PML_RARA_not	0.109714285714286
MCL1	1.67423830095391	0.00016	M4_CBFB_MYH11	M4_CBFB_MYH11_not	0.00354461538461538
MCL1	0.641295343172434	0.000026	M4_MLL	M4_MLL_not	0.000832
JAK2	1.62828224077646	0.035	M5_FLT3	M5_FLT3_not	0.173793103448276
JAK2	1.34124551293129	0.032	M4_NPM1	M4_NPM1_not	0.170666666666667
JAK2	0.60181344561868	0.056944444	M4_PML_RARA	M4_PML_RARA_not	0.0674742857142857
JAK2	1.50848114661595	0:11	M4_CBFB_MYH11	M4_CBFB_MYH11_not	0.0916666666666667
JAK2	0.733286346483175	0.00000048	M2_RUNX1_RUNX1T1	M2_RUNX1_RUNX1T1_not	0.00004608
JAK2	0.561175056102604	5.4e-10	M4_MLL	M4_MLL_not	0.00000007776
BOK	1.05252173387062	0.047	M4_MLL	M4_MLL_not	0.197485714285714
BOK	1.09243333969954	0.034	M2_FLT3	M2_FLT3_not	0.171789473684211
BOK	1.08912325130482	0.04722222	M1_NPM1	M1_NPM1_not	0.0593454545454545
BOK	1.13890182509818	0.0000058	M2_RUNX1_RUNX1T1	M2_RUNX1_RUNX1T1_not	0.000238628571428571
BID	1.17927062363548	0.033	M1_FLT3	M1_FLT3_not	0.171789473684211
BID	0.861824762058086	0.031	M2_RUNX1_RUNX1T1	M2_RUNX1_RUNX1T1_not	0.168452830188679
BID	1.17370261014633	0.023	M4_Normal_Karyotype	M4_Normal_Karyotype_not	0.127384615384615
BID	1.38415191748071	0.05625	M4_NPM1	M4_NPM1_not	0.0674742857142857
BID	1.29372407439415	0:15	M4_MLL	M4_MLL_not	0.01728
BID	1.22964368155286	0:11	M1_Normal_Karyotype	M1_Normal_Karyotype_not	0.0916666666666667
BID	0.387532618002298	0.00032	M4_PML_RARA	M4_PML_RARA_not	0.00542117647058824
BID	1.30726034160321	0.00000074	M2_Normal_Karyotype	M2_Normal_Karyotype_not	0.00005328
BCL2L2	1.12618045156325	0.006	M4_Normal_Karyotype	M4_Normal_Karyotype_not	0.055741935483871
BCL2L2	1.14476868253821	0.00031	M2_Normal_Karyotype	M2_Normal_Karyotype_not	0.00542117647058824
BCL2L2	1.24396484490867	0.00015	M1_Normal_Karyotype	M1_Normal_Karyotype_not	0.00354461538461538
BCL2L11	1.13465097088763	0.043	M4_MLL	M4_MLL_not	0.194953846153846
BCL2L11	0.708712610261583	0.034	M4_PML_RARA	M4_PML_RARA_not	0.171789473684211
BCL2L11	0.689433444956833	0.021	M4_Complex_Karyotype	M4_Complex_Karyotype_not	0.0875
BCL2L11	1.11317224078842	0.016	M1_Normal_Karyotype	M1_Normal_Karyotype_not	0.109714285714286
BCL2L11	1.2213135078751	0.00024	M2_Normal_Karyotype	M2_Normal_Karyotype_not	0.004608
BCL2L1	1.19547815172798	0.043	M0_FLT3	M0_FLT3_not	0.194953846153846
BCL2L1	0.781148122411102	0.039	M2_RUNX1_RUNX1T1	M2_RUNX1_RUNX1T1_not	1.Mar
BCL2L1	0.742261182267481	0.022	M1_FLT3	M1_FLT3_not	0.12672
BCL2L1	2.53961519518251	0.0680555555	M4_PML_RARA	M4_PML_RARA_not	0.0742736842105263
BCL2L1	0.710124862023932	0:29	M1_NPM1	M1_NPM1_not	0.0309333333333333
BCL2L1	0.59791219049376	0:29	M0_RUNX1	M0_RUNX1_not	0.0309333333333333
BCL2L1	0.662600782521901	0.00002	M4_CBFB_MYH11	M4_CBFB_MYH11_not	0.00072
BCL2A1	1.55750398222968	0.048	M1_Normal_Karyotype	M1_Normal_Karyotype_not	0.197485714285714
BCL2A1	1.65920964456813	0.022	M4_Normal_Karyotype	M4_Normal_Karyotype_not	0.12672
BCL2A1	2.22686664880868	0.017	M4_NPM1	M4_NPM1_not	0.113860465116279
BCL2A1	1.58642657574795	0.06597222	M2_RUNX1_RUNX1T1	M2_RUNX1_RUNX1T1_not	0.0739459459459459
BCL2A1	0.151745146078337	0.00054	M4_PML_RARA	M4_PML_RARA_not	0.00864
BCL2	0.733797221400413	0.048	M5_NPM1	M5_NPM1_not	0.197485714285714
BCL2	0.860405437834124	0.045	M1_FLT3	M1_FLT3_not	0.196363636363636
BCL2	1.28119581653159	0.044	M3_PML_RARA	M3_PML_RARA_not	0.194953846153846
BCL2	0.852592588798731	0.018	M3_FLT3	M3_FLT3_not	0.8
BCL2	0.67451524953953	0.013	M5_FLT3	M5_FLT3_not	0.65
BCL2	0.82269339973893	0:42	M4_NPM1	M4_NPM1_not	0.0417103448275862
BCL2	0.850232600007102	0.00021	M4_Normal_Karyotype	M4_Normal_Karyotype_not	0.00432
BCL2	0.751107654233825	0.000052	M5_Normal_Karyotype	M5_Normal_Karyotype_not	0.0014976
BCL2	1.29859627544566	0.0000049	M4_MLL	M4_MLL_not	0.0002352
BCL2	0.838851404076079	0.0000026	M2_RUNX1_RUNX1T1	M2_RUNX1_RUNX1T1_not	0.00014976
BBC3	0.798200609781568	0.046	M3_FLT3	M3_FLT3_not	0.197485714285714
BBC3	0.784040934259313	0.044	M5_NPM1	M5_NPM1_not	0.194953846153846
BBC3	0.831310526735062	0.06527777	M1_FLT3	M1_FLT3_not	0.0739459459459459
BBC3	0.811121389993591	0.047222222	M1_NPM1	M1_NPM1_not	0.0593454545454545
BBC3	0.778278216529712	0.005	M4_CBFB_MYH11	M4_CBFB_MYH11_not	0.048
BBC3	1.23589818369627	0.00064	M2_RUNX1_RUNX1T1	M2_RUNX1_RUNX1T1_not	0.00936
BBC3	1.72833190839971	5.9e-13	M4_MLL	M4_MLL_not	1.6992e-10
BAX	0.778002319049533	0:04	M0_Complex_Karyotype	M0_Complex_Karyotype_not	0.188852459016393
BAX	1.57665571078159	0.012	M2_FLT3	M2_FLT3_not	0.0886153846153846
BAX	1.28313987970808	0:39	M1_NPM1	M1_NPM1_not	0.0401142857142857
BAX	1.52310439266921	0:11	M3_FLT3	M3_FLT3_not	0.0916666666666667
BAX	1.37826360031991	0.00089	M1_FLT3	M1_FLT3_not	0.0122057142857143
BAX	1.57243937736906	0.00008	M4_NPM1	M4_NPM1_not	0.00209454545454545
B2M	1.08817349938241	0.037	M4_NPM1	M4_NPM1_not	0.180610169491525
B2M	0.794876633296565	0.023	M4_PML_RARA	M4_PML_RARA_not	0.127384615384615
B2M	0.936691458305754	0:02	M4_MLL	M4_MLL_not	0.122553191489362
B2M	1.25873564626617	0.018	M1_Complex_Karyotype	M1_Complex_Karyotype_not	0.8
B2M	1.10562717059934	0.00065	M4_Normal_Karyotype	M4_Normal_Karyotype_not	0.00936

Supplemental Table S6. List of pathways enriched in M0/1/2 or M4/5 groups based on GSEA analysis

Gene Sets used	# Gene Sets
BIOCARTA_MsigDB_c2	217
KEGG_MsigDB_c2	186
MsigDB_HALLMARKS	46
NCI_NATURE_V4_PID	212
REACTOME_MsigDB_c2	669
WIKIPW	268

Description
Phenotypes compared: FAB M4 and M5 vs. M0 and M1 FDR cutoff 0.1 used for filtering in both Hemap and TCGA data sets Tabs 1-2 contain GSEA results upregulated in M4 and M5 groups, compared to M0 and M1 groups. Pathway FDR and NES values shown in Figure 4C are highlighted for Hemap GSEA results (**a**: Hemap_pathways_M4_M5). Similar/Same pathways are highlighted for TCGA AML data set (**b**: TCGA_pathways_FAB_M4_M5). **c-d** contain GSEA results upregulated in M0 and M1 groups, compared to M4 and M5 groups.

a. Hemap pathways M4 M5

NAME	SIZE	NES	NOM p-val	FDR q-val	FWER p-val
LYSOSOME-KEGG_MSIGDB_C2	115	2.3478072	0.0	0.0	0.0
COMPLEMENT-MSIGDB_HALLMARKS	195	2.343244	0.0	0.0	0.0
INFLAMMATORY_RESPONSE-MSIGDB_HALLMARKS	198	2.3351223	0.0	0.0	0.0
TNFA_SIGNALING_VIA_NFKB-MSIGDB_HALLMARKS	198	2.3276932	0.0	0.0	0.0
AUTOPHAGY_PERERA	126	2.3188524	0.0	0.0	0.0
INNATE_IMMUNE_SYSTEM-REACTOME_MSIGDB_C2	228	2.250565	0.0	0.0	0.0
INTERFERON_GAMMA_RESPONSE-MSIGDB_HALLMARKS	192	2.1368678	0.0	1.7228287E-4	0.001
CHEMOKINE_RECEPTORS_BIND_CHEMOKINES-REACTOME_MSIGDB_C2	47	2.1088302	0.0	3.0182963E-4	0.002
LEISHMANIA_INFECTION-KEGG_MSIGDB_C2	62	2.08367	0.0	5.348594E-4	0.004
TOLL_RECEPTOR_CASCADES-REACTOME_MSIGDB_C2	109	2.0506792	0.0	4.8137348E-4	0.004
PEPTIDE_GPCRS_HOMO_SAPIENS-WIKIPW	74	2.043489	0.0	7.6871586E-4	0.007
REGULATION_OF_TOLL_LIKE_RECEPTOR_SIGNALING_PATHWAY_HOMO_SAPIENS-WIKIPW	132	2.0370507	0.0	8.063938E-4	0.008
GRAFT_VERSUS_HOST_DISEASE-KEGG_MSIGDB_C2	34	2.0347688	0.0	7.443635E-4	0.008
ASTHMA-KEGG_MSIGDB_C2	26	2.0329287	0.0	6.911947E-4	0.008
COMPLEMENT_CASCADE-REACTOME_MSIGDB_C2	27	2.026121	0.0	8.8256015E-4	0.011
GLYCOSPHINGOLIPID_METABOLISM-REACTOME_MSIGDB_C2	31	2.0222964	0.0	8.2740013E-4	0.011
DEFENSINS-REACTOME_MSIGDB_C2	20	2.0215194	0.0	7.787295E-4	0.011
LATENT_INFECTION_OF_HOMO_SAPIENS_WITH_MYCOBACTERIUM_TUBERCULOSIS-REACTC	31	2.0187643	0.0	8.029891E-4	0.012
IL6_JAK_STAT3_SIGNALING-MSIGDB_HALLMARKS	84	2.0077882	0.0	8.237802E-4	0.013
TOLL_LIKE_RECEPTOR_SIGNALING_PATHWAY_HOMO_SAPIENS-WIKIPW	94	1.9875175	0.0	0.0013735475	0.023
COAGULATION-MSIGDB_HALLMARKS	135	1.9844366	0.0	0.0013637216	0.024
ALLOGRAFT_REJECTION-MSIGDB_HALLMARKS	196	1.9836742	0.0	0.0013569181	0.025
CYTOKINE_CYTOKINE_RECEPTOR_INTERACTION-KEGG_MSIGDB_C2	241	1.9803885	0.0	0.0014005655	0.026
NOD_PATHWAY_HOMO_SAPIENS-WIKIPW	39	1.9762907	0.0	0.0014428999	0.028
TOLL_LIKE_RECEPTOR_SIGNALING_PATHWAY-KEGG_MSIGDB_C2	93	1.9625736	0.0	0.001962531	0:04
ALLOGRAFT_REJECTION-KEGG_MSIGDB_C2	33	1.9615821	0.0	0.0019347536	0.041
TYPE_I_DIABETES_MELLITUS-KEGG_MSIGDB_C2	38	1.9583794	0.0	0.0019937467	0.044
ENDOGENOUS_TLR_SIGNALING-NCI_NATURE_V4_PID	21	1.9443305	0.0	0.0029056724	0.064
NKT_PATHWAY-BIOCARTA_MSIGDB_C2	28	1.9425817	0.0	0.0028884178	0.066
AUTOIMMUNE_THYROID_DISEASE-KEGG_MSIGDB_C2	43	1.9289705	0.0016891892	0.0034312068	0.082
INITIAL_TRIGGERING_OF_COMPLEMENT-REACTOME_MSIGDB_C2	12	1.9231982	0.0	0.0037407903	0.092
TYPE_II_INTERFERON_SIGNALING_IFNG_HOMO_SAPIENS-WIKIPW	45	1.9084904	0.001858736	0.0049311225	0,086111111
UROKINASE_TYPE_PLASMINOGEN_ACTIVATOR_UPA_AND_UPAR_MEDIATED_SIGNALING-NCI	41	1.9069377	0.0	0.0048520663	0,0875
INTESTINAL_IMMUNE_NETWORK_FOR_IGA_PRODUCTION-KEGG_MSIGDB_C2	43	1.8958616	0.0	0.0055542206	0,102083333
G_ALPHA_I_SIGNALLING_EVENTS-REACTOME_MSIGDB_C2	178	1.8942508	0.0	0.0056667486	0,106944444
INTERFERON_GAMMA_SIGNALING-REACTOME_MSIGDB_C2	54	1.8881397	0.0	0.006112306	0:17
MIR_TARGETED_GENES_IN_LEUKOCYTES_TARBASE_HOMO_SAPIENS-WIKIPW	124	1.8868557	0.0	0.0060744053	0,120138889
NOD_LIKE_RECEPTOR_SIGNALING_PATHWAY-KEGG_MSIGDB_C2	59	1.8848151	0.0	0.0061962404	0,124305556
DRUG_METABOLISM_OTHER_ENZYMES-KEGG_MSIGDB_C2	36	1.8839298	0.0	0.006161087	0,126388889
TRYPTOPHAN_METABOLISM-KEGG_MSIGDB_C2	39	1.8723725	0.0	0.0072437017	0,147222222
XENOBIOTIC_METABOLISM-MSIGDB_HALLMARKS	198	1.8710536	0.0	0.007181866	0,149305556
RESPONSE_TO_ELEVATED_PLATELET_CYTOSOLIC_CA2-REACTOME_MSIGDB_C2	78	1.8676574	0.0	0.0073516537	0,154861111
SPHINGOLIPID_METABOLISM-REACTOME_MSIGDB_C2	60	1.8656232	0.0	0.0073786466	0,158333333
AMINO_SUGAR_AND_NUCLEOTIDE_SUGAR_METABOLISM-KEGG_MSIGDB_C2	44	1.8603723	0.0	0.007975923	0:25
CLASS_A1_RHODOPSIN_LIKE_RECEPTORS-REACTOME_MSIGDB_C2	266	1.8585489	0.0	0.008198349	0:26
BLYMPHOCYTE_PATHWAY-BIOCARTA_MSIGDB_C2	11	1.8583672	0.0	0.008020124	0:26
COMP_PATHWAY-BIOCARTA_MSIGDB_C2	17	1.8539504	0.0037453184	0.008232725	0:27
MHC_CLASS_II_ANTIGEN_PRESENTATION-REACTOME_MSIGDB_C2	85	1.8520563	0.0	0.008308948	0,193055556
ASBCELL_PATHWAY-BIOCARTA_MSIGDB_C2	12	1.8385426	0.0038535646	0.010367282	0,233333333
BETA_DEFENSINS-REACTOME_MSIGDB_C2	15	1.8373345	0.0	0.010327304	0,235416667
GRANULOCYTES_PATHWAY-BIOCARTA_MSIGDB_C2	13	1.8350328	0.0	0.010567534	0:35
PEPTIDE_LIGAND_BINDING_RECEPTORS-REACTOME_MSIGDB_C2	163	1.8329688	0.0	0.010687501	0,249305556
BETA2_INTEGRIN_CELL_SURFACE_INTERACTIONS-NCI_NATURE_V4_PID	28	1.8259956	0.0	0.011866686	0,277083333
COMPLEMENT_AND_COAGULATION_CASCADES_HOMO_SAPIENS-WIKIPW	59	1.8206196	0.0	0.012974642	0,303472222
GLYCOSAMINOGLYCAN_DEGRADATION-KEGG_MSIGDB_C2	20	1.8106389	0.0018518518	0.015000159	0,340972222
VIRAL_MYOCARDITIS-KEGG_MSIGDB_C2	66	1.8059531	0.0	0.016268117	0,370138889
ANTIGEN_PROCESSING_AND_PRESENTATION-KEGG_MSIGDB_C2	69	1.8056929	0.0017271157	0.016046226	0,370833333
REGULATION_OF_COMPLEMENT_CASCADE-REACTOME_MSIGDB_C2	11	1.7962474	0.0	0.018429259	0,406944444
OTHER_GLYCAN_DEGRADATION-KEGG_MSIGDB_C2	14	1.7960724	0.0038910506	0.018177697	0,407638889
IMMUNOREGULATORY_INTERACTIONS_BETWEEN_A_LYMPHOID_AND_A_NON_LYMPHOID_CE	57	1.7958027	0.0033898305	0.01805409	0,408333333
CELLULAR_ROLES_OF_ANTHRAX_TOXIN-NCI_NATURE_V4_PID	20	1.7946202	0.0019193857	0.018011529	0,411111111
ACTIVATED_TLR4_SIGNALLING-REACTOME_MSIGDB_C2	87	1.77979	0.0	0.022874016	0,466666667
AMB2_INTEGRIN_SIGNALING-NCI_NATURE_V4_PID	39	1.7786366	0.0	0.023003928	0,470833333
COMPLEMENT_ACTIVATION_CLASSICAL_PATHWAY_HOMO_SAPIENS-WIKIPW	15	1.7775025	0.0018691589	0.02295853	0,475694444
IL1_AND_MEGAKARYOTYCES_IN_OBESITY_HOMO_SAPIENS-WIKIPW	24	1.7713904	0.0	0.02480294	0,502777778
COMPLEMENT_AND_COAGULATION_CASCADES-KEGG_MSIGDB_C2	67	1.7684401	0.0	0.025404943	0,511805556
FRUCTOSE_AND_MANNOSE_METABOLISM-KEGG_MSIGDB_C2	33	1.76629	0.001858736	0.025670573	0,518055556
SELENIUM_MICRONUTRIENT_NETWORK_HOMO_SAPIENS-WIKIPW	75	1.7659597	0.0	0.025451915	0,520138889
VITAMIN_A_AND_CAROTENOID_METABOLISM_HOMO_SAPIENS-WIKIPW	41	1.7642174	0.0034843206	0.025775777	0,525694444
MIR_TARGETED_GENES_IN_ADIPOCYTES_TARBASE_HOMO_SAPIENS-WIKIPW	18	1.7541918	0.008710802	0.029044293	0,554166667
PROSTAGLANDIN_SYNTHESIS_AND_REGULATION_HOMO_SAPIENS-WIKIPW	30	1.7526916	0.0	0.029093375	0,556944444
PATHOGENIC_ESCHERICHIA_COLI_INFECTION_HOMO_SAPIENS-WIKIPW	48	1.7484798	0.0018552876	0.030593485	0,570833333
ESTROGEN_METABOLISM_HOMO_SAPIENS-WIKIPW	11	1.7388055	0.0	0.034731656	0,602083333
CHEMOKINE_SIGNALING_PATHWAY-KEGG_MSIGDB_C2	174	1.7384808	0.0	0.034390893	0,603472222
ALLOGRAFT_REJECTION_HOMO_SAPIENS-WIKIPW	75	1.7381173	0.0	0.0340606	0,603472222
CLASSIC_PATHWAY-BIOCARTA_MSIGDB_C2	12	1.7356001	0.0	0.03503313	0,6125
CHOLESTEROL_HOMEOSTASIS-MSIGDB_HALLMARKS	70	1.7279915	0.0	0.038405422	0,063194444
NFKB_PATHWAY-BIOCARTA_MSIGDB_C2	22	1.7265931	0.0074626864	0.03868125	0,639583333
INFLAMMASOMES-REACTOME_MSIGDB_C2	16	1.725987	0.0038461538	0.038419243	0,640972222
TRAFFICKING_AND_PROCESSING_OF_ENDOSOMAL_TLR-REACTOME_MSIGDB_C2	11	1.7243962	0.0036231885	0.038673766	0,642361111
GPCR_LIGAND_BINDING-REACTOME_MSIGDB_C2	363	1.7220628	0.0	0.039540596	0,647916667
NUCLEOTIDE_BINDING_DOMAIN_LEUCINE_RICH_REPEAT_CONTAINING_RECEPTOR_NLR_SI(	43	1.7134289	0.0017513135	0.04361832	0,658333333
ACYL_CHAIN_REMODELLING_OF_PC-REACTOME_MSIGDB_C2	21	1.712849	0.001858736	0.043278914	0,658333333
NRF2_PATHWAY_HOMO_SAPIENS-WIKIPW	126	1.7114978	0.0	0.04350631	0,660416667
GALACTOSE_METABOLISM-KEGG_MSIGDB_C2	25	1.7110187	0.0018832391	0.043373715	0,661111111
IL5_PATHWAY-BIOCARTA_MSIGDB_C2	10	1.7108009	0.0076045627	0.042979483	0,661111111
TRANSPORT_OF_ORGANIC_ANIONS-REACTOME_MSIGDB_C2	11	1.7085909	0.0038314175	0.043693453	0,663194444
GLYCOLYSIS_GLUCONEOGENESIS-KEGG_MSIGDB_C2	58	1.7075341	0.0	0.043797065	0,664583333
NATURAL_KILLER_CELL_MEDIATED_CYTOTOXICITY-KEGG_MSIGDB_C2	120	1.706334	0.0	0.04397289	0,666666667
ALPHA9_BETA1_INTEGRIN_SIGNALING_EVENTS-NCI_NATURE_V4_PID	23	1.7053128	0.010928961	0.0440723	0,668055556
LAIR_PATHWAY-BIOCARTA_MSIGDB_C2	15	1.7032646	0.0057471264	0.04469221	0,669444444
PENTOSE_PHOSPHATE_PATHWAY-KEGG_MSIGDB_C2	26	1.700436	0.0072202166	0.045846205	0,675694444
PORPHYRIN_AND_CHLOROPHYLL_METABOLISM-KEGG_MSIGDB_C2	27	1.69813	0.005291005	0.046777774	0,678472222
EPITHELIAL_MESENCHYMAL_TRANSITION-MSIGDB_HALLMARKS	195	1.6976151	0.0	0.046637498	0,679861111
MYD88_MAL_CASCADE_INITIATED_ON_PLASMA_MEMBRANE-REACTOME_MSIGDB_C2	78	1.6952728	0.0	0.04758159	0,68125

APOPTOSIS-MSIGDB_HALLMARKS	154	1.6921626	0.0	0.049193498	0,684722222
PATHOGENIC_ESCHERICHIA_COLI_INFECTION-KEGG_MSIGDB_C2	47	1.6890907	0.0034965035	0.050781187	0,685416667
PROTEOLYTIC_CLEAVAGE_OF_SNARE_COMPLEX_PROTEINS-REACTOME_MSIGDB_C2	16	1.6857909	0.007633588	0.052279808	0,686805556
PHOSPHOLIPID_METABOLISM-REACTOME_MSIGDB_C2	184	1.6856605	0.0	0.051788203	0,686805556
CELL_SURFACE_INTERACTIONS_AT_THE_VASCULAR_WALL-REACTOME_MSIGDB_C2	83	1.6852442	0.0	0.05151062	0,06875
OXIDATIVE_STRESS_HOMO_SAPIENS-WIKIPW	27	1.6797848	0.007707129	0.054458633	0,689583333
CCR5_PATHWAY-BIOCARTA_MSIGDB_C2	16	1.6789361	0.011049724	0.05451289	0,690972222
AFLATOXIN_B1_METABOLISM_HOMO_SAPIENS-WIKIPW	7	1.6753579	0.0039138943	0.056466527	0,692361111
IL10_PATHWAY-BIOCARTA_MSIGDB_C2	17	1.6735388	0.013513514	0.05728159	0,693055556
IL8_AND_CXCR2_MEDIATED_SIGNALING_EVENTS-NCI_NATURE_V4_PID	33	1.6728045	0.006968641	0.05733942	0,693055556
TCA_CYCLE_HOMO_SAPIENS-WIKIPW	15	1.66867	0.014897579	0.0598627	0,69375
HYPOXIA-MSIGDB_HALLMARKS	196	1.668391	0.0	0.059540678	0,69375
TRANSCRIPTIONAL_REGULATION_OF_WHITE_ADIPOCYTE_DIFFERENTIATION-REACTOME_M	71	1.6667705	0.0017123288	0.05997225	1.0
GLYCOLYSIS-MSIGDB_HALLMARKS	197	1.6655061	0.0	0.060486093	1.0
INSULIN_RECEPTOR_RECYCLING-REACTOME_MSIGDB_C2	23	1.6649512	0.009259259	0.06040619	1.0
CREATION_OF_C4_AND_C2_ACTIVATORS-REACTOME_MSIGDB_C2	8	1.6642468	0.018975332	0.0603052	1.0
EXTRACELLULAR_MATRIX_ORGANIZATION-REACTOME_MSIGDB_C2	83	1.6633364	0.0	0.060440727	1.0
METABOLISM_OF_CARBOHYDRATES-REACTOME_MSIGDB_C2	225	1.6589205	0.0	0.06327869	1.0
EICOSANOID_SYNTHESIS_HOMO_SAPIENS-WIKIPW	19	1.6586562	0.007968128	0.06296571	1.0
CITRIC_ACID_CYCLE_TCA_CYCLE-REACTOME_MSIGDB_C2	17	1.658191	0.0056179776	0.06284566	1.0
ACTIVATION_OF_CHAPERONE_GENES_BY_XBP1S-REACTOME_MSIGDB_C2	43	1.6561605	0.0051993066	0.063923225	1.0
PPAR_SIGNALING_PATHWAY-KEGG_MSIGDB_C2	65	1.6538312	0.001669449	0.06500077	1.0
CYTOKINES_AND_INFLAMMATORY_RESPONSE_HOMO_SAPIENS-WIKIPW	26	1.6532228	0.0036429872	0.06488565	1.0
HEMATOPOIETIC_CELL_LINEAGE-KEGG_MSIGDB_C2	80	1.6530755	0.0	0.06445038	1.0
GPCRS_CLASS_A_RHODOPSIN_LIKE_HOMO_SAPIENS-WIKIPW	239	1.6507281	0.0	0.06589687	1.0
IL6_MEDIATED_SIGNALING_EVENTS-NCI_NATURE_V4_PID	47	1.650253	0.008695652	0.065697476	1.0
TRANS_GOLGI_NETWORK_VESICLE_BUDDING-REACTOME_MSIGDB_C2	55	1.6474315	0.0017006802	0.067326166	1.0
INTEGRIN_CELL_SURFACE_INTERACTIONS-REACTOME_MSIGDB_C2	75	1.6473687	0.0	0.066837445	1.0
GLYCEROPHOSPHOLIPID_BIOSYNTHESIS-REACTOME_MSIGDB_C2	79	1.6460551	0.0	0.06735077	1.0
CITRATE_CYCLE_TCA_CYCLE-KEGG_MSIGDB_C2	28	1.6457946	0.007677543	0.067013696	1.0
PYRIMIDINE_CATABOLISM-REACTOME_MSIGDB_C2	11	1.6452745	0.011257036	0.06688107	1.0
ESTROGEN_RESPONSE_LATE-MSIGDB_HALLMARKS	194	1.6426522	0.0	0.068143494	1.0
FLUOROPYRIMIDINE_ACTIVITY_HOMO_SAPIENS-WIKIPW	30	1.6416718	0.005524862	0.06829588	1.0
SRCRPTP_PATHWAY-BIOCARTA_MSIGDB_C2	11	1.6410359	0.01178782	0.06828524	1.0
PASSIVE_TRANSPORT_BY_AQUAPORINS-REACTOME_MSIGDB_C2	11	1.6408049	0.01764706	0.067888156	1.0
TRYPTOPHAN_METABOLISM_HOMO_SAPIENS-WIKIPW	45	1.6398511	0.0035211267	0.067991175	1.0
ACYL_CHAIN_REMODELLING_OF_PI-REACTOME_MSIGDB_C2	14	1.6395913	0.01171875	0.067639105	1.0
SEMAPHORIN_INTERACTIONS_HOMO_SAPIENS-WIKIPW	59	1.6353679	0.012522361	0.07031885	1.0
IL1_SIGNALING-REACTOME_MSIGDB_C2	37	1.634831	0.006980803	0.07018751	1.0
CELL_ADHESION_MOLECULES_CAMS-KEGG_MSIGDB_C2	126	1.6340678	0.0016313214	0.07024489	1.0
ACYL_CHAIN_REMODELLING_OF_PE-REACTOME_MSIGDB_C2	20	1.6337074	0.016759777	0.069967195	1.0
STARCH_AND_SUCROSE_METABOLISM-KEGG_MSIGDB_C2	34	1.633455	0.008833922	0.06968275	1.0
HEPARAN_SULFATE_HEPARIN_HS_GAG_METABOLISM-REACTOME_MSIGDB_C2	49	1.6303673	0.00681431	0.0715993	1.0
THE_ACTIVATION_OF_ARYLSULFATASES-REACTOME_MSIGDB_C2	11	1.6280007	0.009416196	0.0728954	1.0
IL_13_PATHWAY-ST_MSIGDB_C2	7	1.6248584	0.021868788	0.07495972	1.0
ARYL_HYDROCARBON_RECEPTOR_PATHWAY_HOMO_SAPIENS-WIKIPW	40	1.624539	0.012048192	0.07474888	1.0
TRYPTOPHAN_CATABOLISM-REACTOME_MSIGDB_C2	11	1.6241167	0.019148936	0.07451774	1.0
FARNESOID_X_RECEPTOR_PATHWAY_HOMO_SAPIENS-WIKIPW	19	1.6227708	0.015296367	0.07507139	1.0
SIGNALING_BY_ILS-REACTOME_MSIGDB_C2	104	1.6220388	0.004862237	0.075114556	1.0
MMP_CYTOKINE_CONNECTION-SA_MSIGDB_C2	14	1.6217715	0.020295203	0.07485968	1.0
INTERLEUKIN_13_PATHWAY-ST_MSIGDB_C2	7	1.6205595	0.0058479533	0.07530522	1.0
SYNDECAN_1_MEDIATED_SIGNALING_EVENTS-NCI_NATURE_V4_PID	46	1.620366	0.010791367	0.074899785	1.0
TH1TH2_PATHWAY-BIOCARTA_MSIGDB_C2	19	1.6182076	0.017408123	0.07628678	1.0
PYRIMIDINE_METABOLISM-REACTOME_MSIGDB_C2	23	1.6152003	0.017889088	0.07797477	1.0
MTORC1_SIGNALING-MSIGDB_HALLMARKS	190	1.6146309	0.0	0.07799177	1.0
SYNTHESIS_SECRETION_AND_DEACYLATION_OF_GHRELIN-REACTOME_MSIGDB_C2	14	1.6144068	0.013487476	0.077609934	1.0
TOLL_PATHWAY-BIOCARTA_MSIGDB_C2	36	1.6143557	0.0055555557	0.077145904	1.0
ADIPOGENESIS_HOMO_SAPIENS-WIKIPW	131	1.6126872	0.0015923567	0.07807567	1.0
FOXM1_TRANSCRIPTION_FACTOR_NETWORK-NCI_NATURE_V4_PID	40	1.6104096	0.014545455	0.079284914	1.0
IRON_UPTAKE_AND_TRANSPORT-REACTOME_MSIGDB_C2	36	1.6093265	0.01056338	0.0795856	1.0
SEMAPHORIN_INTERACTIONS-REACTOME_MSIGDB_C2	61	1.607096	0.005226481	0.080940954	1.0
PTM_GAMMA_CARBOXYLATION_HYPUSINE_FORMATION_AND_ARYLSULFATASE_ACTIVATION	25	1.6052597	0.02550091	0.08207442	1.0
EXTRINSIC_PATHWAY_FOR_APOPTOSIS-REACTOME_MSIGDB_C2	13	1.6046011	0.015779093	0.08203759	1.0
TRANSFERRIN_ENDOCYTOSIS_AND_RECYCLING-REACTOME_MSIGDB_C2	25	1.6044006	0.013409962	0.081723355	1.0
VITAMIN_D_METABOLISM_HOMO_SAPIENS-WIKIPW	10	1.603438	0,086805556	0.081995435	1.0
SIGNAL_REGULATORY_PROTEIN_SIRP_FAMILY_INTERACTIONS-REACTOME_MSIGDB_C2	12	1.6016104	0:01	0.083169356	1.0
FACILITATIVE_NA_INDEPENDENT_GLUCOSE_TRANSPORTERS-REACTOME_MSIGDB_C2	11	1.6015124	0.018691588	0.08272985	1.0
MEMBRANE_TRAFFICKING-REACTOME_MSIGDB_C2	119	1.5968033	0:16	0.086138286	1.0
ADIPOGENESIS-MSIGDB_HALLMARKS	192	1.5934712	0.0	0.08855022	1.0
SYSTEMIC_LUPUS_ERYTHEMATOSUS-KEGG_MSIGDB_C2	97	1.593325	0.0033112583	0.08819583	1.0
FATTY_ACID_METABOLISM-MSIGDB_HALLMARKS	151	1.5932225	0.0	0.08775134	1.0
IL2_STAT5_SIGNALING-MSIGDB_HALLMARKS	195	1.5931234	0.0014925373	0.08731164	1.0
PLATELET_SENSITIZATION_BY_LDL-REACTOME_MSIGDB_C2	16	1.5926871	0.032136105	0.08717848	1.0
RECYCLING_PATHWAY_OF_L1-REACTOME_MSIGDB_C2	26	1.5920074	0.018214935	0.08729935	1.0
VIBRIO_CHOLERAE_INFECTION-KEGG_MSIGDB_C2	54	1.5905054	0.008896797	0.08819444	1.0
CHYLOMICRON_MEDIATED_LIPID_TRANSPORT-REACTOME_MSIGDB_C2	15	1.5871545	0.026768642	0.0905402	1.0
METABOLISM_OF_LIPIDS_AND_LIPOPROTEINS-REACTOME_MSIGDB_C2	451	1.5862147	0.0	0.09072347	1.0
LYSOSOME_VESICLE_BIOGENESIS-REACTOME_MSIGDB_C2	22	1.5859137	0.029357798	0.090469696	1.0
INSULIN_SIGNALING_PATHWAY-KEGG_MSIGDB_C2	136	1.5853269	0.0032626428	0.09035542	1.0
PRION_DISEASES-KEGG_MSIGDB_C2	35	4,101388889	0.017667845	0.09042277	1.0
INFLAMMATORY_RESPONSE_PATHWAY_HOMO_SAPIENS-WIKIPW	32	1.5844898	0.0120689655	0.090010196	1.0
P53_PATHWAY-MSIGDB_HALLMARKS	192	1.5824254	0.0	0.09131202	1.0
ENDOSOMAL_VACUOLAR_PATHWAY-REACTOME_MSIGDB_C2	8	1.5820465	0.018691588	0.09109514	1.0
PYRUVATE_METABOLISM_AND_CITRIC_ACID_TCA_CYCLE-REACTOME_MSIGDB_C2	37	1.5806319	0.014414415	0.09172881	1.0
ANTIGEN_PRESENTATION_FOLDING_ASSEMBLY_AND_PEPTIDE_LOADING_OF_CLASS_I_MHC	20	1.5803474	0.020408163	0.091519676	1.0
CACAM_PATHWAY-BIOCARTA_MSIGDB_C2	13	1.5784625	0.020446097	0.09277978	1.0
GLUTATHIONE_METABOLISM-KEGG_MSIGDB_C2	41	1.5754027	0.012567325	0.09499628	1.0
TID_PATHWAY-BIOCARTA_MSIGDB_C2	18	1.5753582	0.017667845	0.0945289	1.0
CS_DS_DEGRADATION-REACTOME_MSIGDB_C2	12	1.5745596	0.022944551	0.09476724	1.0
IL1R_PATHWAY-BIOCARTA_MSIGDB_C2	33	1.5736711	0.015706806	0.095026664	1.0
REGULATION_OF_RAS_FAMILY_ACTIVATION-NCI_NATURE_V4_PID	32	1.5717614	0.0144665465	0.09619591	1.0
CA_DEPENDENT_EVENTS-REACTOME_MSIGDB_C2	29	1.5716568	0.01908397	0.095783725	1.0
VITAMIN_B12_METABOLISM_HOMO_SAPIENS-WIKIPW	47	1.5710026	0.003539823	0.09583495	1.0
MONOCYTE_PATHWAY-BIOCARTA_MSIGDB_C2	10	1.5693622	0.029350106	0.096923806	1.0
IKK_COMPLEX_RECRUITMENT_MEDIATED_BY_RIP1-REACTOME_MSIGDB_C2	8	1.5678713	0.017892644	0.09768813	1.0
GLUCOSE_METABOLISM-REACTOME_MSIGDB_C2	62	1.5673448	0.010291595	0.097697824	1.0
SPINAL_CORD_INJURY_HOMO_SAPIENS-WIKIPW	113	1.5668738	0.0016528926	0.09761402	1.0

b. TCGA pathways FAB M4 M5

NAME	SIZE	NES
COMPLEMENT-MSIGDB_HALLMARKS	178	2.4659095
INNATE_IMMUNE_SYSTEM-REACTOME_MSIGDB_C2	203	2.4300048
LYSOSOME-KEGG_MSIGDB_C2	116	2.3901496
INTERFERON_GAMMA_SIGNALING-REACTOME_MSIGDB_C2	55	2.3893356
INFLAMMATORY_RESPONSE-MSIGDB_HALLMARKS	177	2.387301
RESPIRATORY_ELECTRON_TRANSPORT_ATP_SYNTHESIS_BY_CHEMIOSMOTIC_COUPLING_AND_HEAT_PRODUCTION_BY_UNCOUP	80	2.3246846
LEISHMANIA_INFECTION-KEGG_MSIGDB_C2	66	2.275647
NOD_PATHWAY_HOMO_SAPIENS-WIKIPW	39	2.2497606
ASTHMA-KEGG_MSIGDB_C2	22	2.2374625
AUTOPHAGY_PERERA	128	2.2353656
RESPIRATORY_ELECTRON_TRANSPORT-REACTOME_MSIGDB_C2	65	2.2231672
AUTOIMMUNE_THYROID_DISEASE-KEGG_MSIGDB_C2	31	2.1940403
OXIDATIVE_PHOSPHORYLATION-KEGG_MSIGDB_C2	104	2.1628115
INTERFERON_GAMMA_RESPONSE-MSIGDB_HALLMARKS	195	2.1415317
ANTIGEN_PROCESSING_CROSS_PRESENTATION-REACTOME_MSIGDB_C2	71	2.136082
TNFA_SIGNALING_VIA_NFKB-MSIGDB_HALLMARKS	192	2.132777
TOLL_RECEPTOR_CASCADES-REACTOME_MSIGDB_C2	113	2.1202414
OXIDATIVE_PHOSPHORYLATION-MSIGDB_HALLMARKS	200	2.1127346
OXIDATIVE_PHOSPHORYLATION_HOMO_SAPIENS-WIKIPW	52	2.0998044
ALLOGRAFT_REJECTION-KEGG_MSIGDB_C2	31	2.092165
FLUOROPYRIMIDINE_ACTIVITY_HOMO_SAPIENS-WIKIPW	30	2.0869112
ALLOGRAFT_REJECTION-MSIGDB_HALLMARKS	181	2.076678
IMMUNOREGULATORY_INTERACTIONS_BETWEEN_A_LYMPHOID_AND_A_NON_LYMPHOID_CELL-REACTOME_MSIGDB_C2	60	2.0719802
GRAFT_VERSUS_HOST_DISEASE-KEGG_MSIGDB_C2	35	2.0506659
ANTIGEN_PROCESSING_AND_PRESENTATION-KEGG_MSIGDB_C2	67	2.0261755
ELECTRON_TRANSPORT_CHAIN_HOMO_SAPIENS-WIKIPW	89	2.0155275
REGULATION_OF_TOLL_LIKE_RECEPTOR_SIGNALING_PATHWAY_HOMO_SAPIENS-WIKIPW	120	2.0141792
INTESTINAL_IMMUNE_NETWORK_FOR_IGA_PRODUCTION-KEGG_MSIGDB_C2	39	2.0130942
CLASS_A1_RHODOPSIN_LIKE_RECEPTORS-REACTOME_MSIGDB_C2	157	2.0107524
LATENT_INFECTION_OF_HOMO_SAPIENS_WITH_MYCOBACTERIUM_TUBERCULOSIS-REACTOME_MSIGDB_C2	25	1.9904767
ER_PHAGOSOME_PATHWAY-REACTOME_MSIGDB_C2	58	1.9885399
INFLAMMASOMES-REACTOME_MSIGDB_C2	16	1.9859273
TYPE_I_DIABETES_MELLITUS-KEGG_MSIGDB_C2	36	1.98529
PROTEASOME-KEGG_MSIGDB_C2	43	1.9833041
AGE_RAGE_PATHWAY_HOMO_SAPIENS-WIKIPW	63	1.9828796
AUTODEGRADATION_OF_THE_E3_UBIQUITIN_LIGASE_COP1-REACTOME_MSIGDB_C2	47	1.9778697
ENDOGENOUS_TLR_SIGNALING-NCI_NATURE_V4_PID	23	1.9735606
TCA_CYCLE_AND_RESPIRATORY_ELECTRON_TRANSPORT-REACTOME_MSIGDB_C2	116	1.9646785
DRUG_METABOLISM_OTHER_ENZYMES-KEGG_MSIGDB_C2	25	1.9471397
TOLL_LIKE_RECEPTOR_SIGNALING_PATHWAY_HOMO_SAPIENS-WIKIPW	85	1.9327481
REGULATION_OF_ORNITHINE_DECARBOXYLASE_ODC-REACTOME_MSIGDB_C2	47	1.9280182
VIF_MEDIATED_DEGRADATION_OF_APOBEC3G-REACTOME_MSIGDB_C2	49	1.9272819
PROSTAGLANDIN_SYNTHESIS_AND_REGULATION_HOMO_SAPIENS-WIKIPW	27	1.9270098
ALLOGRAFT_REJECTION_HOMO_SAPIENS-WIKIPW	63	1.9225376
XENOBIOTIC_METABOLISM-MSIGDB_HALLMARKS	161	1.9211237
TOLL_LIKE_RECEPTOR_SIGNALING_PATHWAY-KEGG_MSIGDB_C2	85	1.9052279
DESTABILIZATION_OF_MRNA_BY_AUF1_HNRNP_D0-REACTOME_MSIGDB_C2	50	1.8963017
NFKB_PATHWAY-BIOCARTA_MSIGDB_C2	23	1.889935
FC_GAMMA_R_MEDIATED_PHAGOCYTOSIS-KEGG_MSIGDB_C2	89	1.8863786
CHEMOKINE_RECEPTORS_BIND_CHEMOKINES-REACTOME_MSIGDB_C2	41	1.8829919
NKT_PATHWAY-BIOCARTA_MSIGDB_C2	23	1.8826604
AMINO_SUGAR_AND_NUCLEOTIDE_SUGAR_METABOLISM-KEGG_MSIGDB_C2	41	1.8790282
THE_NLRP3_INFLAMMASOME-REACTOME_MSIGDB_C2	11	1.8676031
VIRAL_MYOCARDITIS-KEGG_MSIGDB_C2	56	1.8667616
DEFENSINS-REACTOME_MSIGDB_C2	8	1.8666749
ACTIVATED_TLR4_SIGNALLING-REACTOME_MSIGDB_C2	90	1.8585864
COAGULATION-MSIGDB_HALLMARKS	101	1.8582302
ACTIVATION_OF_IRF3_IRF7_MEDIATED_BY_TBK1_IKK_EPSILON-REACTOME_MSIGDB_C2	13	1.8579633
GPCR_LIGAND_BINDING-REACTOME_MSIGDB_C2	214	1.8578212
REGULATION_OF_COMPLEMENT_CASCADE-REACTOME_MSIGDB_C2	10	1.8549488
TRAF6_MEDIATED_INDUCTION_OF_TAK1_COMPLEX-REACTOME_MSIGDB_C2	13	1.8494451
CROSS_PRESENTATION_OF_SOLUBLE_EXOGENOUS_ANTIGENS_ENDOSOMES-REACTOME_MSIGDB_C2	46	1.842509
GLYCOSAMINOGLYCAN_DEGRADATION-KEGG_MSIGDB_C2	18	1.8317848
PEPTIDE_LIGAND_BINDING_RECEPTORS-REACTOME_MSIGDB_C2	90	1.83125
CITRIC_ACID_CYCLE_TCA_CYCLE-REACTOME_MSIGDB_C2	19	1.8221724
CIRCADIAN_REPRESSION_OF_EXPRESSION_BY_REV_ERBA-REACTOME_MSIGDB_C2	22	1.8207715
TRANSCRIPTIONAL_REGULATION_OF_WHITE_ADIPOCYTE_DIFFERENTIATION-REACTOME_MSIGDB_C2	70	1.8156202
P53_DEPENDENT_G1_DNA_DAMAGE_RESPONSE-REACTOME_MSIGDB_C2	53	1.8148497
IL10_PATHWAY-BIOCARTA_MSIGDB_C2	16	1.804305
BLYMPHOCYTE_PATHWAY-BIOCARTA_MSIGDB_C2	11	1.8005865
TRAFFICKING_AND_PROCESSING_OF_ENDOSOMAL_TLR-REACTOME_MSIGDB_C2	12	1.7990607
SCF_BETA_TRCP_MEDIATED_DEGRADATION_OF_EMI1-REACTOME_MSIGDB_C2	49	1.7969385
CDK_MEDIATED_PHOSPHORYLATION_AND_REMOVAL_OF_CDC6-REACTOME_MSIGDB_C2	46	1.7948238
NOD_LIKE_RECEPTOR_SIGNALING_PATHWAY-KEGG_MSIGDB_C2	55	1.7943594
TCA_CYCLE_HOMO_SAPIENS-WIKIPW	17	1.7932086
COMPLEMENT_CASCADE-REACTOME_MSIGDB_C2	18	1.7920077
CITRATE_CYCLE_TCA_CYCLE-KEGG_MSIGDB_C2	28	1.7867037
PROTEASOME_PATHWAY-BIOCARTA_MSIGDB_C2	28	1.7811247
CYTOKINE_SIGNALING_IN_IMMUNE_SYSTEM-REACTOME_MSIGDB_C2	237	1.7803302
PEPTIDE_GPCRS_HOMO_SAPIENS-WIKIPW	40	1.7793673
INITIAL_TRIGGERING_OF_COMPLEMENT-REACTOME_MSIGDB_C2	10	1.7783943
ANTIGEN_PRESENTATION_FOLDING_ASSEMBLY_AND_PEPTIDE_LOADING_OF_CLASS_I_MHC-REACTOME_MSIGDB_C2	20	1.7662185
NUCLEOTIDE_BINDING_DOMAIN_LEUCINE_RICH_REPEAT_CONTAINING_RECEPTOR_NLR_SIGNALING_PATHWAYS-REACTOME_MSIG	45	1.765774
CYTOKINE_CYTOKINE_RECEPTOR_INTERACTION-KEGG_MSIGDB_C2	189	1.7635928
SCFSKP2_MEDIATED_DEGRADATION_OF_P27_P21-REACTOME_MSIGDB_C2	53	1.763174
STATIN_PATHWAY_HOMO_SAPIENS-WIKIPW	20	1.7624173
NEF_MEDIATES_DOWN_MODULATION_OF_CELL_SURFACE_RECEPTORS_BY_RECRUITING_THEM_TO_CLATHRIN_ADAPTERS-REACT	19	1.7623215
INTERFERON_SIGNALING-REACTOME_MSIGDB_C2	136	1.7598606
MIR_TARGETED_GENES_IN_LEUKOCYTES_TARBASE_HOMO_SAPIENS-WIKIPW	122	1.7527503
IKK_COMPLEX_RECRUITMENT_MEDIATED_BY_RIP1-REACTOME_MSIGDB_C2	10	1.7508737
G_ALPHA_I_SIGNALLING_EVENTS-REACTOME_MSIGDB_C2	114	1.743836
MYD88_MAL_CASCADE_INITIATED_ON_PLASMA_MEMBRANE-REACTOME_MSIGDB_C2	80	1.7409902

RELA_PATHWAY-BIOCARTA_MSIGDB_C2	16	1.739917
OXIDATIVE_STRESS_HOMO_SAPIENS-WIKIPW	24	1.7383341
THE_ROLE_OF_NEF_IN_HIV1_REPLICATION_AND_DISEASE_PATHOGENESIS-REACTOME_MSIGDB_C2	26	1.7372311
ENDOSOMAL_VACUOLAR_PATHWAY-REACTOME_MSIGDB_C2	8	1.7371874
SYSTEMIC_LUPUS_ERYTHEMATOSUS-KEGG_MSIGDB_C2	95	1.7324044
SIGNALING_BY_WNT-REACTOME_MSIGDB_C2	63	1.7322773
COMP_PATHWAY-BIOCARTA_MSIGDB_C2	13	1.7287824
IL6_JAK_STAT3_SIGNALING-MSIGDB_HALLMARKS	78	1.7140067
PYRIMIDINE_METABOLISM-REACTOME_MSIGDB_C2	21	1.709983
PHOSPHORYLATION_OF_CD3_AND_TCR_ZETA_CHAINS-REACTOME_MSIGDB_C2	15	1.7060188
TUMOR_NECROSIS_FACTOR_PATHWAY-ST_MSIGDB_C2	29	1.7051104
ACTIVATION_OF_NF_KAPPAB_IN_B_CELLS-REACTOME_MSIGDB_C2	61	1.7042876
IL4_MEDIATED_SIGNALING_EVENTS-NCI_NATURE_V4_PID	52	1.7025677
GRANULOCYTES_PATHWAY-BIOCARTA_MSIGDB_C2	13	1.7017605
SIGNAL_REGULATORY_PROTEIN_SIRP_FAMILY_INTERACTIONS-REACTOME_MSIGDB_C2	12	1.6977122
ARF1_PATHWAY-NCI_NATURE_V4_PID	19	1.6975638
IL1_AND_MEGAKARYOTYCES_IN_OBESITY_HOMO_SAPIENS-WIKIPW	23	1.6956129
CANONICAL_NF_KAPPAB_PATHWAY-NCI_NATURE_V4_PID	23	1.6938375
TOLL_PATHWAY-BIOCARTA_MSIGDB_C2	37	1.6912892
CDC42RAC_PATHWAY-BIOCARTA_MSIGDB_C2	16	1.6847003
ARYL_HYDROCARBON_RECEPTOR_HOMO_SAPIENS-WIKIPW	40	1.6820769
SHC1_EVENTS_IN_ERBB4_SIGNALING-REACTOME_MSIGDB_C2	17	1.6819034
IL1_SIGNALING-REACTOME_MSIGDB_C2	39	1.6815839
ACYL_CHAIN_REMODELLING_OF_PI-REACTOME_MSIGDB_C2	8	1.6814001
PML_PATHWAY-BIOCARTA_MSIGDB_C2	16	1.6799072
GLYCOSPHINGOLIPID_METABOLISM-REACTOME_MSIGDB_C2	29	1.6764659
BETA_DEFENSINS-REACTOME_MSIGDB_C2	5	1.67569
TH1TH2_PATHWAY-BIOCARTA_MSIGDB_C2	16	1.6710895
TWEAK_SIGNALING_PATHWAY_HOMO_SAPIENS-WIKIPW	40	1.6709334
INTERFERON_ALPHA_BETA_SIGNALING-REACTOME_MSIGDB_C2	49	1.6686558
PDGFR_BETA_SIGNALING_PATHWAY-NCI_NATURE_V4_PID	128	1.6684377
GALACTOSE_METABOLISM-KEGG_MSIGDB_C2	22	1.6669236
TRAF6_MEDIATED_INDUCTION_OF_NFKB_AND_MAP_KINASES_UPON_TLR7_8_OR_9_ACTIVATION-REACTOME_MSIGDB_C2	74	1.666144
CLASS_I_PI3K_SIGNALING_EVENTS-NCI_NATURE_V4_PID	49	1.6656067
LAIR_PATHWAY-BIOCARTA_MSIGDB_C2	14	1.6636237
P53_PATHWAY-MSIGDB_HALLMARKS	193	1.6627256
PARKINSONS_DISEASE-KEGG_MSIGDB_C2	103	1.6623931
PLATELET_SENSITIZATION_BY_LDL-REACTOME_MSIGDB_C2	16	1.6617563
CHEMOKINE_SIGNALING_PATHWAY-KEGG_MSIGDB_C2	157	1.6593677
NFKB_AND_MAP_KINASES_ACTIVATION_MEDIATED_BY_TLR4_SIGNALING_REPERTOIRE-REACTOME_MSIGDB_C2	69	1.6578231
MEMBRANE_TRAFFICKING_HOMO_SAPIENS-WIKIPW	69	1.6453439
APC_C_CDH1_MEDIATED_DEGRADATION_OF_CDC20_AND_OTHER_APC_C_CDH1_TARGETED_PROTEINS_IN_LATE_MITOSIS_EARLY	64	1.6448324
PATHOGENIC_ESCHERICHIA_COLI_INFECTION_HOMO_SAPIENS-WIKIPW	52	1.6431755
NATURAL_KILLER_CELL_MEDIATED_CYTOTOXICITY-KEGG_MSIGDB_C2	107	1.6363239
IL8_AND_CXCR2_MEDIATED_SIGNALING_EVENTS-NCI_NATURE_V4_PID	33	1.6361071

c. Hemap_pathways_M0_M1

NAME	SIZE	NES	NOM p-val
GENERIC_TRANSCRIPTION_PATHWAY-REACTOME_MSIGDB_C2	315	-2.3055868	0.0
MYC_TARGETS_V1-MSIGDB_HALLMARKS	178	-2.0839288	0.0
MRNA_PROCESSING_HOMO_SAPIENS-WIKIPW	121	-2.0505354	0.0
NONSENSE_MEDIATED_DECAY_ENHANCED_BY_THE_EXON_JUNCTION_COMPLEX-REACTOME_MSIGDB_C2	59	-2.0292943	0.0
RIBOSOME-KEGG_MSIGDB_C2	41	-2.01833	0.0
PEPTIDE_CHAIN_ELONGATION-REACTOME_MSIGDB_C2	39	-2.0020952	0.0
3_UTR_MEDIATED_TRANSLATIONAL_REGULATION-REACTOME_MSIGDB_C2	53	-1.9967451	0.0
PROCESSING_OF_CAPPED_INTRON_CONTAINING_PRE_MRNA-REACTOME_MSIGDB_C2	128	-1.9441764	0.0
MRNA_PROCESSING-REACTOME_MSIGDB_C2	146	-1.900145	0.0
CYTOPLASMIC_RIBOSOMAL_PROTEINS_HOMO_SAPIENS-WIKIPW	46	-1.8866994	0.0
MRNA_SPLICING-REACTOME_MSIGDB_C2	100	-1.8830794	0.0
MRNA_3_END_PROCESSING-REACTOME_MSIGDB_C2	32	-1.8646716	0.0
PACKAGING_OF_TELOMERE_ENDS-REACTOME_MSIGDB_C2	37	-1.8609581	0.0
TRANSCRIPTION-REACTOME_MSIGDB_C2	175	-1.8558459	0.0
FORMATION_OF_THE_TERNARY_COMPLEX_AND_SUBSEQUENTLY_THE_43S_COMPLEX-REACTOME_MSIGDB_C2	26	-1.8296608	0.0
SIGNALING_BY_FGFR1_FUSION_MUTANTS-REACTOME_MSIGDB_C2	17	-1.8210053	0.0021413276
SIGNALING_BY_FGFR1_MUTANTS-REACTOME_MSIGDB_C2	28	-1.8160412	0.0
RNA_DEGRADATION-KEGG_MSIGDB_C2	56	-1.8040515	0.0
RNA_POL_I_PROMOTER_OPENING-REACTOME_MSIGDB_C2	42	-1.7719352	0.00456621
CLEAVAGE_OF_GROWING_TRANSCRIPT_IN_THE_TERMINATION_REGION-REACTOME_MSIGDB_C2	40	-1.7631412	0.0023696683
SPLICEOSOME-KEGG_MSIGDB_C2	119	-1.7603718	0.0
METABOLISM_OF_NON_CODING_RNA-REACTOME_MSIGDB_C2	44	-1.7573915	0.0046620048
TELOMERE_MAINTENANCE-REACTOME_MSIGDB_C2	63	-1.7571934	0.0
TRANSPORT_OF_MATURE_TRANSCRIPT_TO_CYTOPLASM-REACTOME_MSIGDB_C2	51	-1.7552595	0.0
RNA_POL_I_RNA_POL_III_AND_MITOCHONDRIAL_TRANSCRIPTION-REACTOME_MSIGDB_C2	97	-1.7552052	0.0
ACTIVATION_OF_THE_MRNA_UPON_BINDING_OF_THE_CAP_BINDING_COMPLEX_AND_EIFS_AND_SUBSEQUENT_BII	30	-1.7525665	0.0021881838
RNA_POL_I_TRANSCRIPTION-REACTOME_MSIGDB_C2	65	-1.7518642	0.0023640662
IL2_SIGNALING_EVENTS_MEDIATED_BY_STAT5-NCI_NATURE_V4_PID	30	-1.7243161	0.0021929825
DEPOSITION_OF_NEW_CENPA_CONTAINING_NUCLEOSOMES_AT_THE_CENTROMERE-REACTOME_MSIGDB_C2	49	-1.723781	0.0025252525
VALINE_LEUCINE_AND_ISOLEUCINE_BIOSYNTHESIS-KEGG_MSIGDB_C2	11	-1.723331	0.006185567
CTCF_PATHWAY-BIOCARTA_MSIGDB_C2	23	-1.7161859	0.0044345898
INFLUENZA_VIRAL_RNA_TRANSCRIPTION_AND_REPLICATION-REACTOME_MSIGDB_C2	55	-1.7034966	0.0
SIGNALING_BY_FGFR_MUTANTS-REACTOME_MSIGDB_C2	42	-1.7021691	0.002232143
INFLUENZA_LIFE_CYCLE-REACTOME_MSIGDB_C2	88	-1.6870109	0.0
COREGULATION_OF_ANDROGEN_RECEPTOR_ACTIVITY-NCI_NATURE_V4_PID	58	-1.6786209	0.0
METABOLISM_OF_RNA-REACTOME_MSIGDB_C2	195	-1.6751395	0.0

d. TCGA pathways M0 M1

NAME	SIZE	NES	NOM p-val	FDR q-val
GENERIC_TRANSCRIPTION_PATHWAY-REACTOME_MSIGDB_C2	326	-2.1041558	0.0	5.302227E-4
OLFACTORY_SIGNALING_PATHWAY-REACTOME_MSIGDB_C2	29	-1.9542017	0.0	0.010386155
OLFACTORY_TRANSDUCTION-KEGG_MSIGDB_C2	46	-1.876282	0.0	0.03250705
MEIOTIC_RECOMBINATION-REACTOME_MSIGDB_C2	61	-1.865564	0.0	0.029584333
RNA_POL_I_PROMOTER_OPENING-REACTOME_MSIGDB_C2	41	-1.8378286	0.0	0.03859896
TASTE_TRANSDUCTION-KEGG_MSIGDB_C2	32	-1.7752548	0.004893964	0.09007122
PACKAGING_OF_TELOMERE_ENDS-REACTOME_MSIGDB_C2	35	-1.7562515	0.0016891892	0.10298665
RNA_POL_I_TRANSCRIPTION-REACTOME_MSIGDB_C2	66	-1.701523	0.0	0.19241117
SIGNALING_BY_FGFR_MUTANTS-REACTOME_MSIGDB_C2	32	-1.6666236	0.008130081	0.27214321
NEUROTRANSMITTERS_PATHWAY-BIOCARTA_MSIGDB_C2	5	-1.6100485	0.007155635	0.46722698
TIGHT_JUNCTION_INTERACTIONS-REACTOME_MSIGDB_C2	18	-1.609526	0.006756757	0.42711195
GLYCINE_SERINE_AND_THREONINE_METABOLISM-KEGG_MSIGDB_C2	27	-1.6079297	0.0099502485	0.39866075
TELOMERE_MAINTENANCE-REACTOME_MSIGDB_C2	62	-1.5963529	0.0016129032	0.41507018
DEPOSITION_OF_NEW_CENPA_CONTAINING_NUCLEOSOMES_AT_THE_CENTROMERE-REACTOME_MSIGDB_C2	50	-1.5660856	0.016949153	0.5240333
AMI_PATHWAY-BIOCARTA_MSIGDB_C2	13	-1.5652649	0.015280136	0.49310243
ION_TRANSPORT_BY_P_TYPE_ATPASES-REACTOME_MSIGDB_C2	27	-1.5518452	0.02173913	0.5278831
MEIOSIS-REACTOME_MSIGDB_C2	86	-1.5492297	0.0031595577	0.5106269
ION_CHANNEL_TRANSPORT-REACTOME_MSIGDB_C2	32	-1.5314323	0.025889968	0.5709465
SIGNALING_BY_FGFR1_MUTANTS-REACTOME_MSIGDB_C2	21	-1.5263451	0.047933884	0.5665365
BIOGENIC_AMINE_SYNTHESIS_HOMO_SAPIENS-WIKIPW	9	-1.522918	0.038655464	0.5545314
HISTONE_MODIFICATIONS_HOMO_SAPIENS-WIKIPW	50	-1.5044528	0.021909233	0.62121296
NICOTINE_ACTIVITY_ON_DOPAMINERGIC_NEURONS_HOMO_SAPIENS-WIKIPW	13	-1.494947	0.05141844	0.6435275
AMINE_DERIVED_HORMONES-REACTOME_MSIGDB_C2	6	-1.493296	0.02977233	0.6241212
RNA_POL_I_RNA_POL_III_AND_MITOCHONDRIAL_TRANSCRIPTION-REACTOME_MSIGDB_C2	99	-1.4880145	0.0075872536	0.6254596
FGFR_LIGAND_BINDING_AND_ACTIVATION-REACTOME_MSIGDB_C2	10	-1.4769261	0.04753521	0.66242075
MEIOTIC_SYNAPSIS-REACTOME_MSIGDB_C2	55	-1.4744071	0.018151816	0.64965343
PROXIMAL_TUBULE_BICARBONATE_RECLAMATION-KEGG_MSIGDB_C2	18	-1.4582627	0.04472272	0.7136957
RAPID_GLUCOCORTICOID_SIGNALING-NCI_NATURE_V4_PID	7	-1.4577448	0.06081081	0.69123477
INHIBITION_OF_INSULIN_SECRETION_BY_ADRENALINE_NORADRENALINE-REACTOME_MSIGDB_C2	21	-1.442105	0.06101695	0.7569545
SIGNALING_BY_FGFR1_FUSION_MUTANTS-REACTOME_MSIGDB_C2	18	-1.4355049	0.06514084	0.7702666
TRANS_SULFURATION_PATHWAY_HOMO_SAPIENS-WIKIPW	10	-1.4296039	0.085141905	0.78006935
HEDGEHOG_SIGNALING_PATHWAY_HOMO_SAPIENS-WIKIPW	13	-1.4256426	0.0822898	0.77888834
CELL_CELL_JUNCTION_ORGANIZATION-REACTOME_MSIGDB_C2	37	-1.4113475	0.041269843	0.8395694
GLUCURONIDATION-REACTOME_MSIGDB_C2	5	-1.4042214	0.05820106	0.8586595
AMYLOIDS-REACTOME_MSIGDB_C2	50	-1.4023662	0.04262295	0.84534746
GLOBO_SPHINGOLIPID_METABOLISM_HOMO_SAPIENS-WIKIPW	18	-1.4002512	0.073426574	0.8345487
MYOGENESIS-REACTOME_MSIGDB_C2	22	-1.3998605	0.07177814	0.81428343

Supplemental Table S7. List of mutations and associated drug sensitivities

	drug	gene	wilcox_pval	t_test	mean_wt_DSS	mean_mut_DSS
1	Venetoclax	Diagnosis vs. Refractory	0,00226	0,00897	29,2	12,8
2	Venetoclax	FAB M1 vs. M5_diag.	0,00866	0,00851	37,3	25,1
3	Cytarabine	RAS	0,01416	0,08591	9,6	24,1
4	Venetoclax	Relapse vs. Refractory	0,01865	0,02447	26,1	12,8
5	Trametinib	RAS	0,02620	0,09738	6,0	16,3
6	Trametinib	Diagnosis vs. Relapse	0,03101	0,06435	4,2	11,8
7	Everolimus	Frozen_Fresh	0,03606	0,09881	2,4	5,7
8	Trametinib	FAB M1 vs. M5_diag.	0,03680	0,07187	8,9	1,9
9	Trametinib	NPM1	0,03940	0,01243	9,6	3,1
10	Everolimus	Diagnosis vs. Refractory	0,11444	0,22043	3,0	5,8
11	Sunitinib	FAB M1 vs. M5_diag.	0,12121	0,19059	4,3	1,4
12	Idarubicin	RAS	0,12282	0,10532	22,8	29,8
13	Idarubicin	FAB M1 vs. M5_diag.	0,12554	0,16490	30,5	24,5
14	Everolimus	FAB M1 vs. M5_diag.	0,13203	0,13618	6,3	0,5
15	Idarubicin	Frozen_Fresh	0,13301	0,12420	22,0	26,3
16	Ruxolitinib	NPM1	0,14537	0,02299	9,6	4,2
17	Trametinib	Diagnosis vs. Refractory	0,16187	0,15477	4,2	10,8
18	Everolimus	Relapse vs. Refractory	0,17871	0,32378	3,2	5,8
19	Venetoclax	Frozen_Fresh	0,18082	0,10716	28,1	21,6
20	Idarubicin	Diagnosis vs. Refractory	0,19172	0,28736	25,3	20,8
21	Venetoclax	RAS	0,19777	0,27290	26,8	20,8
22	Idarubicin	Diagnosis vs. Relapse	0,19909	0,15054	25,3	20,6
23	Sunitinib	Complex	0,20222	0,32328	2,7	4,5
24	Ruxolitinib	RAS	0,22438	0,31416	7,2	11,9
25	Venetoclax	NPM1	0,26701	0,26567	24,5	29,0
26	Sunitinib	FLT3	0,26981	0,21163	2,4	5,6
27	Everolimus	RAS	0,27145	0,46084	3,1	5,0
28	Ruxolitinib	Diagnosis vs. Relapse	0,28587	0,49977	6,5	8,5
29	Trametinib	Complex	0,29516	0,27705	4,9	10,0
30	Ruxolitinib	Diagnosis vs. Refractory	0,30088	0,31062	6,5	10,7
31	Venetoclax	IDH	0,32818	0,28148	24,6	28,8
32	Trametinib	IDH	0,33092	0,16948	8,7	4,8
33	Ruxolitinib	FAB M1 vs. M5_diag.	0,35281	0,35408	10,5	4,8
34	Sunitinib	NPM1	0,35483	0,31272	2,5	4,6
35	Sunitinib	RAS	0,35519	0,00655	3,6	0,6
36	Ruxolitinib	Complex	0,37353	0,68062	6,8	8,0
37	Cytarabine	Complex	0,37478	0,08931	12,0	7,0
38	Cytarabine	IDH	0,39743	0,13498	12,8	9,0
39	Trametinib	Frozen_Fresh	0,39946	0,52127	6,4	8,3
40	Venetoclax	Complex	0,41278	0,38479	26,1	18,8
41	Trametinib	FLT3	0,41773	0,70657	7,1	8,4
42	Ruxolitinib	Frozen_Fresh	0,45627	0,76764	7,4	8,2
43	Idarubicin	NPM1	0,47450	0,55698	23,1	24,9
44	Cytarabine	NPM1	0,47450	0,59499	12,1	10,3
45	Idarubicin	Complex	0,48350	0,58502	23,4	20,8
46	Everolimus	Complex	0,49618	0,58626	3,0	4,8
47	Everolimus	Diagnosis vs. Relapse	0,49632	0,95280	3,0	3,2
48	Idarubicin	IDH	0,50185	0,51823	24,4	22,3
49	Venetoclax	FLT3	0,53232	0,55355	25,4	28,0
50	Cytarabine	FAB M1 vs. M5_diag.	0,53680	0,69828	10,8	12,0
51	Sunitinib	Relapse vs. Refractory	0,54002	0,19564	4,8	1,8
52	Ruxolitinib	FLT3	0,55562	0,74704	7,6	8,6
53	Sunitinib	Frozen_Fresh	0,58439	0,56017	3,1	4,1
54	Ruxolitinib	Relapse vs. Refractory	0,62160	0,60323	8,5	10,7
55	Sunitinib	Diagnosis vs. Relapse	0,63677	0,50101	3,3	4,8
56	Venetoclax	Diagnosis vs. Relapse	0,64343	0,37570	29,2	26,1
57	Cytarabine	FLT3	0,66599	0,27110	12,2	9,3
58	Cytarabine	Frozen_Fresh	0,69956	0,32953	10,0	13,9
59	Ruxolitinib	IDH	0,75332	0,41310	8,6	6,3
60	Idarubicin	FLT3	0,77370	0,80359	23,5	24,3
61	Sunitinib	IDH	0,78133	0,66622	3,4	2,7
62	Cytarabine	Diagnosis vs. Relapse	0,79264	0,51644	11,7	9,9
63	Everolimus	IDH	0,79897	0,61098	3,7	2,7
64	Everolimus	NPM1	0,79897	0,69477	3,6	2,8
65	Everolimus	FLT3	0,87788	0,93862	3,3	3,5
66	Cytarabine	Diagnosis vs. Refractory	0,92148	0,95802	11,7	12,0
67	Cytarabine	Relapse vs. Refractory	0,94328	0,71522	9,9	12,0
68	Idarubicin	Relapse vs. Refractory	0,94328	0,96927	20,6	20,8
69	Sunitinib	Diagnosis vs. Refractory	0,96094	0,33278	3,3	1,8
70	Trametinib	Relapse vs. Refractory	0,97902	0,84063	11,8	10,8

* Mutation comparison involves all samples. FAB M1 vs M5 comparision is comprised of diagnosis samples.

Supplemental Figures

A

	1	2	3	4	5	6	7	8	9	10	11	12
A	BzCl	0.1	KOMB1	KOMB2	KOMB3	KOMB4	KOMB5	KOMB6	KOMB7	KOMB8	KOMB9	
B	BzCl	1	10	1	0.1	10	0.25	0.1	KOMB10	KOMB11	KOMB12	KOMB13
C	KOMB26	10	100	10	1	100	2.5	1	KOMB14	KOMB15	KOMB16	KOMB17
D	DMSO	DMSO	DMSO	DMSO	DMSO	DMSO	DMSO	DMSO	DMSO	DMSO	DMSO	DMSO
E	KOMB27	50	300	30	3	300	25	10	BzCl	KOMB18	KOMB19	KOMB20
F	KOMB28	100	1000	100	10	1000	75	100	KOMB21	KOMB22	KOMB23	BzCl
G	KOMB29	1000	10000	1000	100	3000	250	1000	KOMB24	KOMB25	KOMB26	KOMB27
H	DMSO	DMSO	DMSO	DMSO	DMSO	DMSO	DMSO	DMSO	DMSO	BzCl	DMSO	DMSO
		Venetoclax	Cytarabine	Idarubicin	Everolimus	Ruxolitinib	Trametinib	Sunitinib				

B

	1	2	3	4	5	6	7	8	9	10	11	12
A												
B		DMSO	0.1	1	0.1	0.01	1	0.025	0.1	0.1	DMSO	
C		DMSO	0.3	3	0.3	0.03	3	0.75	0.3	0.3	DMSO	
D		DMSO	1	10	1	0.1	10	0.25	1	1	DMSO	
E		DMSO	3	30	3	0.3	30	0.75	3	3	DMSO	
F		DMSO	10	100	10	1	100	2.5	10	10	DMSO	
G		BzCl	50	300	30	3	300	7.5	30	30	BzCl	
H		BzCl	100	1000	100	10	1000	25	100	100	BzCl	
I		BzCl	300	30000	300	30	30000	75	300	300	BzCl	
J		BzCl	1000	100000	1000	100	100000	250	1000	1000	BzCl	
K		BzCl	KOMB1	KOMB2	KOMB3	KOMB4	KOMB5	KOMB6	KOMB7		BzCl	
L			KOMB8	KOMB9	KOMB10	KOMB11	KOMB12	KOMB13	KOMB14			
M			KOMB15	KOMB16	KOMB17	BzCl	KOMB18	KOMB19	KOMB20			
N			KOMB21	KOMB22	KOMB23	BzCl	KOMB24	KOMB25	KOMB26	KOMB27		
O												
P												
			Venetoclax	Cytarabine	Idarubicin	Everolimus	Ruxolitinib	Trametinib	Sunitinib	Quizartinib		

Supplemental Figure S1. Drug plate layouts. (A) 96-well plate for FC assay and **(B)** 384-well plate for CTG assay. To compare the DSS scores between FC and CTG-based assay, only the concentrations present in the FC layout were used. Drug concentrations used for each combination are presented in manuscript Table 1.

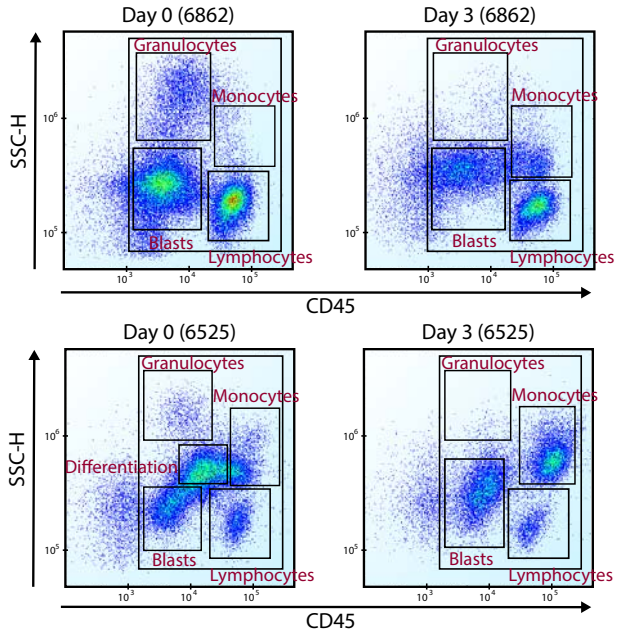

Supplemental Figure S2. *Ex vivo* cell culturing causes changes in cell compositions. Representative scatter plots (SSC *vs*. CD45+) of two AML samples measured by FC at day 0 and day 3. The granulopoietic cell population (represented by the SSChigh/CD45dim gates) was diminished and/or side scatter decreased in several samples as shown with the 6862 sample. Differentiation of monoblasts/promonocytes towards more mature monocytes based on the increment of SSCmid/CD45high and CD14+ cell populations was observed in many M5 cases as illustrated with the 6525 sample. *Ex vivo* culturing resulted in two clear separate cell populations in the SSC/CD45 scatter plots in several M5 samples.

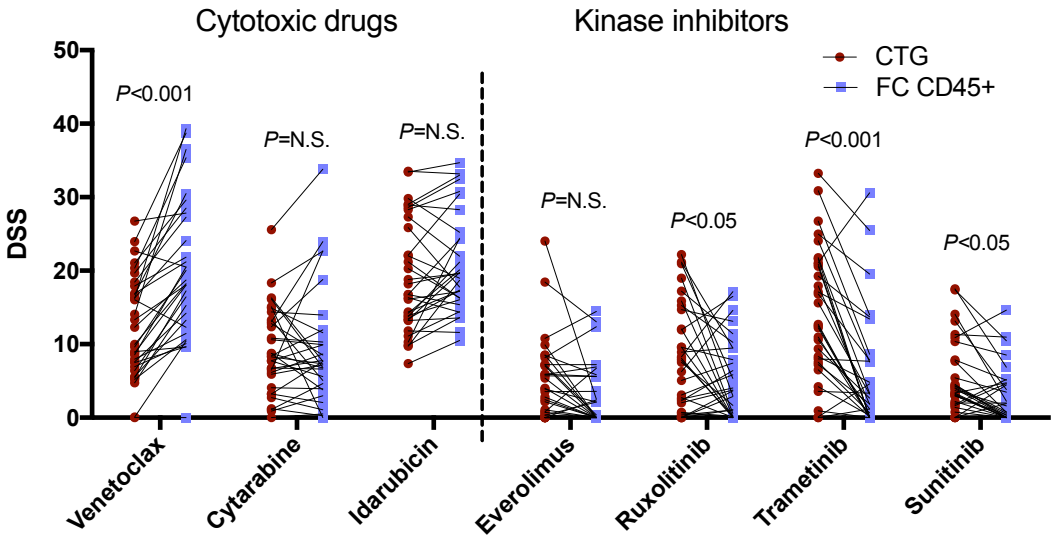

Supplemental Figure S3. Drug sensitivity comparison between CTG and FC-based assay on individual drugs. The comparison was made between drug sensitvity scores calculated from CTG-based bone marrow mononuclear cell and FC-based CD45+ leukocyte viability. Each dot represents one patient and the line connects the two readouts from the same patient. Venetoclax shows higher DSS scores (lower IC50) when measured with flow cytometry whereas trametinib, sunitinib and ruxolitinib shows higher DSS scores (lower IC50) when measured with CTG. CTG measures the ATP levels and thus the metabolic activity of the cells, whereas FC measure the number of live cells present after 72h drug treatment.

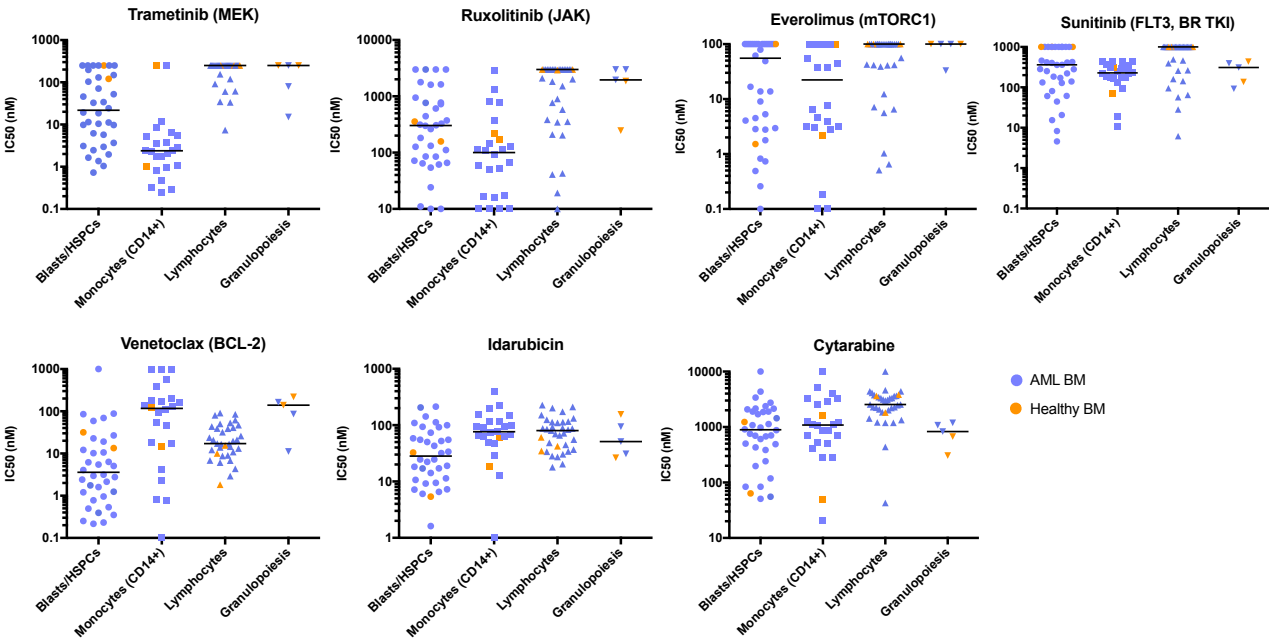

Supplemental Figure S4. IC50 values for distinct cell populations in AML and 2-3 healthy control samples. Blue dots represent AML samples (n=33) and orange dots represent healthy control samples (n=2 or 3). The black line indicates the median IC50 value.

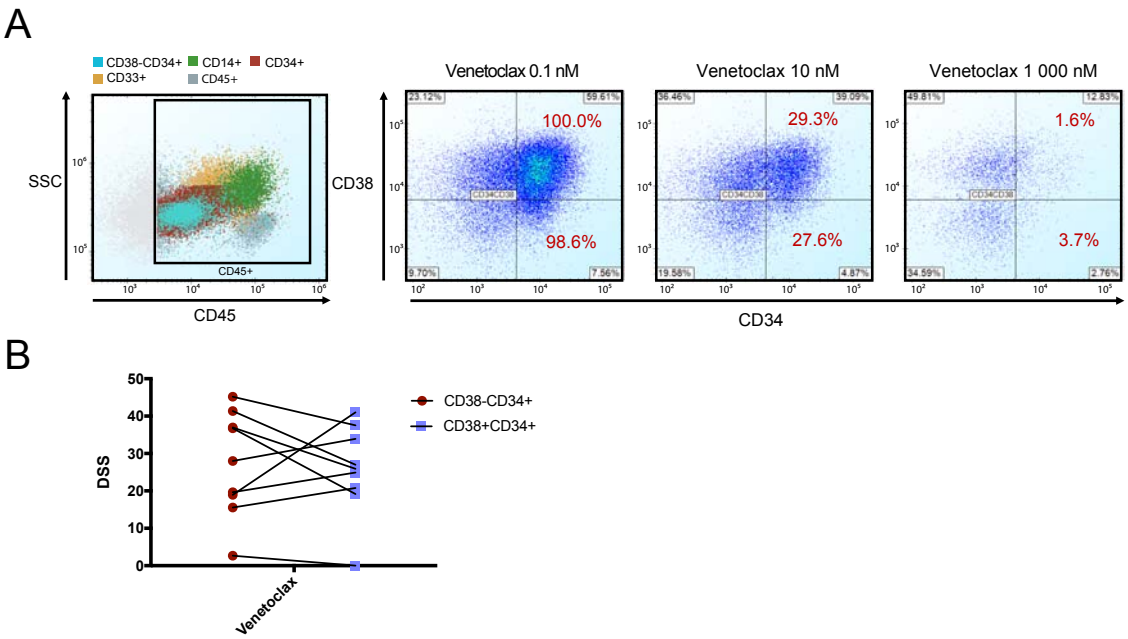

Figure S5. Venetoclax effect on CD34+CD38- LSCs *vs*. bulk CD34+CD38+ blasts. (A) A FC scatter plot representation of venetoclax effect on CD34+CD38- *vs*. bulk CD34+38+ blasts of patient sample 6688_2. The red highlighted value is the percentage of live cells relative to DMSO control treated wells at day 3. **(B)** Comparison for nine AML samples, which had distinct CD34+CD38- and CD34+CD38+ populations. The line connects the cell population specific effect for the same sample.

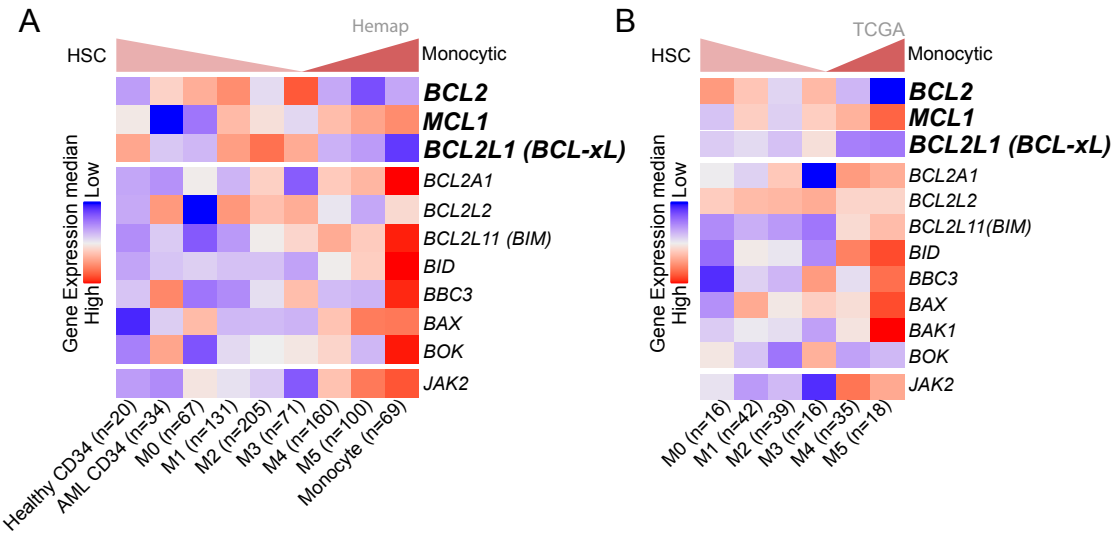

Supplemental Figure S6. *BCL2* family expression for each FAB class analyzed from Hemap and TCGA data sets. Heatmap representation of gene expression levels in different AML subtypes or healthy cells derived from the **(A)** Hemap data set or the **(B)** TCGA data set.

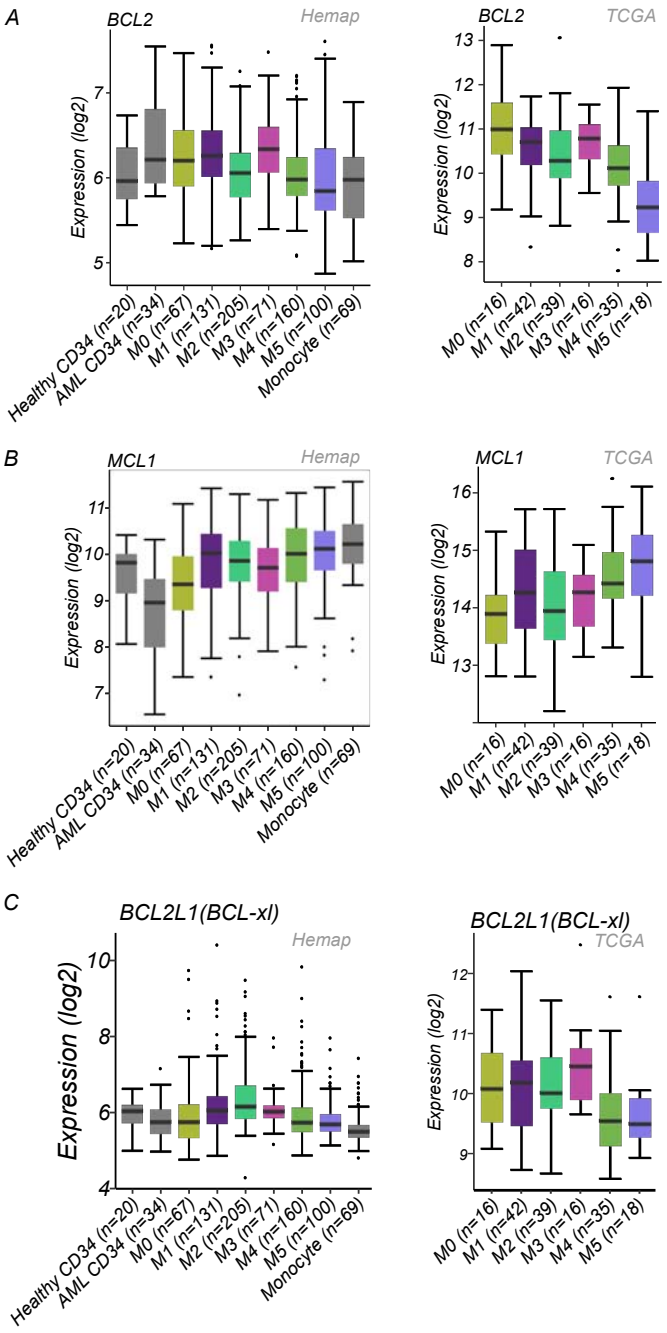

Supplemental Figure S7. *BCL2*, *MCL1*, *BCL2L1* expression for each AML FAB class and control samples. Expression of *BCL2* **(A)**, *MCL1* **(B)** and *BCL2L1* **(C)** in different AML subtypes and healthy controls from Hemap (left panels) and TCGA (right panels) data sets.

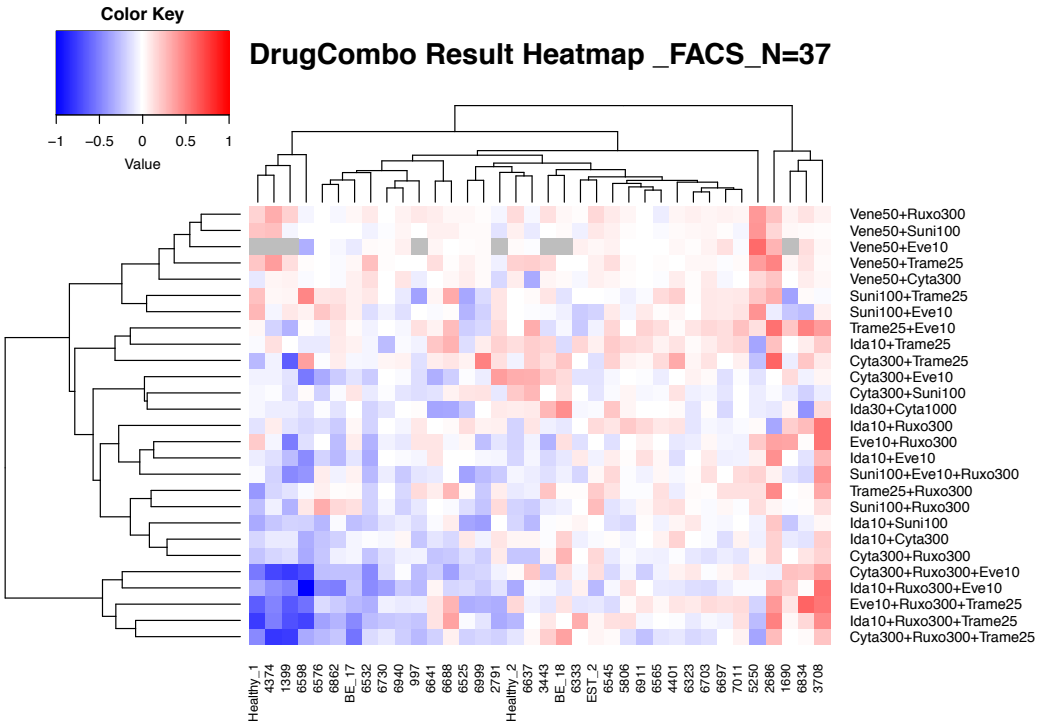

Supplemental Figure S8. Synergistic activity of different rational drug combinations in AML. Heatmap of the calculated BLISS synergy scores for the indicated drug combinations. The number after the short drug names represents the drug concentration (nM) used in the combinations.

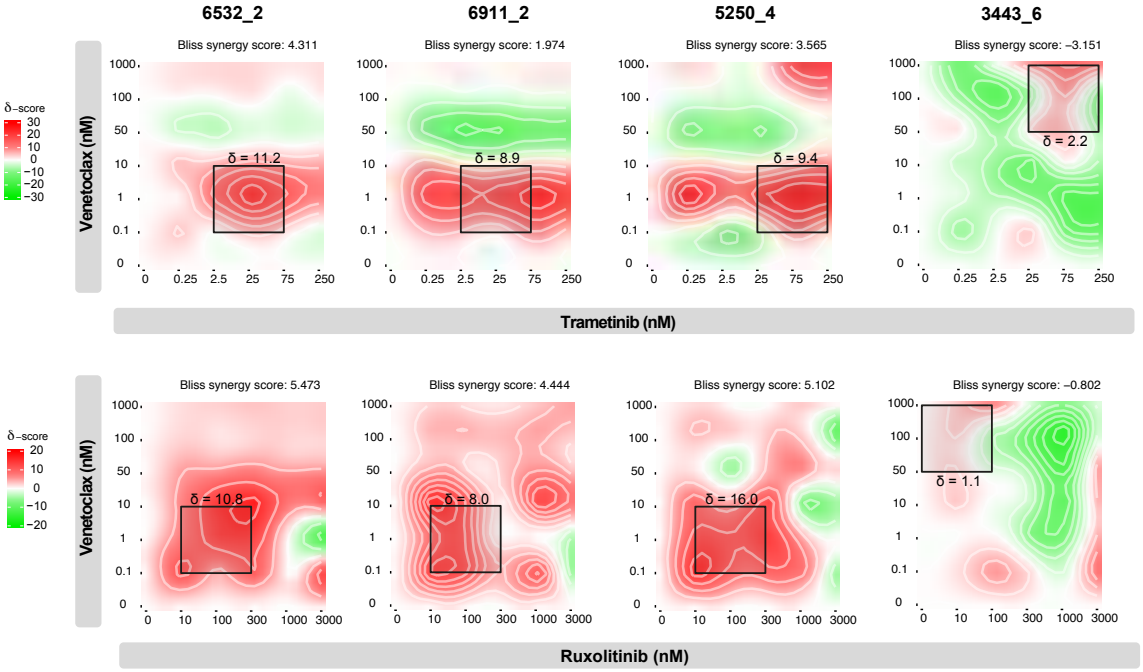

Supplemental Figure S9. Synergy between MEK inhibitor trametinib and JAK1/2 inhibitor ruxolitinib with Bcl-2 inhibitor venetoclax in AML. Dose–response matrices of delta synergy scores achieved at indicated doses of venetoclax combined with trametinib (top panels) or ruxolitinib (lower panels) in four patient samples. The black boxes represent the highest synergy score areas. The BLISS synergy method was used to calculate delta synergy scores.